

**Polymer Micro Photosynthetic Power Cell: Design, Fabrication,  
Parametric Study and Testing**

M. Shahparnia

*A Thesis*

*In*

*The Department*

*Of*

*Mechanical and Industrial Engineering*

Presented in Partial Fulfillment of the Requirements

For the Degree of Master of Applied Science (Mechanical Engineering) at

Concordia University

Montreal, Quebec, Canada

July 2011

© M. Shahparnia, 2011

CONCORDIA UNIVERSITY

School of Graduate Studies

This is to certify that the thesis prepared

By: *Mehdi Shahparnia*

Entitled: *Polymer Micro Photosynthetic Power Cell: Design, Fabrication, Parametric Study and Testing* and submitted in partial fulfillment of the requirements for the degree of *Master of Applied Science (Mechanical Engineering)* complies with the regulations of the University and meets the accepted standards with respect to originality and quality.

Signed by the final examining committee:

Dr. Mamoun Medraj \_\_\_\_\_ Chair

Dr. Sheldon Williamson \_\_\_\_\_ Examiner

Dr. Narayanswamy Sivakumar \_\_\_\_\_ Examiner

Dr. Muthukumaran Packirisamy \_\_\_\_\_ Supervisor

Dr. Valter Zazubovich \_\_\_\_\_ Co-Supervisor

Approved by \_\_\_\_\_ Dr. Martin Pugh \_\_\_\_\_

Chair of Department

\_\_\_\_\_ Dr. Robin Drew \_\_\_\_\_

Dean of Faculty

September 3, 2011

## ABSTRACT

### **Polymer Micro Photosynthetic Power Cell: Design, Fabrication, Parametric Study and Testing**

Energy and its importance are undoubtedly some unquestionable topics of all times. Not only the environmental impact of our main energy source – fossil fuels – but also their limited quantity made the human-kind find alternate sources of energy. Moreover, in the recent years there has been lots of attention on green energy. The challenge however, is finding suitable energy sources and developing appropriate energy harvesting devices.

Photosynthesis is among the most frequent and vital processes occurring all over the planet and recently, it has been found to be a potential promising energy source. The challenge still remains developing an appropriate energy harvesting device. Micro Electro Mechanical Systems (MEMS) enables fabrication of devices that the human-kind was not able to produce before.

So far there has been a vast research and investment on solar cells and fuel cells. However, the potential energy source mentioned earlier (photosynthesis) has not received as much attention. This work is an attempt to develop a device capable of harvesting energy from photosynthesis using nontraditional materials and processes used in MEMS.

A Micro Photosynthetic Power Cell ( $\mu$ PSC) was fabricated and tested for performance. Then, using no-load performance optimal fabrication parameters were suggested. Some environmental and operational parameters were studied and properties

such as *voltage-current* characteristics and long-term behavior were studied. The results and outputs of the  $\mu$ PSC developed in this study were presented in forms of power and current densities for comparison purposes and eventually, some points were suggested for future studies.

Open circuit voltage of more than 900 mV was measured. The measured current varied from zero (open circuit) to 840  $\mu$ A (short circuit). At the peak power generation of 175  $\mu$ W, approximate voltage and current correspond to 400 mV and 400  $\mu$ A. These results correspond to a noticeable power generation of 36.1  $\mu$ W/cm<sup>2</sup> which is comparable to that of  $\mu$ PSCs fabricated previously by other groups.

## Acknowledgment

I would like to have this as an opportunity to show my sincere gratitude to those who supported and assisted me in this work.

Working at Optical Bio MEMS laboratory of Concordia University under supervision of **Dr. Muthukumaran Packirisamy** with his noble ideas and my co-supervisor **Dr. Valter Zazubovits** (Department of physics) is truly considered as an honor for me. I am greatly thankful to Dr. **M. Packirisamy** for accepting my presence in his team in the first place as well as supporting this work financially and mentoring me how to apply my theoretical knowledge to practical problem solving throughout the completion of this thesis.

I am grateful to **Dr. Matthieu Nannini** – manager of McGill MicroFab Laboratory – who assisted me in one of the most critical parts of fabrication process involved in this work.

This thesis would not have been possible without the great support of **Dr. Philippe Juneau** – Department of Biological Sciences, Université du Québec à Montréal (UQAM) – and **Mr. Francis Racine** – Graduate Research Assistant – for preparing and testing all the cultures and photosynthetic micro-organisms used in this work.

It is a pleasure to thank my *colleagues* at the Optical Bio MEMS laboratory with whom I have been working for almost 3 years and who cooperated with me in form of advice, suggestion and benchmarking.

I owe my deepest gratitude to *my family* who were always by my side and supported me the best they could in all aspects of life.

I am indebted to my great friend **Arash Naseri** – Mechanical Engineer (Concordia University) and Analyst (Bombardier Transport) – from whom I heard of The Concordia University for the first time and who made me acquainted with opportunities in Montreal and Concordia University. It would be reasonable to note that I owe him many achievements of mine during this period.

*“At the age of 55, I realized that small decisions are made by the brain and great ones by the heart”*, Gabriel García Márquez. I would like to express my thankfulness to my dearest, those who helped me making great decisions and made available their support in various ways: **Behdad Kheirkhah, Matin Tavkolli, Yalda Farshchian, Maryam Akhavan, Paolo Vergalito, Nora Sebestyen, Samine Mojaver, Gohar Tajic, Kenji Doshida, Vanja Kragulj, Roham Mactabi, Karolina Przek, Slavisa Lukic, Lelissa Savic, Mirna Kragulj and Robert Duncan Ross.**

Lastly, I offer my regards and thanks to all of those who supported me in any respect during the completion of the project.

Mahdi Shahparnia

*Dedicated to Pasqualino Sanzo – friend of mine whom I lost in spring 2011*

*You will be always in minds Pasqualino*

# Contents

Acknowledgment .....	v
List of Figures .....	xii
List of Tables .....	xvii
1 Introduction .....	19
1.1.1 Energy, Technologies and devices.....	19
1.1.2 Fuel cells .....	20
1.1.3 Heat engines.....	22
1.1.4 Thermophotovoltaic devices.....	23
1.1.5 Solar cells.....	24
1.1.6 Combined devices.....	27
1.1.7 Photosynthetic power cells (PSC).....	28
1.2 Energy conversion mechanism.....	29
1.3 Principles of operation .....	30
1.3.1 The Device .....	30
1.3.2 The Mechanism.....	31
1.4 History .....	33
1.5 Thesis motivation .....	36
1.6 Thesis objectives and scopes.....	36
1.7 Organization of the thesis in manuscript-based format.....	38

2	Photosynthesis .....	41
2.1	Basics of photosynthesis .....	41
2.2	Light and dark reactions .....	44
2.3	Photosynthesis and respiration .....	47
2.4	Photosystems and light harvesting complexes .....	48
2.5	Electron Transfer in photosynthesis and respiration .....	52
2.6	Parameters affecting photosynthesis .....	54
2.6.1	Temperature .....	54
2.6.2	Light .....	56
2.6.3	Carbon dioxide .....	62
2.6.4	Glucose addition .....	62
3	Fabrication: Low stress microfabrication of electrode integrated proton exchange membrane for polymer based photosynthetic power cell .....	64
3.1	Introduction .....	64
3.1.1	Photosynthesis .....	65
3.1.2	Respiration .....	67
3.1.3	Electron transfer .....	67
3.2	$\mu$ PSC Structure and Principle of Operation .....	67
3.2.1	Operational principle .....	67
3.2.2	Structure .....	68

3.3	Fabrication.....	69
3.3.1	Half- cells.....	69
3.3.2	Proton Exchange Membrane (PEM).....	73
3.3.3	Electrodes.....	76
3.3.4	Assembly.....	82
3.3.5	External circuit.....	83
3.4	Results .....	84
3.5	Conclusions .....	86
4	Experimental setup .....	88
4.1	Setup.....	88
4.2	Experimental verification.....	90
4.3	Calculations.....	96
5	Results: Effect of Proton Exchange Membrane Electrode Configuration and Other Design Parameters on the Performance of Micro Photosynthetic Power Cell ( $\mu$ PSC) ....	99
5.1	Introduction .....	99
5.1.1	Energy harvesting devices .....	99
5.1.2	Photosynthesis.....	101
5.1.3	Photosynthetic Power Cell.....	102
5.2	Fabrication.....	103
5.2.1	Photosynthetic Power Cell.....	103

5.2.2	Measurement setup .....	106
5.3	Experiments.....	107
5.3.1	Effect of proton exchange membrane and electrode configuration .....	108
5.3.2	Effect of potassium ferricyanide concentration .....	114
5.3.3	Effect of volume and concentration of algae .....	116
5.3.4	Effect of illumination.....	121
5.3.5	V-I Characteristics .....	123
5.3.6	Long-term Behavior Analysis.....	125
5.4	Conclusion.....	127
6	Experiments with other photosynthetic organisms.....	130
6.1	Introduction .....	130
6.1.1	Glucose addition .....	130
6.1.2	Photosynthetic organisms .....	136
6.1.3	Mediators .....	138
7	Conclusions and future works .....	150
7.1	Conclusions .....	150
7.2	Future works.....	152
8	References .....	154
	Appendices.....	160
	A1: Parametric study of the performance of the micro photosynthetic power cell.....	160

A2: No-load performance of $\mu$ PSCs with Nafion 212 and various electrode configurations.....	163
A3: No-load performance of $\mu$ PSCs with Nafion 115 and various electrode configurations.....	164
A4: No-load performance of $\mu$ PSCs with Nafion 117 and various electrode configurations.....	165
A5: First trial experiment with external load of 1kOhms .....	166
A6: Variations of voltage and current with three different external loads (PEM212/D3) .....	167
A7: Variations of power and current densities with three different external loads (PEM212/D3).....	168
A8: Variations of voltage and current with three different external loads (PEM115/D3) .....	169
A9: Variations of power and current densities with three different external loads (PEM115/D3).....	170
A10: Voltage-Current ( $V-I$ ) characteristics of two $\mu$ PSCs.....	171
A11: Power generation curves of two $\mu$ PSCs.....	172
A12: Mold design for PDMS fabrication.....	173

## List of Figures

Figure 1-1: Most common fuel cell types [3] .....	21
Figure 1-2: Schematic of $\mu$ PSC .....	31
Figure 1-3: Operation of $\mu$ PSC .....	32
Figure 2-1: Leaf structure [44].....	43
Figure 2-2: Mesophyll cell structure [44] .....	43
Figure 2-3: Chloroplast structure [44] .....	43
Figure 2-4: Schematic presentation of algae structure – Green algae, <i>Chlamydomonas reinhardtii</i> , strains <i>CC125</i> [45].....	44
Figure 2-5: Higher plant photosynthesis: Light and dark reactions [50] .....	46
Figure 2-6: Products of light and dark reactions.....	47
Figure 2-7: Schematic presentation of light harvesting complexes of some species [43] .....	50
Figure 2-8: Electron transport chain in photosynthesis [50].....	52
Figure 2-9: Electron transport chain in respiration [52] .....	52
Figure 2-10: Schematic presentation of the effect of temperature on photosynthesis .....	55
Figure 2-11: Electromagnetic spectrum [60] .....	57
Figure 2-12: Daylight spectrum [59] .....	58
Figure 2-13: Spectrum of blue sky Vs red sunset [59] .....	58
Figure 2-14: Absorption spectrum of Chlorophyll a, b and Carotenoids [59].....	59
Figure 2-15: Underwater light spectra [61] .....	59
Figure 2-16: In vivo absorption spectra of intact cells of 20 phototrophic species [61] ..	60
Figure 3-1: Operational mechanism of $\mu$ PSC.....	68

Figure 3-2: $\mu$ PSC structure .....	69
Figure 3-3: Half-cell design .....	70
Figure 3-4: Designed mold .....	70
Figure 3-5: Fabricated mold – a. with cylindrical features for circular channels, b. close up of the cylindrical features.....	71
Figure 3-6: Fabricated PDMS chip showing pins removal.....	72
Figure 3-7: Schematic of half-cell assembly .....	72
Figure 3-8: Ionic conductivity test.....	75
Figure 3-9: Variation in pH of water using Nafion NRE 212.....	76
Figure 3-10: Electrode pattern design.....	77
Figure 3-11: Integrating electrodes on Nafion.....	79
Figure 3-12: Some electrode patterns on Nafion .....	80
Figure 3-13: External connection of the electrodes .....	81
Figure 3-14: Exploded view of the $\mu$ PSC.....	82
Figure 3-15: Assembled $\mu$ PSC with fluid ports and external connections.....	82
Figure 3-16: The external circuit .....	83
Figure 3-17: Output voltage and current.....	84
Figure 3-18: Current and power densities.....	85
Figure 4-1: Experimental setup.....	88
Figure 4-2: Experimental verification with voltage generator (a) and AAA battery (b) using the external circuit and data acquisition system (c) .....	90
Figure 4-3: Experimental setup using power supply, multi meter and DAS .....	91
Figure 4-4: Experimental verification – DAS Vs voltage generator .....	93

Figure 4-5: Experimental verification with $\mu$ PSC .....	94
Figure 4-6: Experimental verification with $\mu$ PSC – Cont'd .....	95
Figure 5-1: Main components of PSC .....	102
Figure 5-2: Unassembled $\mu$ PSC model.....	104
Figure 5-3: Assembled proposed $\mu$ PSC.....	105
Figure 5-4: Schematics of the $\mu$ PSC tested .....	105
Figure 5-5: Schematics of the experiment setup.....	105
Figure 5-6: Experiment measurement setup .....	106
Figure 5-7: Changes in the electrode surface to volume ratio with number of pores.....	111
Figure 5-8: Variation of OCV with electrode configurations on Nafion 212.....	112
Figure 5-9: Variations of the maximum OCV with various electrode configurations on different PEMs.....	113
Figure 5-10: Variations of the mean OCV with various electrode configurations on different PEMs.....	113
Figure 5-11: Variations of the maximum OCV with PEMs having the same electrode configuration.....	113
Figure 5-12: Variations of the mean OCV with PEMs having the same electrode configuration.....	113
Figure 5-13: OCV variations with different catholyte concentrations in a $\mu$ PSC with Nafion 117 and electrode configuration D2.....	115
Figure 5-14: Maximum and mean OCV with different concentrations of potassium ferricyanide with Nafion 117 and electrode configuration D2 .....	115
Figure 5-15: Effect of the algae concentration with maximum volume (2 ml) .....	117

Figure 5-16: Variations of closed circuit voltage with normalized concentration for different chamber volumes .....	118
Figure 5-17: Axonometric plot of the closed circuit voltage variations with algae volume and concentration .....	118
Figure 5-18: Contour plot of the output voltage variations with algae's volume and concentration.....	119
Figure 5-19: Closed circuit voltage of 300 mV and more under 20 k $\Omega$ load .....	120
Figure 5-20: Variations of voltage and current with illumination under load and no-load conditions.....	122
Figure 5-21: V-I characteristics of a $\mu$ PSC with Nafion 117 and electrode pattern D2 ..	123
Figure 5-22: Power generation curve of a $\mu$ PSC with Nafion 117 and electrode pattern D2 .....	124
Figure 5-23: long-term behavior of PSC .....	126
Figure 6-1: Glucose solutions of different concentrations.....	131
Figure 6-2: Effect of glucose addition with $\mu$ PSC with Nafion 115 and electrode D2 ..	132
Figure 6-3: Effect of glucose addition with $\mu$ PSC with Nafion 117 and electrode D2 ..	133
Figure 6-4: Effect of glucose addition on performance of a $\mu$ PSC with Nafion 115 and electrode D3 and external load of 1k $\Omega$ .....	134
Figure 6-5: Effect of glucose addition and injection time on the closed circuit voltage under 1k $\Omega$ resistance and $\mu$ PSC with Nafion 115 and electrode D3 .....	135
Figure 6-6: Comparison of V-I characteristics of $\mu$ PSCs with different photosynthetic samples.....	137
Figure 6-7: Power generation of different photosynthetic samples .....	137

Figure 6-8: Effect of mediators on growth rate of green algae.....	140
Figure 6-9: Effect of mediators on growth rate of cyanobacteria.....	140
Figure 6-10: Incubator's light spectrum .....	141
Figure 6-11: Room light spectrum used for the experiments .....	142
Figure 6-12: Absorption spectrum of Algae with mediators .....	142
Figure 6-13: Absorption spectrum of cyanobacteria with mediators.....	143
Figure 6-14 Absorption spectrum of media with mediators - $T = 0$ .....	144
Figure 6-15 Absorption spectrum of media with mediators - $T = 1$ [Day].....	145
Figure 6-16 Absorption spectrum of media with mediators - $T = 2$ [Day].....	146
Figure 6-17 Absorption spectrum of media with mediators - $T = 4$ [Day].....	147

## List of Tables

Table 1-1: Comparison of the power generation of fuel cells [3].....	21
Table 1-2: Comparison of Photovoltaic Devices [15] .....	26
Table 1-3: Laboratory efficiency of some PV cells [17] .....	27
Table 2-1: Available and utilized solar energy [43] .....	41
Table 2-2: Core and peripheral antenna complexes of some photosynthetic bacteria [43] .....	49
Table 2-3: Names and main pigments of organisms in Figure 2-11 [61].....	61
Table 3-1: Properties of 3 types of Nafion® .....	74
Table 3-2: Electrode design properties .....	77
Table 4-1: Experimental verification using $\mu$ PSC .....	92
Table 5-1: Nafion® properties.....	109
Table 5-2: Electrodes configuration.....	109
Table 6-1: Parameters of the cultures used .....	136
Table 6-2: Samples used for studying the effect of mediators.....	139

# **Chapter 1**

## ***Introduction***

# 1 Introduction

## 1.1.1 Energy, Technologies and devices

Energy is probably the most important issue of the current century. New sources, approaches and systems have been explored in order to find suitable and more reliable power sources and energy harvesting devices. One class of these approaches has been proposed by a relatively new field of science – MEMS (Micro Electro Mechanical Systems). Acceptance and adaptation of new products and technologies might require some time. MEMS acceptance is no exception and can be clearly understood by comparing the time when the first MEMS device was demonstrated (1979, Stanford University – MEMS accelerometer [1]) and the time it became practically accepted and used (after 15 years – airbag safety systems) [2]. Same ideology can be applied to new products as well. By now MEMS has already been accepted in industries and has very fast growth rate. What is discussed in this work also falls under the category of MEMS products. Hence, the device and power generation scale are micro scale.

Below we present some categories of power generating devices and compare their advantages and disadvantages.

Batteries are probably the most predominant technology for portable power generation. The main disadvantages of this category of energy generation devices however are relatively high cost, environmental impact and low energy density. Lots of alternative systems have been proposed and investigated ranging from passive man power to energy harvesting systems such as fuel cells, micro heat engines, etc. These

technologies are being raised with the promise of energy density increase. The following is a brief discussion of these systems [3].

### **1.1.2 Fuel cells**

Fuel cells are one of the most promising systems being investigated. They are generally an alternative to conventional methods of power generation and can be traced back to 1830s. In contrast to the batteries, fuel cells use continuously replenished reactants. No moving parts are required in fuel cells and no thermal conversion routes are necessary. They were first proposed by W. Grove [4] in 1830s and have been under development to the date. One of the disadvantages of the fuel cells is the insufficient ionic conductivity in the electrolyte. However, micro fuel cells are to make an improvement by reducing the path length of ionic charge through the electrolyte. The most common fuel cell types are: alkaline fuel cell (AFC), Polymer electrolyte membranes fuel cell (PEMFC), phosphoric acid fuel cell (PAFC), molten carbonate fuel cell (MCFC) and solid oxide Fuel cell (SOFC) [3,5]. Figure 1-1 illustrates the basic differences of the mentioned fuel cells.

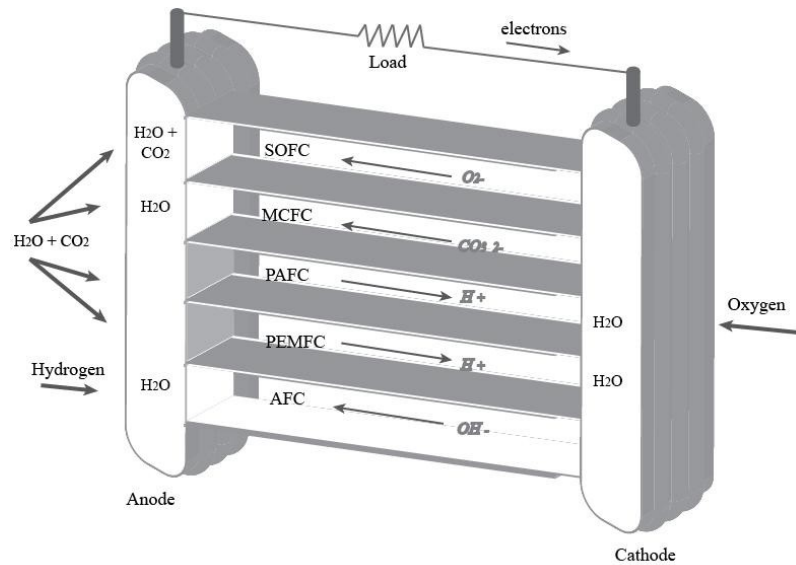


Figure 1-1: Most common fuel cell types [3]

These above types of fuel cells were investigated on micro scale as well.

Comparison of their power generation capabilities is presented in Table 1-1.

Characterization		Power density	Operating temperature [°C]
Device Name		[mW cm <sup>-2</sup> ]	
Double chamber	SOFC	200-400	350-400
	μSOFC	6-145	390-600
	μPEMFC	100	60
Single chamber fuel cell		~ 250	N/A
Membrane-less FC (Laminar flow micro fuel cell)		200	N/A

Table 1-1: Comparison of the power generation of fuel cells [3]

### 1.1.3 Heat engines

For many large-scale power plants heat engines are the primary choice of power conversion devices. Depending on the power generation level, different sources are used varying from natural gas to coal to nuclear. But even micro scale heat engines burning hydrocarbon fuels allow achieve larger energy densities in comparison with lithium-ion battery [3]. Main challenges regarding the micro scale heat engines are small size, low Reynolds number, large viscous losses and high heat transfer. Many silicon-based micro-scale heat engines have been studied over years. In 1990s a very first micro-scale heat engine was developed at MIT [6]. Soon after, internal combustion engines and steam engines were developed. The goal of the project developed at MIT was to obtain 5% conversion efficiency followed by an increase to 10%. [3].

H. Epstein *et al.* [7] fabricated a turbine at MIT consisting of a stack of five silicon wafers bonded together. The middle wafer contained the rotor with the blades. The 2<sup>nd</sup> and the 4<sup>th</sup> contained the bearings providing axial support and the outer wafers (1<sup>st</sup> and 5<sup>th</sup>) contained the required channels. Pressurized nitrogen was used for operation of the turbine and rotor speed of 1.4 million rpm was obtained.

Similar to the engine mentioned above, micro turbochargers have been designed as well. The major difference is that the turbocharger's rotor includes a turbine on one side and a compressor on the other side. Micro scale internal combustion heat engines have been studied as well. The main challenge in these engines is the limited available volume for the reaction [3]. Some of these attempts are now being commercialized such as a swing engine fabricated by W. Dahm *et al.* [8] which produces 20 W and is being

commercialized by Powerix Technologies. There also have been some attempts to integrate the electric generator concepts into the gas turbine mentioned above [9].

#### **1.1.4 Thermophotovoltaic devices**

Another category of electricity generating devices is Thermophotovoltaics (TPV) in which the power generation is based on absorbing photons generated by heated emitter. These photons are absorbed by a photocell and are converted to electricity. This concept was proposed in 1960s by H. Kolm at MIT. However, it did not receive much attention till late 1980s [10]. TPV technology is very close to that of the solar cells. The basic difference is in the source of radiation. In the TPV a heated local emitter is used instead of the sun as the source of radiation. Reported system efficiencies are as high as 12.3% [11] and the power density can be much higher than for the solar energy harvesting systems. These higher power densities can be achieved because the emitter and the photocell can be placed in close proximity. However, due to the noticeable difference in the temperature of the radiation sources (sun versus heated emitter), the emitted photons in TPV have lower energy. Since there is no moving part in TPV, it is less subjected to wear comparing to turbines and other engines. In addition, problems associated with large thermal stress in the photocell itself do not occur. There are challenges, however, regarding design and fabrication, such as choice of the photocell material and fabrication of the emitter. The photocell material should be chosen according to the emitter temperature and emission spectrum and its temperature should be kept as low as possible. However, in case of the MEMS devices, the emitter and the photocell are placed in close proximity where the emitted power is proportional to the fourth power of temperature. Therefore, the challenge in TPV fabrication is the thermal

isolation of the emitter which is required in order to maintain high temperature when high emitted power is desired. Since the heat transfer is proportional to the surface to volume ratio, scaling down of the device will increase this ratio. Hence, microfabrication of TPV should be done with great care; otherwise it will result in a low efficiency of the system [3].

Two main examples of MEMS TPV were reported. A prototype micro TPV suggested by W. M. Yang *et al.* [12] generated a total power of over 1 W with highest efficiency of 0.66% where the emitter's temperature was 1052 °C. In the other project titled "A prototype microthermophotovoltaic power generator", O. M. Nielsen *et al.* [13] achieved 1 mW of output power. The efficiency and power density were calculated as 0.08% and 32 mWcm<sup>-2</sup> respectively. The emitter's temperature was 700 °C and an efficiency of 2.4% and power density of 250 mWcm<sup>-2</sup> was estimated by increasing the emitter's temperature to 1000 °C and using photocells on both sides of the emitter under vacuum.

### **1.1.5 Solar cells**

The photo-effects in semiconductors are due to the generation of electrons and holes by light absorption [14,15]. A. Fujishima and K. Honda [16] studied an electrochemical photocell based on an n-type TiO<sub>2</sub> electrode in contact with aqueous electrolyte and Pt counter electrode. The reported result was a voltage of 0.5 V and quantum efficiency of 0.1 %. By 1941, the light-to-electricity conversion efficiency of selenium devices reached about 1 percent and later on with growth and development of p-n junction, single crystal cells were fabricated. By mid 1950s the conversion efficiency reached 6 percent [17]. A. Hermann [18] reviewed various polycrystalline thin-film solar

cells. Different solar cells were compared based on the materials used as well as the scale of the devices. For small area cells efficiency of up to 15.8% was reported with OCV varying from 0.59 to 2.9 volts [18].

Photovoltaic devices can be divided into the following sub-classes [15]:

1. Wet photovoltaic cells or liquid junction solar cells are composed of n or p type semiconductor photo electrode, a solution of a redox couple according to the photo electrode and a counter electrode kept in dark with a reverse redox. By 1980s reported power conversion efficiency of such devices reached up to 15%.
2. Fuel producing cells are the most common category of photo electrochemical devices using semiconductor electrodes and is divided to three subcategories:
  - a. Photo-electrolysis cells in which the two electrodes are immersed into the same solution of constant pH. Efficiency of such devices was reported to be between 3 and 7.8%.
  - b. Photo-assisted electrolysis cells operated under illumination plus an assisting bias, e.g. chemically biased cell with different electrolytes in the two half cells with an efficiency of 3 – 12%.
  - c. Photovoltaic electrolysis cells producing both electrical power and fuel with a low-energy electrolyte reaction. The efficiency of devices of this category was reported as 7 %.
3. Photo electrochemical storage cells are considered as secondary batteries. These devices are recharged by absorption of light. Up to 11.3 % conversion efficiency

was reported for one of the devices developed by Texas Instruments with U.S. Department of Energy Support.

Table 1-2 compares the devices mentioned above. It seems unlikely that these devices would be competitive with solid state PV cells with their over 70 % efficiency. However it should be noted that significant amount of research and development work has been done on solar cells for more than four decades and since they are fairly developed by now, the focus has been shifted towards the development of complimentary products, design optimizations and innovative systems. Other devices mentioned above, however, got much less attention and were not a focus of much research.

Table 1-3 includes the recorded laboratory efficiency of some photovoltaic cells.

Name	Description	Efficiency [%]
Liquid junction solar cells (wet photovoltaic cells)	Electrode ,counter electrode and redox couple	15
Fuel producing cells		
Photo electrolysis cells	Two electrodes immersed into the same solution	3 – 7.8
Photo-assistant electrolysis cell	Illumination plus an assisting bias required	3 – 12
Photovoltaic electrolysis cells	Production via low energy electrolyte reaction	7
Photo electrochemical storage cells	Rechargeable secondary batteries	11.3

**Table 1-2: Comparison of Photovoltaic Devices [15]**

PV Cell Type	Laboratory Efficiency [%]
Single cell	23.1
Poly crystal silicon	18.0
Gallium arsenide	29.2
Thin film amorphous silicon	13.8
Thin film cadmium telluride	12.3
Thin film copper indium diselenide	14.1

Table 1-3: Laboratory efficiency of some PV cells [17]

### 1.1.6 Combined devices

A typical PV module converts 4 – 17 % of the solar radiation into electrical energy. The portion of the solar radiation which is not converted to electrical energy will be converted to heat, which results in an extreme cell working temperature. The main two negative consequences are a drop in the cell efficiency and a probable permanent structural damage due to the thermal stress. Combination of a photovoltaic and thermal system results in production of both electricity and heat from one integrated system. Different examples and application were reviewed by T. T. Chow [19] where the calculated thermal efficiency of the systems under investigation was in the range of 45 – 70%. One interesting example of such a device is combining TPV and solar assisted heat pump (SAHP) systems by direct coupling of a TPV panel to a heat pump. The TPV panel is designed for direct expansion of the refrigerant. This has been seen as an alternative approach for achieving higher temperature of hot water supply and a better PV cooling.

Liquid refrigerant vaporizes at the tubing underneath flat-plate collector which is now the TPV evaporator [19].

### **1.1.7 Photosynthetic power cells (PSC)**

Another category of small-scale power generating devices which needs to get more attention is PSC. It is very similar to fuel cells from some points of view however there are some major differences and advantages compared to fuel cells, solar cells and other devices mentioned earlier. Main differences and the advantages of PSC are mentioned below. In order to better understand the progress and developments of PSC during different periods of time, the main mechanism as well as the history of electrochemical cells will be described.

As appears from the device's name, Micro Photosynthetic Power Cell utilizes the light energy through bio-chemical processes performed by micro-organisms. Summary of PSC is given below.

- The device is similar to fuel cells; however no fuel is required.
- Since no fuel is required, the difficulties regarding supply and exhaust are not of concern.
- Like the solar cells PSC is operated under illumination; however unlike the solar cells it is able to produce electrical energy in the dark as well, resulting in continuous dual functionality.
- Due to the dual functionality of the device and its effect on the micro-organisms, PSC is considered as a self-restoring device.

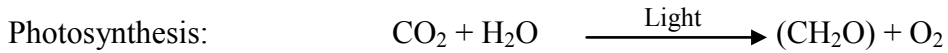
- Since live cultures are used for photosynthesis, PSC is considered as a bio-system. Nowadays bio-systems are getting a lot of attention due to the environmental impacts and pollution issues.
- Unlike some of the devices mentioned earlier, there are no moving parts involved in PSC. Consequently wear is of no concern.
- Unlike for the solar cells and some other devices, thermal stress is not an issue in PSC.
- Fuel cells generally require a higher operating temperature comparing to PSC.
- Geometry and material selection are not as sophisticated as for other photovoltaic devices.
- Like some other mentioned devices, PSC is modular and can be sized to meet particular demands.
- Low operating and maintenance cost

It is to be mentioned that PSC is still at a preliminary stage of development. That is why the results and outputs are still not comparable to solar cells or systems which have been under development for decades. The factors which make it quite interesting for researches are its advantages compared to other devices mentioned above.

## **1.2 Energy conversion mechanism**

Photosynthetic power cells (PSC) convert solar energy to electricity through biochemical processes occurring in different micro-organisms. However, unlike the solar

cells, PSC is able to produce power in dark as well and unlike the fuel cells there is no fuel required in PSC. The operation of the device is based on photosynthesis and respiration which are processes with opposite direction. That is how the dual functionality of PSC and its self-restoring operations are explained.



Details will be explained in another Chapter 2 where the focus is on biological points and issues. However, it is useful to mention that both photosynthesis and respiration involved electron transfer chains. In PSC these electrons are diverted to pass through an external circuit [25,42].

## 1.3 Principles of operation

### 1.3.1 The Device

The device consists of two identical half cells. That is because the anode and cathode in  $\mu\text{PSC}$  are interchangeable. The device is covered with glass covers on both sides and in between the two compartments there is a layer of sulfonated copolymer called Nafion that serves as Proton Exchange Membrane (PEM). The chambers at either side of the membrane just between the glass covers and the electrodes are for anolyte and catholyte solutions, respectively. Schematic of the device is shown in Figure 1-2.

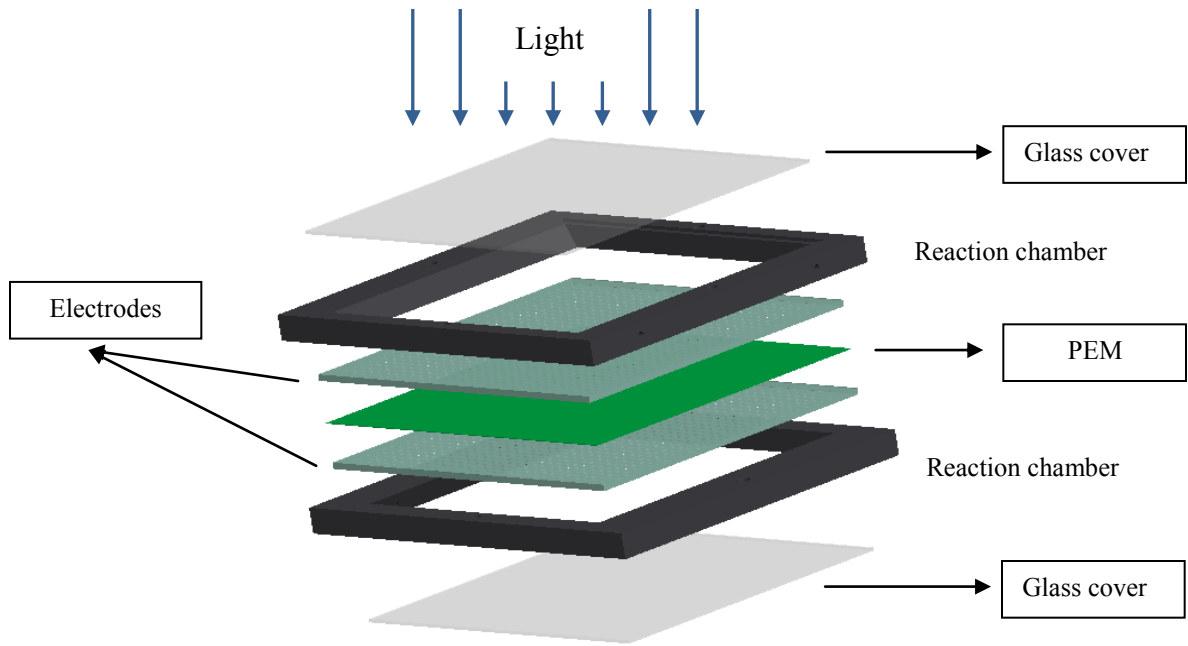
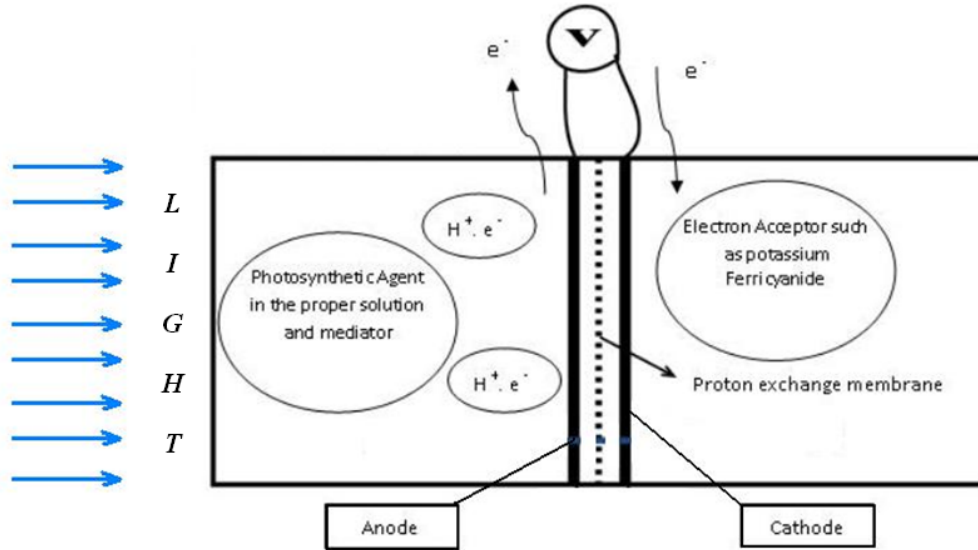


Figure 1-2: Schematic of  $\mu$ PSC

The fabrication of these main components is one of the main differences between this work and the previous ones. This will be discussed in details in the following chapter where each component is explained separately. One of the main differences to be mentioned is that unlike in all the previous works which were about silicon based devices, the device developed in this work is a polymer-based MEMS device.

### 1.3.2 The Mechanism

The operation of the device can be visualized with the help of Figure 1-3.



**Figure 1-3: Operation of  $\mu$ PSC**

In the anodic compartment, a photosynthetic micro-organism is suspended in a mediator solution. The mediator is selected such that it is able to oxidize NADP or NADPH and in turn can be oxidized by the anode (gold electrode) [20]. In the presence of light, the live culture captures the photon energy. As a result, H<sub>2</sub>O molecules will be oxidized. The electrons will be transferred along the electron transfer chain and eventually participate in oxidation of NADP. The released electrons travel through an external circuit. Concomitantly, the electron transport induces a pH gradient which is balanced by the proton exchange membrane (PEM). PEM is a polymer electrolyte membrane with a specific behavior. It is designed to conduct positive ions while it is impermeable to gases. That is why it is serving as a separator of the two compartments while being a barrier for the electrodes and a path to facilitate protons exchange [21,23].

During respiration – occurring in dark – a reverse process which also involves electron transfer takes place. The sugars accumulated during the light phase are

consumed and part of energy is again converted to electricity. That is why  $\mu$ PSC is able to produce electricity both under illumination and in the dark which counts as an advantage of  $\mu$ PSC comparing to the other devices of the same category.

It is generally assumed that photosynthesis occurs in the presence of light while respiration happens in dark. More precisely, some degree of respiration (depending on light intensity, temperature, etc) always occurs under illumination as well but photosynthesis is the predominant process. Hence, generally photosynthesis and respiration are called the main reactions in light and dark, respectively. The proportion and contribution of the two reactions to the power generation in light however, is not exactly known and requires further investigations.

As will be discussed in the next chapter, the micro-organisms contain the light capturing pigments which are mostly chlorophyll. The use of mediator and the oxidant optimal for a particular micro-organism used in the cell is one of the factors which should be considered for optimization of the device. On the other hand, in order to increase the performance of the device, electron and ionic transfer should be facilitated by optimizing components such as: electrodes, PEM and the external circuit.

## **1.4 History**

First Microbial Fuel Cell (MFC) was reported by K. Plotter [24] and involved generating electrical energy from living cultures with the aid of platinum electrodes. This was however neglected until 1931 when Cohen brought Plotter's MFC back to life. The operational principle of Plotter's MFC is extraction and transfer of electrons from cells to the anode electrode. The redox potential difference between dissimilar solutions (anolyte

– catholyte) causes the electrons to travel from anode to cathode via the external circuit. When live cell cultures are used in the anodic compartment, the mediators penetrate the cells and interact with the reducing agents in the cell. Consequently they become reduced themselves. This (as well as water-splitting reactions) releases protons which travel through a proton selective membrane due to the resulting proton gradient [24,25].

One of the early practical studies of PSC goes back to late 1970s when M. Allen and A. Crane [26] demonstrated a photosynthetic power cell with isolated thylakoids. So far, some people utilized live whole-cell photosynthetic organisms. However, some other experiments have been performed in which subcellular photosynthetic components have been utilized [20-40]. One of the earliest works of this type was that performed by E. Gross *et al* [40] in early 1980s.

In 1978, M. Aizawa [27] used chlorophyll with platinum electrodes and an alkaline solution. He tested chlorophyll with an acid solution as well. A positive potential shift was observed by using MnChl in a PSC.

A. Drachev and A. Jasaitis [28,29], K. Pakham and P. Mueller [30,31] isolated the reaction centers and performed their tests with certain redox mediators. Their measurements indicated a potential of 0.2 V approximately.

In 1980, A. F. Janzen [32] described photoelectrochemical conversion using reaction center electrodes and isolated reaction center-functionalized and utilized them as a film on SnO<sub>2</sub>. An open circuit voltage (OCV) of 0.08 V with a current density of 0.5  $\mu\text{A}/\text{cm}^2$  was observed.

In 1985, K. Tanaka *et al* [33,34] utilized Cyanobacterium *Anabaena* as the photosynthetic agent and HNQ (2-hydroxy-1,4-naphthoquinone) as the redox mediator. Measurements both in dark and light were reported.

In 1993, T. Yagishita *et al.* [35-37] performed tests with various micro-organisms in various PSCs in which they used HNQ as the mediator. The open circuit voltage test resulted in an output of 800 mV. When they performed the experiments with external load, they found a current density of 320  $\mu\text{A}/\text{cm}^2$ . They also tested cycles of light and dark and observed conversion efficiencies varying from 0.2 % to 3.3 %. In 1997 to 1999 they studied the influence of different parameters such as concentration of the micro-organism, effect of light intensity and glucose addition to the cells [38,39].

Use of isolated chloroplast with various mediators by W. Haehnel and *et al* [41] yielded OCV of 220 mV and 16  $\mu\text{A}/\text{cm}^2$  current density.

In 2003, K. Lam *et al.* [42] fabricated a PSC. They performed measurements with a 10 ohm load both in dark and light and obtained current and power densities of 30  $\mu\text{A}/\text{cm}^2$  and 61  $\mu\text{W}/\text{L}$ , respectively. The measured open circuit voltage was 400 mV.

In one of the recent works in 2006, M. Chiao *et al.* [22] used bulk silicon micromachining technology for fabricating the compartments of the PSC. They used two different micro-organisms – baker's yeast (*Saccharomyces Cerevisiae*) and blue green algae (Phylum Cyanophyta). More precisely, the former led to a microbial fuel cell (MFC) and the latter led to a photosynthetic power cell (PSC). The measured power density was 2.3  $\text{nW}/\text{cm}^2$  and 0.04  $\text{nW}/\text{cm}^2$ , respectively. This was measured with 10 ohm load and resulted in OCV of 300-400 mV.

Just a month later, another work was published by K. Lam *et al* [21]. They calculated a theoretical maximum current density of  $9.6 \text{ mA/cm}^2$  under illumination of  $2000 \text{ } \mu\text{mol photons/m}^2/\text{s}$ . However what they measured was only  $1 \mu\text{A/cm}^2$ . The measured values for OCV in light and dark were 470 and 330 mV respectively which are comparable to those for the other micro fabricated fuel cells.

In this work live whole-cell photosynthetic organisms are utilized.

## **1.5 Thesis motivation**

Green energy is a topic receiving lots of attention and investment these days. As the fossil fuels are coming to an end, more and more attention is given to renewable energy sources and new and appropriate energy harvesting devices. Photosynthesis has been vital for the development of life on this planet and its efficiency and reliability suggest it may be beneficial to harness it. This work is an attempt to propose, fabricate and test a Micro Photosynthetic Power Cell using green algae as the photosynthetic agent. It also tries to optimize fabrication parameters and suggest some optimal environmental and operational conditions.

## **1.6 Thesis objectives and scopes**

Objective of this thesis is to develop a micro scale power generation device by fabricating an appropriate energy harvesting device – Micro Photosynthetic Power Cell – utilizing algal photosynthesis. Simple and low-cost fabrication providing flexible geometry to be used in various applications is to be considered in the proposal. The specific objectives of the proposed research are:

1. Literature review on energy harvesting devices and technologies

- a. Sources, small scale power generating devices, technologies, advantageous and disadvantageous and comparisons
  - b. History of electrochemical cells and operational principle of photosynthetic electrochemical cells
2. Studying photosynthesis and respiration
- a. processes and mechanisms, photosynthetic agents and light harvesting pigments
  - b. Photochemical conversion of solar energy, electron transport chain and affecting parameters
3. Designing, fabrication and development of a Micro Photosynthetic Power Cell
- a. Studying the influence of each component and proposing modifications with the aim of performance optimization
  - b. Proposing materials and processes involved in the fabrication
  - c. Testing each component and the final assembly for functionality
  - d. Design parametric study
  - e. Testing the proposed Photosynthetic Power Cell for performance
  - f. Proposing optimal fabrication and operational parameters based on the experiments

## 1.7 Organization of the thesis in manuscript-based format

This manuscript-based thesis is organized in seven chapters. In the present chapter, a brief introduction to energy harvesting devices and technologies,  $\mu$ PSC's operational principles and history, the motivation, the scope and objective of this thesis are presented. Chapters three and five are based on manuscripts prepared for journal publications. These chapters are organized in a cohesive manner to address the objectives of the thesis defined in section 1.6 and formatted according to "Thesis Preparation and Thesis Examination Regulations (version-2011)" of the School of Graduate Studies at Concordia University. In the duplicated articles, sections, figures, equations, and tables are numbered according to the thesis preparation regulations. A single comprehensive reference list rather than reference lists for individual papers is presented in the Reference section. Conclusions of the thesis and the future recommendations are presented in chapter 7.

Chapter 2 presents a brief discussion on photosynthesis and the affecting parameters. This chapter covers the objectives 2-a and 2-b of the thesis defined in section 1.6.

Chapter 3 is based on the following manuscript prepared for SPIE journal of micro/nanolithography, MEMS and MOEMS (JM<sup>3</sup>) and patent submitted – *Scalable Polymer Based Power Cells using Photosynthesis.*

*M. Shahparnia, M. Packirisamy and Philippe Juneau, "Low stress microfabrication of electrode integrated proton exchange membrane for polymer based photosynthetic power cell"*

This chapter covers the objectives 3-a to 3-c of the thesis defined in section 1.6.

Chapter 4 presents experimental setup, measuring systems and the proposed parametric study. This chapter covers the objectives 3-d of the thesis defined in section 1.6.

Chapter 5 is based on the following manuscript prepared for publication in the IEEE/ASME Journal of Microelectromechanical Systems (JMEMS).

*M. Shahparnia, M. Packirisamy, P. Juneau and V. Zazubovich, “Effect of Proton Exchange Membrane Electrode Configuration and Parametric Study on the Performance of Micro Photosynthetic Power Cell ( $\mu$ PSC)”*

This chapter covers the objective 3-d and 3-f of the thesis defined in section 1.6.

Chapter 6 includes additional experiments which were carried out with alternate photosynthetic bio-organisms.

Chapter 7 presents conclusions and summary of the thesis along with future recommendations.

## **Chapter 2**

# ***Photosynthesis***

## 2 Photosynthesis

This chapter covers the objectives 2-a and 2-b of the “Objective and scope of the thesis” in Section 1.6.

### 2.1 Basics of photosynthesis

Photosynthesis is conversion of light energy to chemical energy by living organisms. The name photosynthesis comes from the Greek words: “photo” meaning light and “synthesis” meaning putting together. It is a complex process taking place in higher plants, phytoplankton and bacteria with some minor differences. In green plants, algae and Cyanobacteria, water and carbon dioxide are required as the raw materials. Photosynthesis splits water to liberate O<sub>2</sub> and uses energy ultimately originating from sunlight to fix CO<sub>2</sub> into sugar. Accumulation of oxygen in atmosphere enables living creatures to consume the photosynthesized foods and derive energy from them by respiration – process in which organic compounds are oxidized back to carbon dioxide and water.

Description	kcal (1 kcal = 1.162 Watt hours)
Annual fall of sunlight energy on the earth’s surface	1.2 e 21 (1.4 e 18 kWh)
Reflected fraction by atmosphere	4x10 <sup>20</sup>
Absorbed fraction by atmosphere (this powers many processes at the earth’s surface such as winds, ocean currents, hurricanes, etc)	2x10 <sup>20</sup>
Fraction falling onto oceans	4.2x10 <sup>20</sup>
Fraction falling onto the lands	1.8x10 <sup>20</sup>
Estimated energy stored by green plants and algae	6x10 <sup>17</sup>
Annual electric power consumption per capita (2008) [44]	2.5x10 <sup>5</sup> (2874.6 kWh)

Table 2-1: Available and utilized solar energy [43]

Table 2-1 presents a general idea about the available solar energy and the amount actually utilized as well as the portion involved in photosynthesis in particular. According to the above table, it appears that the efficiency utilized by photosynthesis is less than 0.3%.

Absorption of light is performed by the so called “light harvesting pigments”. A pigment is any substance that absorbs light. The color of the pigment is determined by the wavelengths of the light reflected. There exist various light harvesting pigments with different absorption spectrum. The absorption spectrum of the pigment also depends on its local environment. For example, pure chlorophyll in dilute solutions displays a simple absorption spectrum with relatively narrow bandwidths. Absorption bands of chlorophyll *in vivo* are usually displaced to longer wavelengths as a result of being bound to protein and the bands are also much broader. Primarily, plants absorb light using pigment chlorophyll, which is the reason that most plants have a green color [43].

Leaf is the main site of photosynthesis in plants. Hence different forms and orientations of leaves can be found due to the environmental conditions and photosynthetic requirements of the plant such that optimal photosynthetic rate is achieved. For simplicity, photosynthesis processes are often explained considering higher plants. Figure 2-1 presents schematics of a leaf structure.

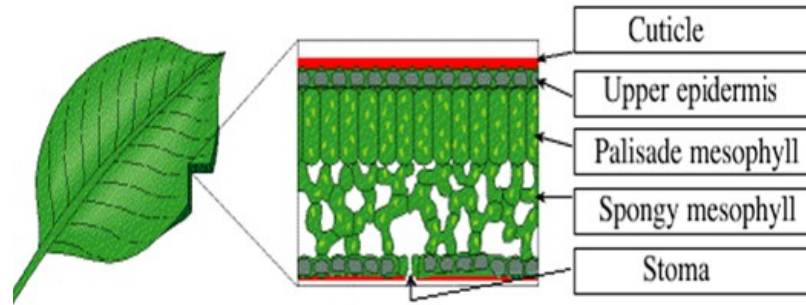


Figure 2-1: Leaf structure [45]

This can be broken down further by having a closer look at mesophyll cells containing chloroplasts as presented in Figure 2-2. Going even further, chloroplast structure is presented in Figure 2-3.

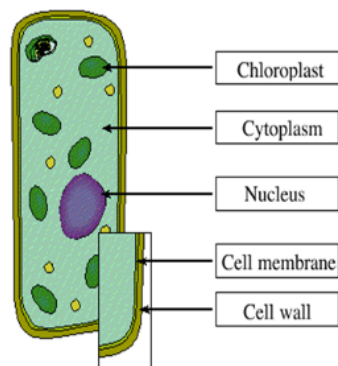


Figure 2-2: Mesophyll cell structure [45]

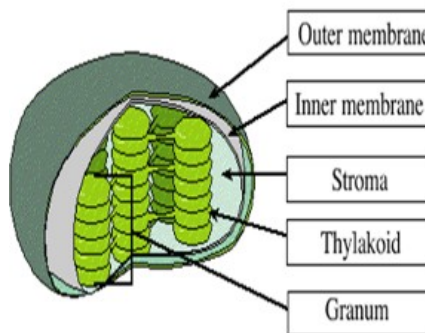


Figure 2-3: Chloroplast structure [45]

Main species used in this work is green algae (*Chlamydomonas reinhardtii*, strain CC125). Figure 2-4 is a closer look at the structure of this single-celled species.

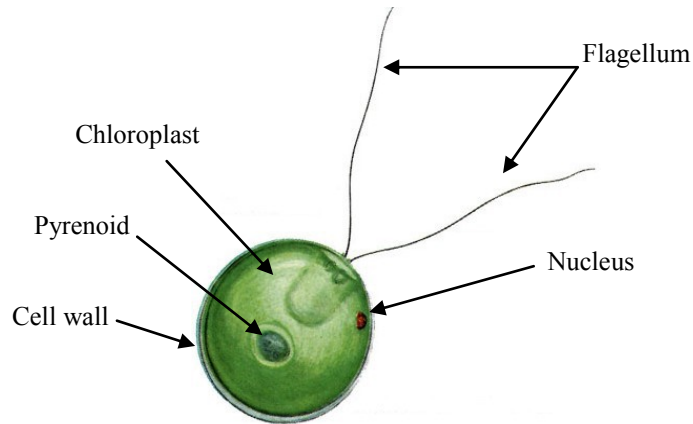


Figure 2-4: Schematic presentation of algae structure – Green algae, *Chlamydomonas reinhardtii*, strains CC125

[46]

This is a single-celled organism present in ocean, fresh water, soil and even mountain tops. It is approximately 10 micron in diameter, swims around with two anterior flagellums and senses the light by its nucleus. Pyrenoid located within the chloroplast is the center of carbon fixation [46].

The reactions related to carbon fixation can be classified into light and dark reactions discussed below.

## 2.2 Light and dark reactions

Visible light drives photosynthesis. Solar energy is composed of electromagnetic energy that travels through space. The shorter wavelength, the greater is the energy for each unit (photon) of electromagnetic radiation. Not all wavelengths of light can support photosynthesis. Depending on the accessory pigments involved, non-absorbed part of the light spectrum is what gives photosynthetic organisms their color and is the least effective for photosynthesis in the respective organisms. The action spectrum of

photosynthesis is the relative effectiveness of different wavelengths of light at inducing various reactions.

If a pigment absorbs light energy, one of the following three things may occur: energy is dissipated as heat; the energy may be emitted immediately at a longer wavelength, a phenomenon known as fluorescence; or energy may be transferred non-radiatively between the pigments and trigger a chemical reaction as in photosynthesis [43]. Due to that energy transfer a part of energy of the higher excited states dissipates as heat to the surroundings through vibration.

Photosynthesis occurs in two stages: light dependent or photosynthetic reactions and light independent or dark reactions known as Calvin-Benson cycle. In the former, the light energy is captured and used to produce high energy molecules whereas in the dark reactions these high energy molecules are used to power the process of capturing carbon dioxide and making carbohydrates. Light (photon) is absorbed by a molecule when the provided frequency of incident light meets the criteria:

$$h.\nu = h.c/\lambda = \Delta E \quad (2.1)$$

Where:

$\Delta E$ : energy level difference between the initial (ground) and final (excited) states

$\nu$ : frequency

$\lambda$ : wavelength

$c$ : velocity of the light

$h$ : Planck's constant

Absorption of light is understood to produce a primary photochemical charge separation between a chlorophyll (or group of chlorophylls) acting as primary electron

donor and the primary electron acceptor, resulting in the reactions going through a series of intermediate electron-transfer steps [43,47-50].

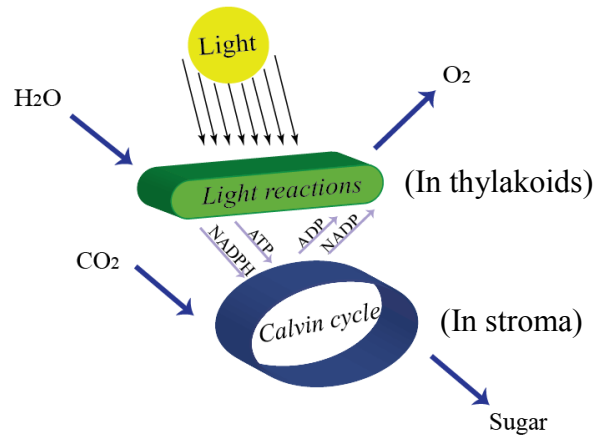


Figure 2-5: Higher plant photosynthesis: Light and dark reactions [51]

Passing through some stages, the electron transport chain starts leading to the ultimate reduction of NADP to NADPH<sup>+</sup>. The chlorophyll regains the lost electron by taking one from a water molecule through a process called photolysis which releases oxygen.

In the dark reactions, enzymes capture CO<sub>2</sub> and 3-carbon sugars are released, which are later combined to form sucrose and starch. Equation 2.2 presents the general photosynthesis process followed by Equation 2.3 a more detailed explanation of light dependant reactions.



Sunlight and oxidation-reduction reactions are the two sources of energy for living organism. Products of the light dependent reactions are: ATP (adenosine

triphosphate) from photophosphorylation (production of ATP using the energy of sunlight) and NADP (Nicotinamide adenine dinucleotide phosphate) from photoreduction (reduction reaction taking place in presence of light, adding an electron to a photoexcited species).

ATP, ADP, NADPH and NADP are coenzymes used in cells for intercellular energy transfer. They are oxidized or reduced in a cyclic manner to form one another.

Figure 2-6 illustrates the products of light and dark reactions.

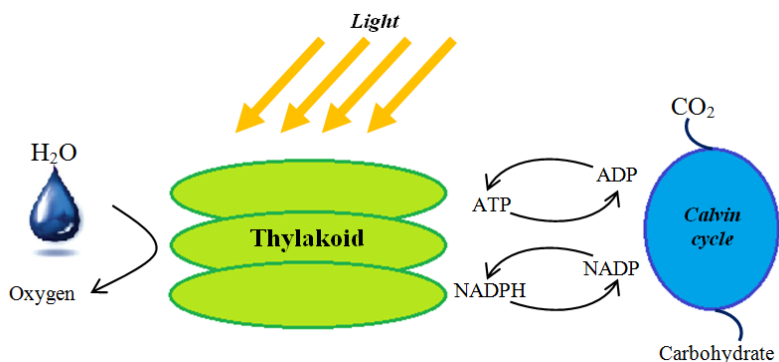
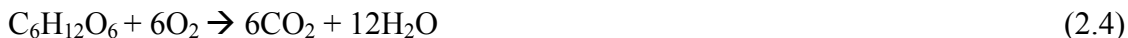


Figure 2-6: Products of light and dark reactions

### 2.3 Photosynthesis and respiration

Photosynthesis and respiration are reversible chemical reactions, meaning that the products of one process are the reactants of the opposite process. Hence cellular respiration is the opposite of photosynthesis. Glucose or other carbohydrates oxidise to produce carbon dioxide, water and chemical energy. Photosynthesis was already mentioned by Equation 2.2. Below is the corresponding cellular respiration reaction.



Glucose + Oxygen → Carbon dioxide + Water

As mentioned earlier, both photosynthesis and respiration are involve electron transport chains. That is why PSC can be operated in either light or dark conditions. However for best efficiencies and maximum lifetime of the device, cycles of light and dark conditions are suggested which restores the organisms as well.

It was also mentioned that the concept of photosynthesis is the same even though there are slight differences comparing different species. Algae come in different forms. Although they are not as complex as plants, the biochemical process of photosynthesis is the same. Very much like plants, algae have chloroplast and chlorophyll is the main pigment, but various accessory pigments are not present in algae. Photosynthetic bacteria do not have chloroplast. Instead photosynthesis takes place directly within the cell. Cyanobacteria contain thylakoid membranes very similar to those in chloroplast and are the only prokaryotes that perform oxygen generating photosynthesis. Most of the time photosynthetic process uses water and releases oxygen. However, some photosynthetic bacteria don't produce oxygen. Some bacteria oxidize hydrogen sulphide instead of water producing sulphur as waste [43,47-49].

## **2.4 Photosystems and light harvesting complexes**

Light-driven primary processes of photosynthesis occur in two main photosynthetic complexes, Photosystem I (PSI) and Photosystem II (PSII). All photosystems have similar design with some minor variations. They are composed of three major components: the reaction center that carries out photochemical charge separation and electron transport, the core antenna or inner antenna consisting of pigment proteins that are an integral part of the reaction center complex, and the peripheral or outer antenna. The energy-transfer pathway is from the peripheral antenna complex to the inner antenna

and finally to the reaction center. Some examples of the core and peripheral antenna of different species are mentioned in Table 2-2 (Letter “B” indicates “Bulk pigment” and the number in front refers to the absorbance wavelength [43].)

Photosynthetic bacteria	Peripheral antenna (LH2)	Core antenna (LH1)
Rhodospirillum rubrum		B890
Rhodopseudomonas viridis		B1015
Rhodobacter sphaeroides	B800-850	→ B875
Rhodobacter capsulate		
Chromatium vinosum	B800-820	→ B800-850 → B890
Rhodopseudomonas acidophila		

**Table 2-2: Core and peripheral antenna complexes of some photosynthetic bacteria [43]**

There exist two types of light-harvesting complexes. The longer wavelength-absorbing “core” (or inner or proximal) antenna, also known as light-harvesting complex 1 (LH1) which is present in all photosynthetic bacteria and is intimately associated with reaction center. The shorter wavelength-absorbing peripheral or distal complexes known as light-harvesting complex 2 (LH2), associated with the peripheral antenna.

The antenna complexes transfer absorbed light energy along a gradient of excitation energy extending from the outermost, shorter wavelength complex toward the reaction center. Unlike the core antenna, which is present in a fixed stoichiometry relative to the reaction center, the relative number of chlorophyll molecules in the peripheral antenna may vary as a result of adaptation to the environmental conditions such as light and temperature, enabling the organism to regulate the amount and size of the

photosynthetic units. Figure 2-7 is a schematic presentation of light harvesting complexes of different species.

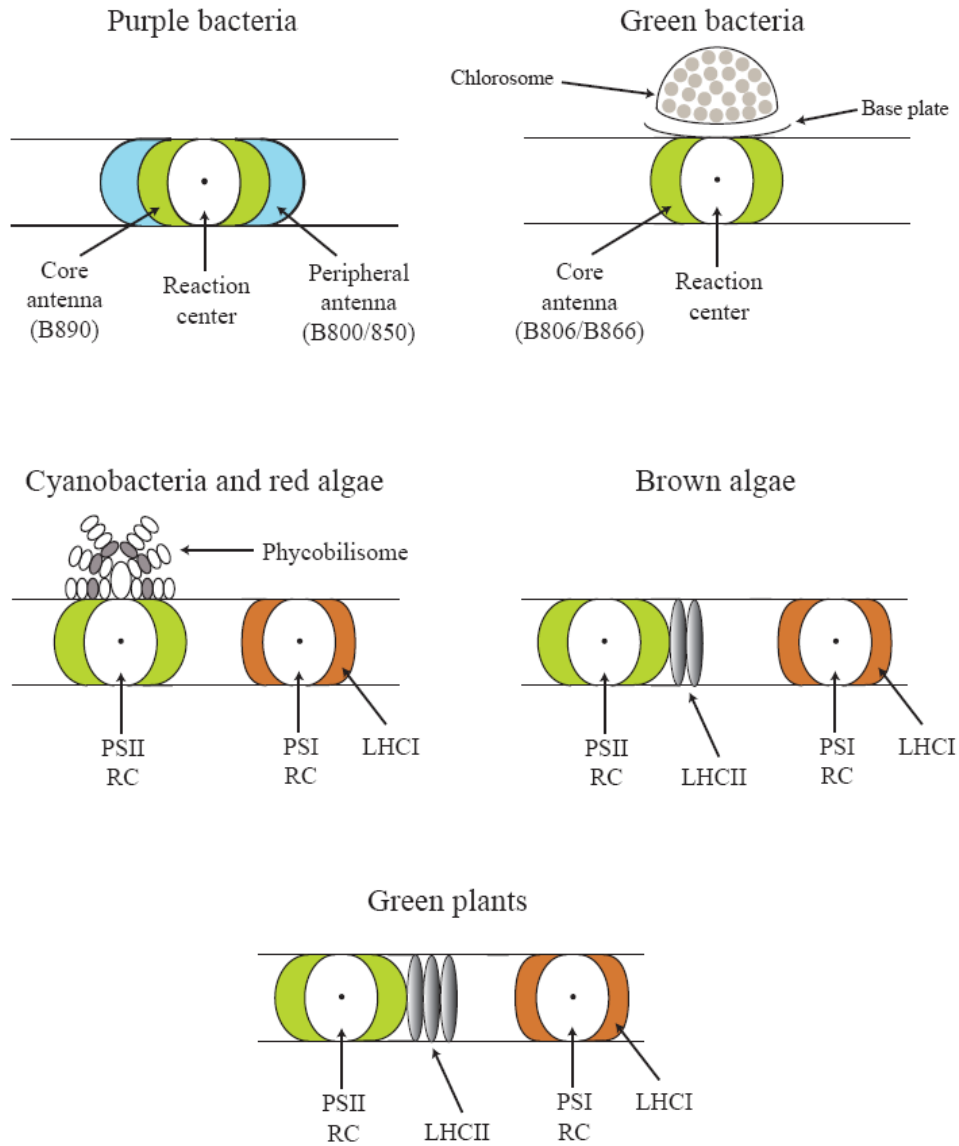


Figure 2-7: Schematic presentation of light harvesting complexes of some species [43]

Besides the major light harvesting pigments, there are two classes of accessory pigments namely carotenoids and phycobilins which absorb light in the wavelength regions where the major light harvesting pigments do not absorb strongly. Carotenoids and phycobilins

are present in photosynthetic organisms including higher plants, algae, and photosynthetic bacteria.

Light harvesting complexes that drive photosynthesis are present in diverse forms. In prokaryotic cyanobacteria (blue-green algae) and eukaryotic red algae, light harvesting is carried out in the main by supramolecular assemblies called phycobilisomes (PBS) which are attached to the stroma surface of the photosystem II core in thylakoid membrane. Each PBS consists of a group of colored phycobiliproteins (PBP) each of which in turn contains covalently bonded pigments or chromophores called phycobilins (PB). The primary function of this remarkable light-harvesting apparatus is to allow the organism to survive in weak light conditions. As green and yellow light is transmitted unattenuated through great depth of water where the organisms reside, PBS possess the particular ability to absorb photons in these spectral regions where light is only weakly absorbed by chlorophyll, and funnel this absorbed energy to the PS II reaction centers with efficiencies greater than 95 %.

Photosystem II: Light reactions taking place in photosynthetic reaction centers depend on a supply of light energy harvested by a number of antenna chlorophyll-protein complexes. Basically, there is a core antenna complex closely associated with the reaction center, plus some slightly more distant, peripheral antenna complexes. Photosystem I: It has been characterized as the long wavelength system, in contrast to PSII as it can be activated by light having wavelengths greater than 690 nm. PSI consists of a reaction center core complex (CCI) and a light harvesting complex (LHCI). Main function of PSI is the photo-induced reduction of ferredoxin by plastocyanin, itself being reduced by PSII [43-48,52].

## 2.5 Electron Transfer in photosynthesis and respiration

Electron transfer or moving of electrons from one site to another is among the most common chemical processes. However, it is one of the most critical and sophisticated processes to be studied. Figure 2-8 illustrates the electron transport chain in photosynthesis followed by the electron transport chain in respiration in Figure 2-9.

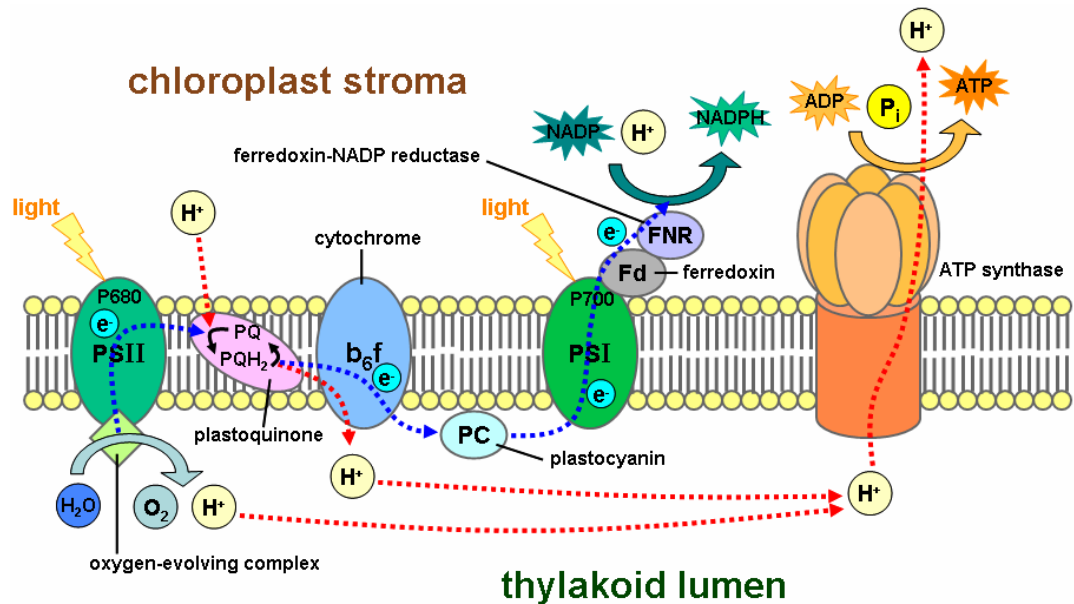


Figure 2-8: Electron transport chain in photosynthesis [51]

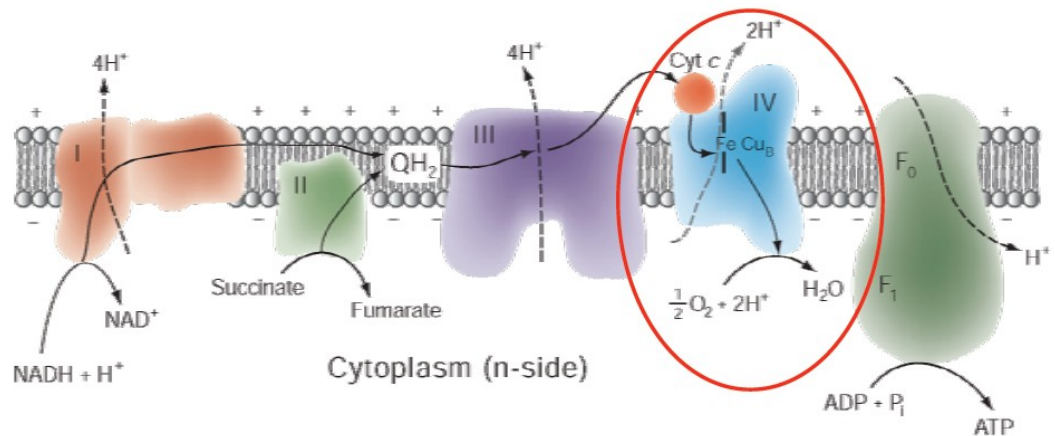


Figure 2-9: Electron transport chain in respiration [53]

Both photosystem I and photosystem II consist of multiple protein subunits, most of which are embedded in the thylakoid membrane. As mentioned earlier, in the light reactions in photosystems one electron is released per one photon absorbed. The released electron goes through several stages involving various *electron donors and acceptors*. The primary electron donor in photosystems is often called “special pair”. The term “primary electron donor” signifies that it is the first species undergoing a charge separation following the absorption of a photon of energy by the antenna pigment. Upon charge separation in Photosystem II reaction center, the excited primary donor loses an electron to the adjacent primary electron acceptor ( $Q_A$ ) and thus becomes oxidized. This is a several-step process.  $Q_B$  is a secondary electron acceptor in the sense that it receives electrons from the “stable” primary electron acceptor  $Q_A$ .

The primary photochemical charge-separation process requires that there is a reaction partner to accept the electron released by the primary donor. A so called “open” reaction center requires the primary electron donor to be in reduced state and the primary electron acceptor in the oxidized state. In other words, if the donor is already oxidized or the primary acceptor is already reduced, the reaction center cannot be photochemically active, and the reaction center is said to be closed. Therefore the extent of photochemical activity depends on the fraction of the donor initially present in the reduced state or of the acceptor initially present in the oxidized state.

PS II splits water into molecular oxygen, electrons and protons. Oxygen evolved is released to the atmosphere while the electrons and protons are used to reduce  $Q_A$  and  $Q_B$ . The latter is a mobile acceptor which carries electrons away. The proton release also creates an electrochemical trans-membrane gradient which is used to drive ATP

synthesis. Photosystem I undergoes redox reactions by using the electrons transferred from photosystem II to reduce  $\text{NADP}^+$ . The NADPH in turn provides the reducing power for  $\text{CO}_2$  fixation [43,47-49]. Transition metals such as copper and iron play leading roles in electron transport. Cytochromes are heme proteins<sup>1</sup> in which the four N-atoms of the heme are attached to an iron atom. These electron-transfer proteins are present in all biological organisms, including photosynthetic bacteria, green plants and algae.

## **2.6 Parameters affecting photosynthesis**

Rate of photosynthesis is affected by the concentration of carbon dioxide, intensity of light and temperature. One of the common ways to study these parameters in plants releasing oxygen is to measure oxygen and carbon dioxide content of the air in a closed experimental chamber.

### **2.6.1 Temperature**

The effect of temperature on photosynthesis is a very important consideration. Though the photochemical reaction is not dependent on the temperature, the rate of photosynthesis does increase with increasing temperature until an optimum value. Photosynthetic rate tends to flatten at about 25 °C as shown in Figure 2-10. Respiration however, continues to rise rapidly above this temperature. Respiration increases strongly with temperature and at temperatures above 35 °C all the produced food is used to support respiration [55-56]

---

<sup>1</sup> A heme protein (or hemoprotein or haemoprotein), or heme protein, is a metalloprotein containing a heme prosthetic group, either covalently or noncovalently bound to the protein itself. The iron in the heme is capable of undergoing oxidation and reduction (usually to +2 and +3, though stabilized  $\text{Fe}^{+4}$ ) [51]

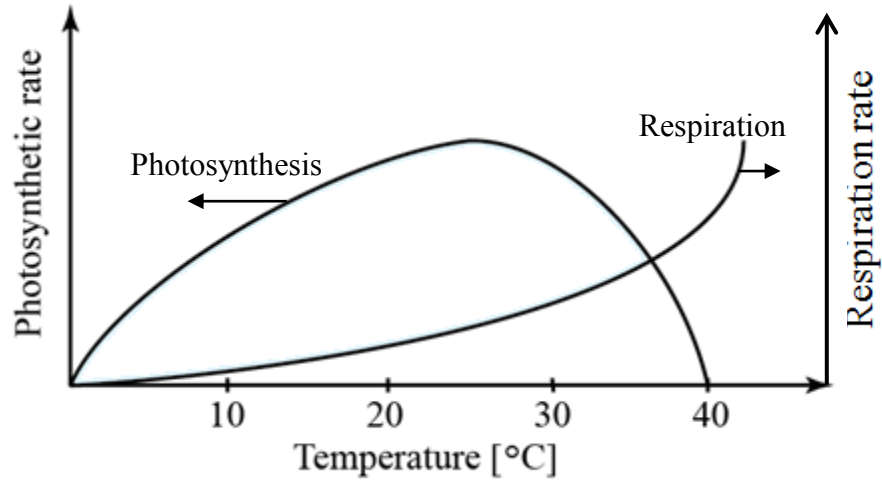


Figure 2-10: Schematic presentation of the effect of temperature on photosynthesis

J. P. Decker [55] studied the effect of temperature on photosynthesis and respiration. His studies were based on red and loblolly pines and he found that in many plants the most favourable temperature for photosynthesis is lower than that for respiration. Photosynthesis to respiration ratio (P/R) decreases with temperature above the optimum temperature for photosynthesis. Under illumination the main reaction occurring in plants is photosynthesis. However, respiration also occurs simultaneously. Once the temperature exceeds the optimal value for photosynthesis, respiration rate increases and causes a shift of carbohydrate balance in the plant. The decrease in photosynthesis rate is due to the fact that some plants close their vents in hot weather so that they do not lose water and protect the plant. It should be noted that if respiration is allowed to continue for too long it leads to deterioration and ultimate death of the plant.

J. P. Decker [55,56] studied photosynthesis and respiration at 20°, 30° and 40° C. Photosynthesis rate was approximately the same at 20° and 30° C and decrease of about 45% was observed when the temperature was increase from 30° to 40° C. Respiration rate

however was doubled when the temperature was increased from 30° to 40° C. P/R was about 13 at 20°, 6.8 at 30° and 3 at 40° C.

### **2.6.2 Light**

Plants only react to certain wavelengths and use specific energy to manufacture food through photosynthesis. Other wavelengths are not useful and sometimes even harmful to the plants.

The rate of photosynthesis is proportional to the light intensity received by plants up to a certain value. Above this level it results in excess heat and increases the temperature. The dividing line between day lengths favourable to vegetative growth and those to cause seed and flower formation is called the critical light period. For most species the critical light period is between 11 to 16 hours. The relative length of the daily light and dark periods controlling flowering of many kinds of plants is a phenomenon called photoperiodism [57].

Continuous running of electrochemical cell (under illumination) results in a decrease in current output of the cell. On the other hand, it was mentioned that long respiration period results in an ultimate death of the plant. Yagishita *et al* [58] studied the effects of light on current outputs in PSC. They obtained an increase in the current output when the light was switched off after certain amount of discharge time. Their results suggested periods of light and dark conditions for the optimal operation of PSCs.

P. Kramer and J. Decker [59] studied the relation between light intensity and rate of photosynthesis of loblolly pine and certain hardwood. They determined the rate of photosynthesis of their samples for one-hour periods at a constant temperature of 30° C

approximately. The variable parameter was light intensity from 300 to 10000 foot-candles. They concluded that lack of sufficient light for maximum photosynthesis can be considered as a significant failure factor in pine seedlings. However, some other species such as some hardwood seedlings were able to carry on relatively more photosynthesis in the shade and could develop more root systems.

Visible light spectrum is shown in Figure 2-11 [61]. Figure 2-12 shows the daylight spectrum [60] followed by the blue sky and red sunset spectrum in Figure 2-13. Depending on the photosynthetic samples absorbance wavelength varies. Absorption spectrum illustrates the portion of the light which is useful for photosynthesis. Hence, providing the required wavelength can support photosynthesis. This however as mentioned earlier is dependent on the type of plant, algae, bacteria and light harvesting pigments involved. Absorption spectrums of some species are demonstrated in Figure 2-14 as examples.

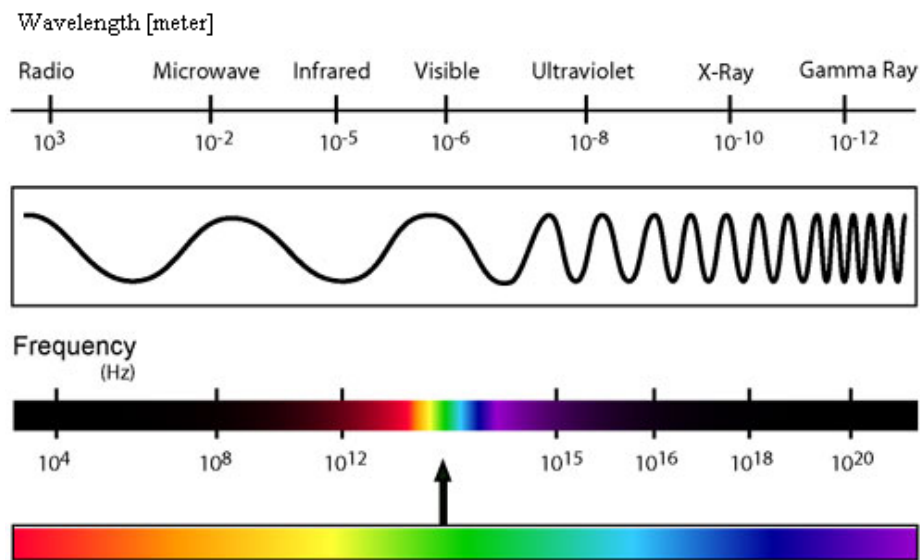


Figure 2-11: Electromagnetic spectrum [61]

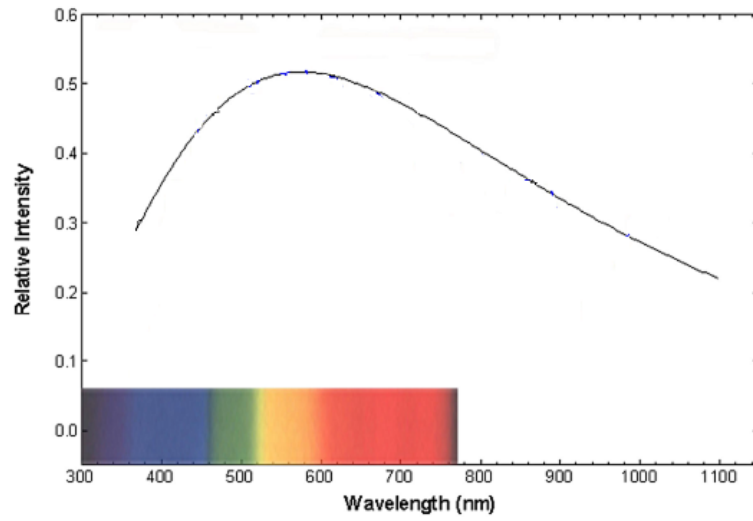


Figure 2-12: Daylight spectrum [60]

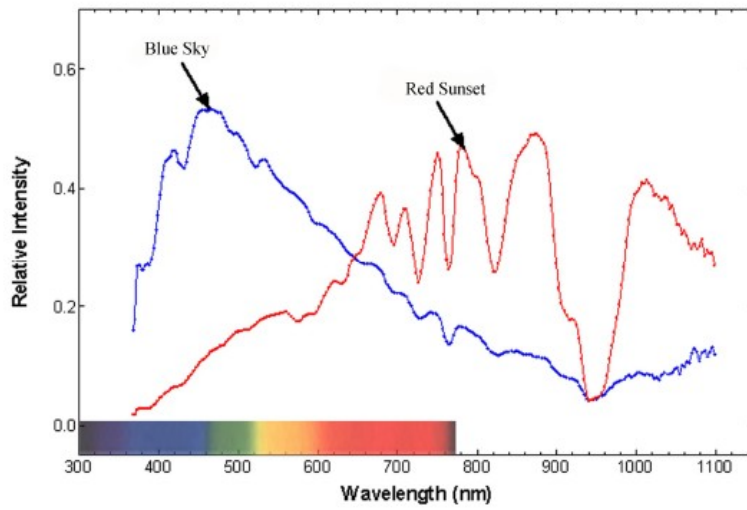


Figure 2-13: Spectrum of blue sky Vs red sunset [60]

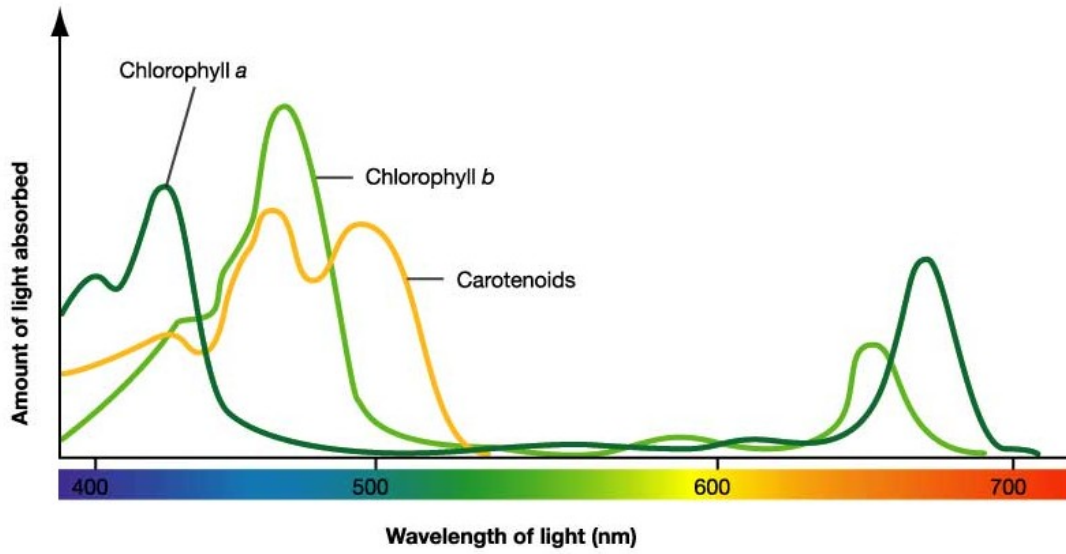


Figure 2-14: Absorption spectrum of Chlorophyll a, b and Carotenoids [60]

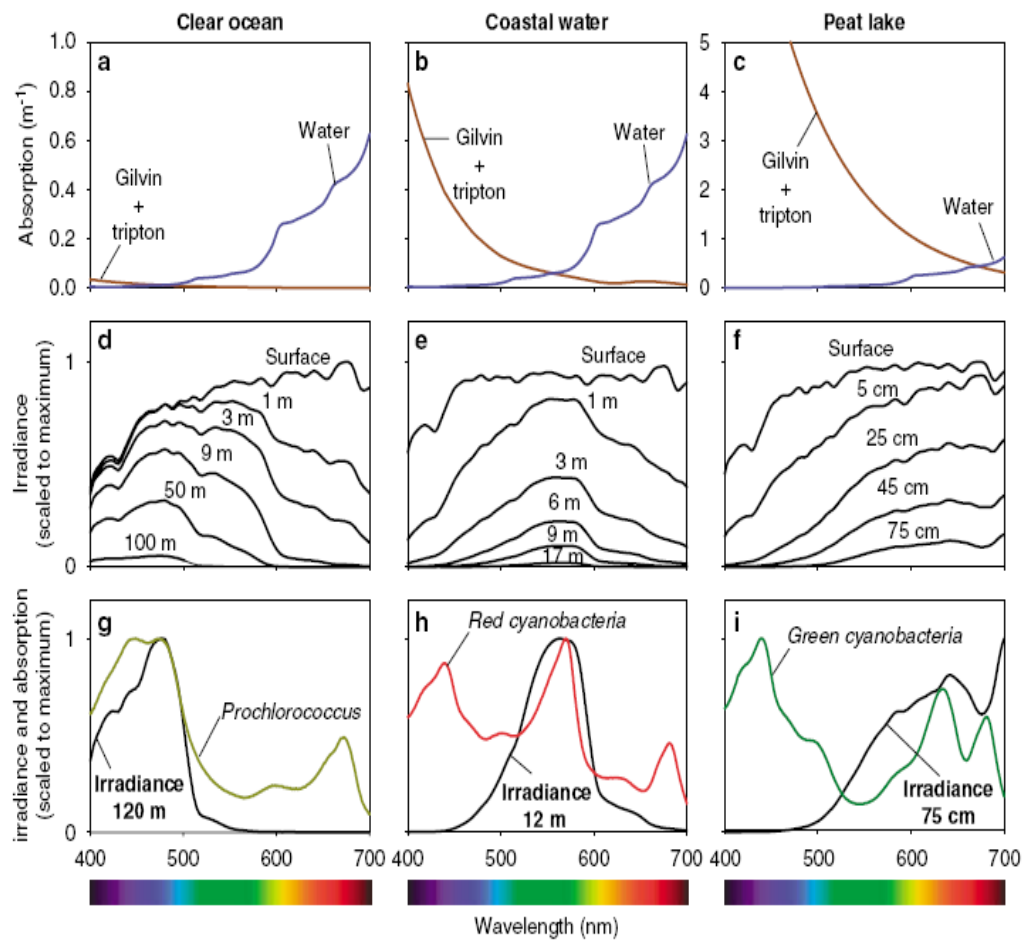


Figure 2-15: Underwater light spectra [62]

Figure 2-15 is the result of the study by M. Stomp *et al* [62] to find penetration of different wavelengths of light into water. Three locations are investigated as different water sources: Subtropical Pacific Ocean, Coastal waters of the Baltic Sea (near Gulf of Finland) and Lake Groote Moost (a Peat lake in Netherlands). It can be found that green light penetrates deep in the Baltic Sea, blue light into Pacific Ocean and red light in the Lake Groote Moost. Figure 2-16 demonstrates the absorption spectra of different species. The numbers in Figure 2-16 refers to the names and main photosynthetic pigments given in Table 2-3 [62].

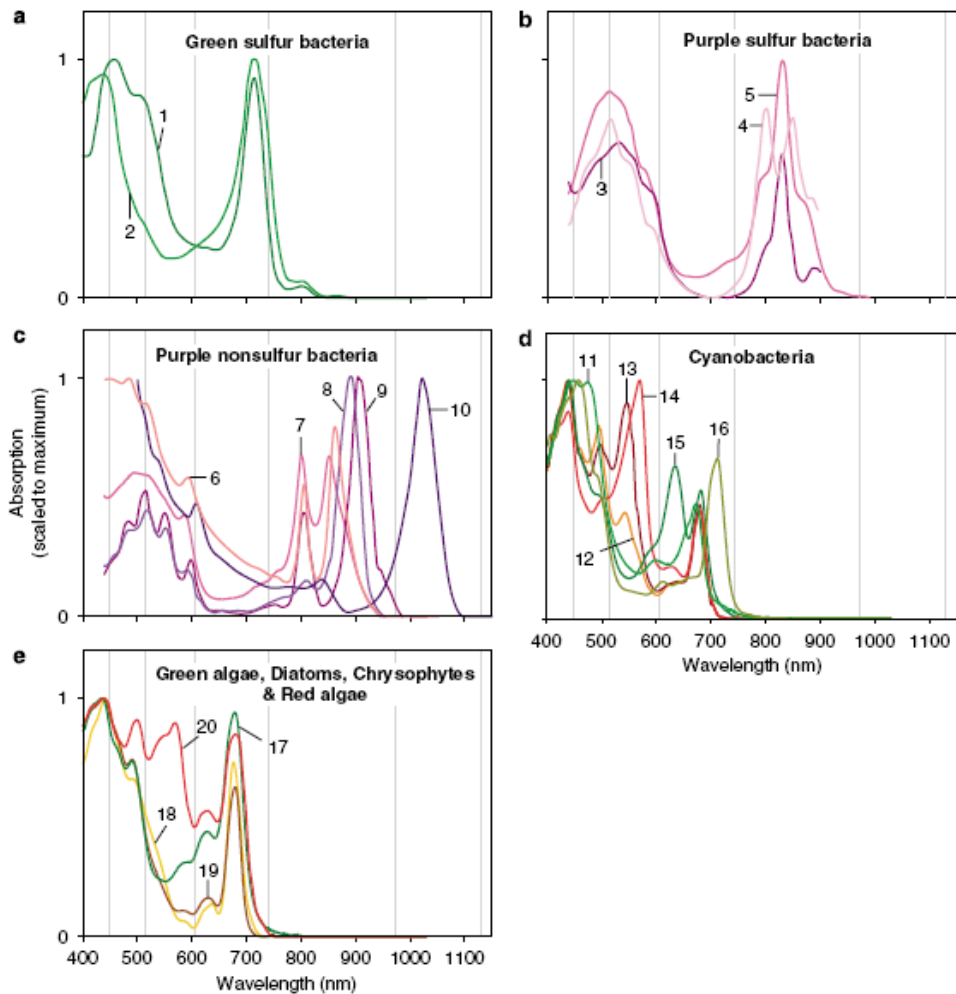


Figure 2-16: In vivo absorption spectra of intact cells of 20 phototrophic species [62]

<b>Number</b>	<b>Species</b>	<b>Main pigments</b>
<b>Green sulfur bacteria</b>		
1	<i>Pelodictyon phaeoclathratiforme</i>	BChl <i>e</i>
2	<i>Prosthecochloris aestuarii</i>	BChl <i>a, c</i>
<b>Purple sulfure bacteria</b>		
3	<i>Thiocapsa marina</i>	BChl <i>a</i>
4	<i>Thiocapsa roseopersicina</i>	BChl <i>a</i>
5	<i>Chromatium okenii</i>	BChl <i>a</i>
<b>Purple non-sulfur bacteria</b>		
6	<i>Rhodobacter capsulatus</i>	BChl <i>a</i>
7	<i>Rhodobacter sphaeroides</i>	BChl <i>a</i>
8	<i>Rhodospirillum rubrum</i>	BChl <i>a</i>
9	<i>Roseospirillum parvum</i>	BChl <i>a</i>
10	<i>Blastochloris viridis</i>	BChl <i>b</i>
<b>Cyanobacteria</b>		
11	<i>Prochlorococcus sp.</i>	Divinyl-Chl <i>a, b</i>
12	<i>Synechococcus WH7803</i>	Chl <i>a</i> , PUB/PEB
13	<i>Synechococcus WH8103</i>	Chl <i>a</i> , PUB/PEB
14	<i>Synechococcus BS5</i>	Chl <i>a</i> , PC, PE
15	<i>Synechococcus BS4</i>	Chl <i>a</i> , PC
16	<i>Acaryochloris marina</i>	Chl <i>d</i>
<b>Green algae</b>		
17	<i>Chlamydomonas sp.</i>	Chl <i>a, b</i>
<b>Diatoms</b>		
18	<i>Phaeodactylum tricornutum</i>	Chl <i>a</i>
<b>Chrysophytes</b>		
19	<i>Isochrysis sp.</i>	Chl <i>a</i>
<b>Red algae</b>		
20	<i>Palmaria palmata</i>	Chl <i>a</i> , PE

Table 2-3: Names and main pigments of organisms in Figure 2-11 [62]

### **2.6.3 Carbon dioxide**

In plants producing oxygen during photosynthesis, the change in concentration of either oxygen or carbon dioxide in a closed chamber is very often used as a measure of photosynthesis rate. However, during respiration the process is reversed and CO<sub>2</sub> is released. Moreover, this type of photosynthesis mainly takes place in higher plants. On the other hand in this study algae and bacterium are the main samples under investigation. Thus, even though there have been studies about the effects of CO<sub>2</sub> concentration on photosynthesis, the details are not discussed here. It can be noted however that during photosynthesis (under illumination), an increase in CO<sub>2</sub> concentration leads to a higher rate of photosynthesis [57].

### **2.6.4 Glucose addition**

Current output of electrochemical cell is dependent of the photosynthetic and respiratory activities. T. Yagishita *et al* [58] investigated the effect of glucose addition on current outputs in PSC. They observed that addition of glucose to the anode compartment leads to a rapid increase in the current outputs of the cell under both dark and light conditions. They believed that current output from oxidation of glucose was added to that from photosynthesis. Moreover they realized that addition of glucose will have a better result if done under illumination. Under discharge conditions, glucose metabolism in the cells might continue and thus is enhanced after pre illumination. Hence, they concluded that by adding glucose, duration of current output of the device can be extended.

This chapter dealt with basis of photosynthesis. The next chapter presents fabrication of the  $\mu$ PSC proposed in this work.

# **Chapter 3**

## ***Fabrication***

### **3 Fabrication: Low stress microfabrication of electrode integrated proton exchange membrane for polymer based photosynthetic power cell**

This chapter is based on a manuscript prepared for SPIE journal of micro/nanolithography, MEMS and MOEMS (JM<sup>3</sup>) and submitted patent: “*Scalable Polymer Based Power Cells using Photosynthesis*”. This chapter covers the objectives 3-a to 3-c of the “Objective and scope of the thesis” in Section 1.6.

#### **3.1 Introduction**

Energy is probably the most important issue of the current century. New sources, approaches and systems have been studied in order to find suitable and more reliable power sources and energy harvesting devices. MEMS (Micro Electro Mechanical Systems) allow for the generation of power at the micro level. However, additional new technologies and methods should be developed in order to realize devices using MEMS.

This work is an attempt to fabricate and develop a photosynthetic power cell using the photosynthesis process in micro-organisms. The operation of the device prepared in this work is based on the electrochemical reactions during photosynthesis. Compared to other published works [21-22] that use silicon, polymer is used in this paper and new micro-fabrication processes are developed for realizing micro photosynthetic power cell while reducing cost and increasing geometrical flexibility and power density.

### 3.1.1 Photosynthesis

As mentioned earlier, the main focus of this work is the fabrication process of the developed  $\mu$ PSC. Hence the operational principle as well as previous method of PSC fabrication is mentioned very briefly in order to be able to compare the current  $\mu$ PSC with similar fabricated devices.

In engineering sense, photosynthesis is the mechanism of converting light energy to chemical energy. It is a complex process taking place in higher plants, phytoplankton and bacteria. In order to perform photosynthesis, these organisms require light, water and carbon dioxide. Carbon dioxide and water are used as the raw material. Photosynthesis splits water, liberates oxygen and combines hydrogen with the carbon dioxide for carbon fixation – a process leading to production of sugars. Accumulation of oxygen in the atmosphere enables living creatures to consume the photosynthesized food and derive energy from it by respiration – process in which organic compounds are oxidized back to carbon dioxide and water [63,64].

Photosynthesis occurs in two stages: light dependent or photosynthetic reactions and light independent or dark reactions known as Calvin-Benson cycle. In the former, the light energy is captured (By using the light of appropriate frequency and wavelength, molecules can be transformed from ground to excited electronic state [63,64].) and used to make high energy molecules whereas in the dark reactions the high energy molecules are used to capture carbon dioxide and make carbohydrates.

In the light reactions, one electron is released per one photon absorbed. Passing through various stages, the electron transport chain leads to the ultimate reduction of NADP (nicotinamide adenine dinucleotide phosphate) to  $\text{NADPH}^+$  (nicotinamide adenine

dinucleotide phosphate-oxidase). NADP is a coenzyme used in anabolic reactions, such as lipid and nucleic acid synthesis. NADPH<sup>+</sup> is a membrane-bound enzyme complex which generates super-oxide by transferring electrons from NADP inside the cell across the membrane and coupling these to molecular oxygen to produce the super-oxide. NADP is reduced in the last step of the light reactions producing NADPH which is then used as reducing power for the biosynthetic reactions in the Calvin cycle of photosynthesis. Concomitantly, the electron transport induced a pH gradient, across the thylakoid membrane, which is needed for the formation of ATP (source of energy used in the biochemical reactions). The chlorophyll regains the lost electron by taking one from a water molecule through a process called photolysis which releases oxygen. In the dark reactions, enzymes capture CO<sub>2</sub> and in the Calvin-Benson cycle releases 3-carbon sugars, which are later combined to form sucrose and starch [43]. The reactions of photosynthesis can be summarized by the following equations:



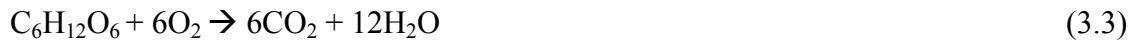
Where:

ATP: Coenzyme: Adenosine triphosphate – from photophosphorylation (One molecule of ATP contains three phosphate groups, and it is produced by ATP synthase from inorganic phosphate and adenosine diphosphate (ADP) or adenosine monophosphate (AMP))

NADP: Nicotinamide adenine dinucleotide phosphate – from photoreduction

### 3.1.2 Respiration

Photosynthesis and respiration are reversible bio-chemical reactions, meaning that the products of one process are the reactants for the opposite process. Hence cellular respiration is the opposite of photosynthesis; glucose or other carbohydrates oxidise to produce carbon dioxide, water and chemical energy. Below is the cellular respiration reaction corresponding to the photosynthesis reaction mentioned earlier [43].



Glucose + Oxygen  $\rightarrow$  Carbon dioxide + Water

### 3.1.3 Electron transfer

As seen above, both photosynthesis and respiration are involved with electron transport chains. As a result,  $\mu\text{PSC}$  can be operated in either light or dark condition. However, for best efficiencies and maximum lifetime of the device, cycles of light and dark conditions are suggested.

Electron transfer or moving of electrons from one site to another is among the most common chemical processes. As mentioned earlier, in the light reactions, one molecule of the pigment chlorophyll absorbs one photon and loses one electron. The released electron goes through several stages involving various electron donors and acceptors [43].

## 3.2 $\mu\text{PSC}$ Structure and Principle of Operation

### 3.2.1 Operational principle

The idea is to interfere with the electron transfer chain mentioned earlier and guide the electrons in the desired direction through the external load to obtain electrical

current. Figure 3-1 illustrates the operational principle of  $\mu$ PSC [21,22]. After absorption of photons, resulting released electrons, carried by the mediator, travel through the media in which photosynthetic agents are present. These electrons are taken up by the anode and travel externally through a load. Then they arrive to the other compartment of the  $\mu$ PSC where cathode is oxidized by potassium ferricyanide (an electron acceptor solution).

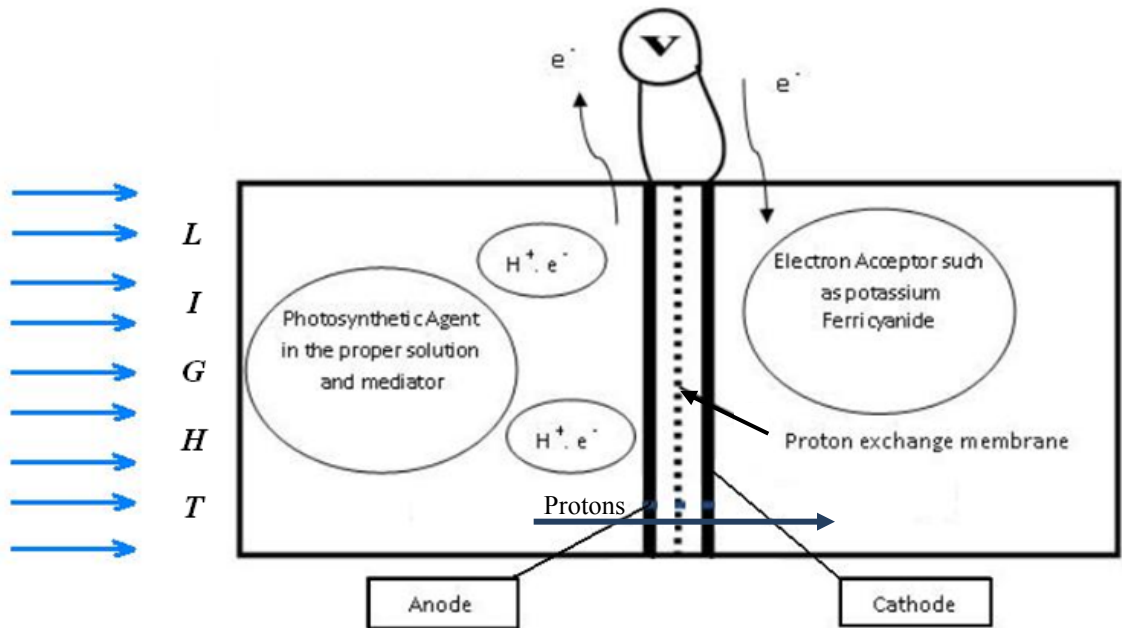
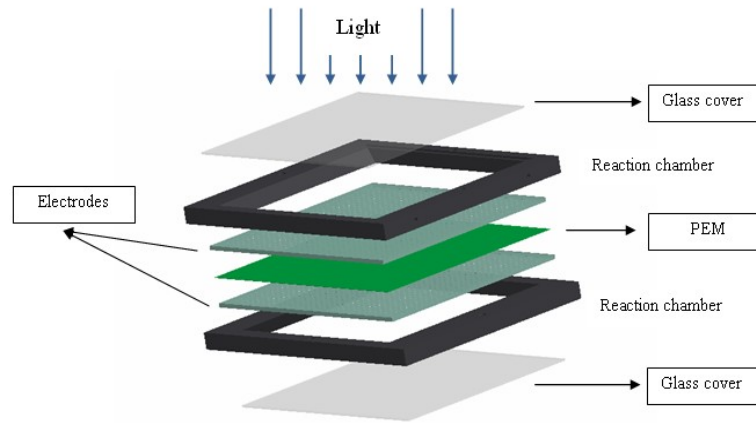


Figure 3-1: Operational mechanism of  $\mu$ PSC

### 3.2.2 Structure

$\mu$ PSC consists of two identical half cells as anode and cathode are interchangeable. The device is covered with glass covers on both sides and in between the two compartments there exists is a separating layer of Proton Exchange Membrane (PEM). On either side of the device, the anolyte and catholyte solutions are contained in chambers formed between the glass covers and the electrodes.



**Figure 3-2:  $\mu$ PSC structure**

Most of the previous fabricated  $\mu$ PSCs are silicon based, hence, the reaction chambers are fabricated by silicon micromachining [21,22]. The other side of the silicon wafer is also etched (patterned) to be used as the base for the electrodes which are fabricated by sputtering chrome and gold with approximate overall thickness of 2500 Å over the patterned silicon. PEM is sandwiched between the two half cells and electrolytes are injected to the chambers using syringes. Details of previous fabrication methods are explained in [21-22]

### **3.3 Fabrication**

#### **3.3.1 Half- cells**

As mentioned earlier the device consists of two identical half-cells. In this paper, polymer Polydimethylsiloxane (PDMS) is used as the base material for making these compartments. PDMS is non-toxic, non-flammable and optically clear polymeric compound. It is easy to handle and work with and it does not require special laboratory

conditions. Moreover, fabrication processes are less expensive than for silicon with a wide application range.

PDMS kit employed consists of PDMS base and curing agent. In this work, they are mixed in the weight ratio of 1:10, degasified and treated thermally afterwards.

Fabricating a part out of PDMS requires a mold. In the current work special consideration has been given to designing the mold so that inlets, outlets, fluid channels and chambers are fabricated in one step. Figure 3-3 illustrates the half-cell to be fabricated with PDMS using the mold shown in Figure 3-4. Circular micro channels were obtained in this process as opposed to the standard rectangular channels obtained using traditional MEMS processes.

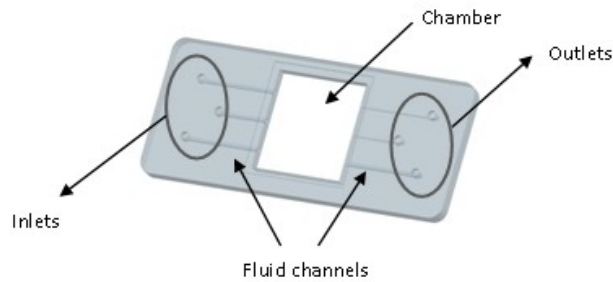


**Figure 3-3: Half-cell design**



**Figure 3-4: Designed mold**

The mold is fabricated by CNC machining of a brass block and the inner surface is coated with gold by electro plating in order to minimize the interaction between PDMS and mold. Cylindrical features with outside diameter of 0.5 mm are coated with gold using Edwards Sputter Coater and glued to the mold as shown in Figure 3-5. PDMS base and curing agents are thoroughly mixed as mentioned earlier. The mixture is then poured into the mold.

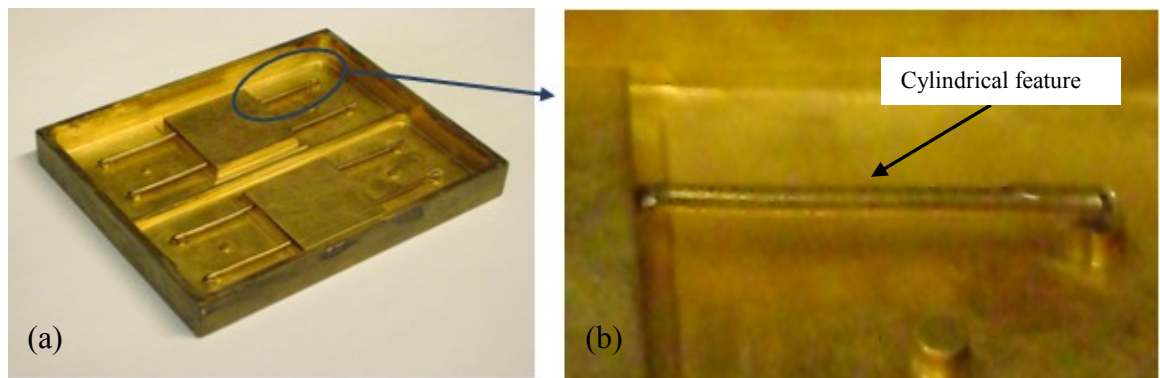
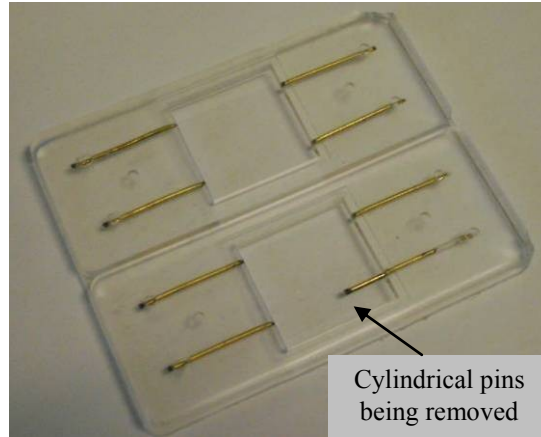


**Figure 3-5: Fabricated mold – a. with cylindrical features for circular channels, b. close up of the cylindrical features**

After pouring the uncured PDMS into the mold, the mixture is degasified using a vacuum chamber. This is in to remove micro bubbles which are induced into the mixture while mixing the base and curing agent. Degasifying time depends on the amount of bubbles and accuracy required and it took approximately 15 minutes in this work.

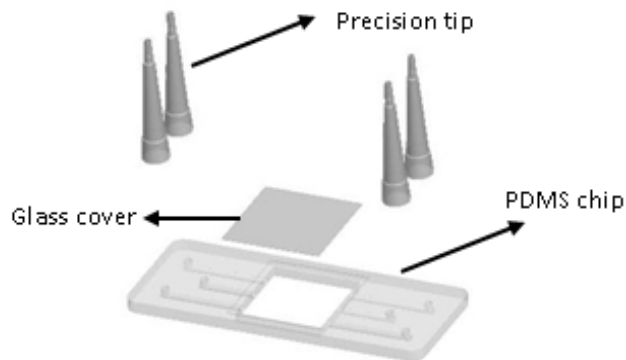
Baking is performed in order to finish the treatment and converting the phase from liquid to solid. Various baking times and temperatures have been used in various works. In this work the mixture was heated at 75 °C for 12 hours. Although baking can be performed in only 30 minutes under 125 °C for instance, lower temperature and longer time provide a better bonding in general.

Figure 3-6 shows the removal of the cylindrical pins used for forming circular channels along the fabricated chip.



**Figure 3-6: Fabricated PDMS chip showing pins removal**

A glass cover (microscope slide) and enough number of precision tips are bonded to the PDMS chip in order to complete the half-cell fabrication. Precision tips are attached using PDMS glue and the glass cover is bonded to the PDMS chip using oxygen/nitrogen plasma treatment and reinforced with PDMS glue. Figure 3-7 illustrates the half-cell assembly of  $\mu$ PSC.



**Figure 3-7: Schematic of half-cell assembly**

Before assembly, fluid ports and channels are observed under microscope equipped with CCD camera for any defects. After assembly, bondings and sealings are checked for leakage by pumping water using a Gilson Peristaltic Pump. Since the channels are not fabricated by etching as in the case of silicon, circular channels were fabricated successfully. Circulation of the chemicals through the chamber and channels is possible with the same LOC (Lab-on-a-chip) setup. Fabrication steps adopted in this paper eliminate many clean-room processes, decrease the costs and make the Micro Photosynthetic Power Cell faster to fabricate.

### **3.3.2 Proton Exchange Membrane (PEM)**

Proton exchange membrane is an important component of electrochemical cells including fuel cells and photosynthetic cells. Hence, many experiments and trials have been performed with various PEMs in order to find optimal PEMs. Likewise in this work, we attempted to suggest optimal PEM for photosynthetic cell application [65-66].

P. Beattie *et al* [67] investigated the ionic conductivity of a series of proton exchange membranes. Some of the membranes explored by them are Nafion<sup>®</sup>, BAM<sup>®</sup>, DAIS<sup>®</sup> and ETFE-g-PSSA<sup>®</sup>. They reported that water content, ionic sites and overall proton concentration of the membrane will affect the membrane conductivity. Moreover, among the mentioned membranes, Nafion<sup>®</sup> is the most widely studied one due to high proton conductivity, excellent stability, good mechanical strength and commercial availability [67].

Thickness of the membrane is an important parameter influencing the performance. The thinner the membrane, the more efficient the membrane is expected to

be [68]. Y. Sato *et al* [69] developed Nafion<sup>®</sup> membrane for PEMFC (proton exchange membrane fuel cell). Nafion<sup>®</sup> is a sulfonated tetrafluorethylene ionomer (synthetic polymer with ionic properties). Some lab procedures have also been developed [70,71] with the aim of improving the electrical properties of Nafion<sup>®</sup>. In the current study Nafion<sup>®</sup> is selected as the PEM and an attempt is made to increase its ionic conductivity by the following procedure [72]. Table 3-1 includes three types of Nafion<sup>®</sup> which are used in the current study.

PEM	Typical Thickness [ $\mu\text{m}$ ]	Basic weight [ $\text{g}/\text{m}^2$ ]
Nafion <sup>®</sup> NRE – 212	50.8	100
Nafion <sup>®</sup> N – 115	127	250
Nafion <sup>®</sup> N – 117	183	360

**Table 3-1: Properties of 3 types of Nafion<sup>®</sup>**

After removing protective layers on both sides, the membrane is further treated to increase the ionic conductivity of the membrane. The treatment is performed in the following six steps.

- 30 minutes in distilled water at 75 °C, which hydrates the membrane and dissolves surface contamination.
- 30 minutes in hydrogen peroxide (3%) at 70 °C, which removes organic contaminations from the surface.
- 30 minutes in diluted sulfuric acid (10%) at 60 °C, which removes metal ion contaminations and sulfonates the membrane.
- Rinsing with three-times of 30 minutes in distilled water at 75 °C.

An experiment was conducted in order to verify the increase in ionic conductivity of the membrane.

Two compartments were fabricated from PDMS, each containing a chamber. One of the chambers was filled with diluted sulfuric acid (10%  $\text{H}_2\text{SO}_4$ ) and the other one with water. pH of solutions in both chambers were monitored as an indication of ion exchange. A Nafion<sup>®</sup> membrane (NRE – 212) was treated and sandwiched between the two compartments. Changes in pH of water versus time were monitored. Similar experiment was performed with an untreated Nafion<sup>®</sup> membrane of the same type.

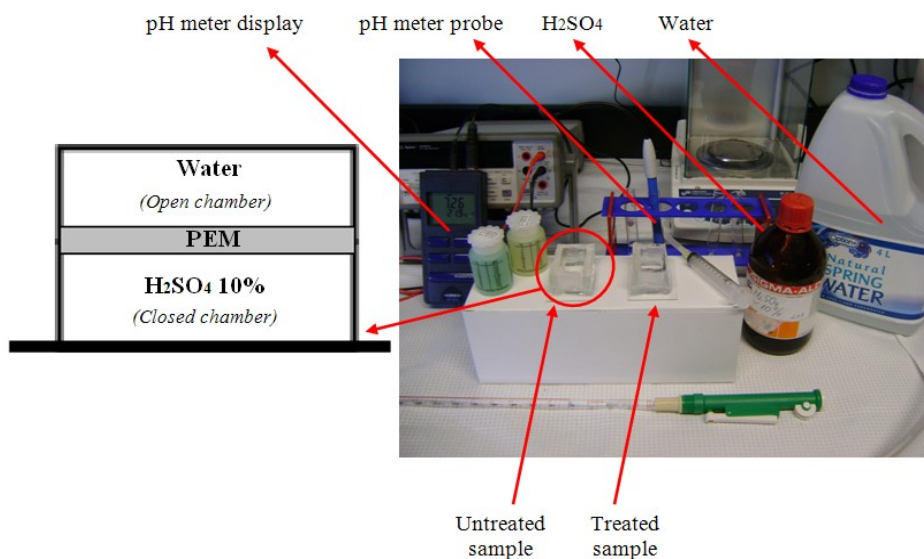


Figure 3-8: Ionic conductivity test

From the results shown in Figure 3-9, it is observed that rate of change of pH using a treated PEM is faster comparing to an untreated membrane. Hence it would be beneficial to use a treated PEM for electrochemical cell applications.

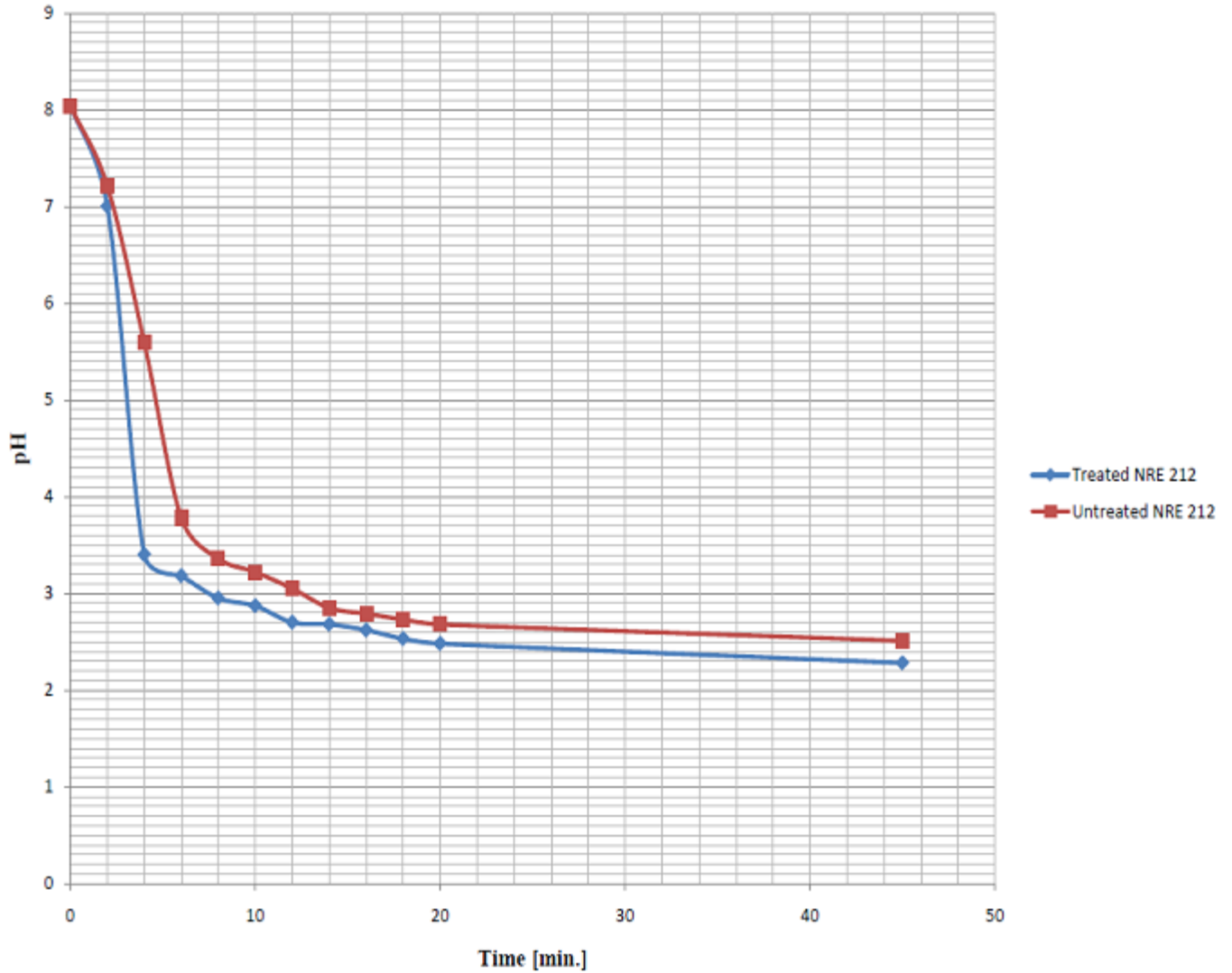
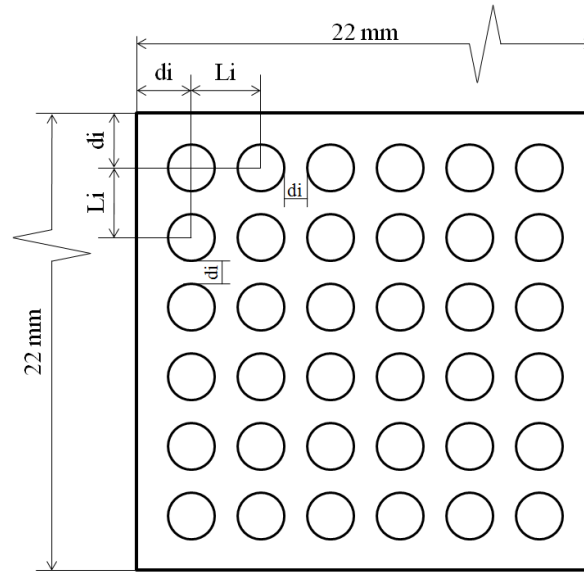


Figure 3-9: Variation in pH of water using Nafion NRE 212

### 3.3.3 Electrodes

In order to best utilize the active zone around the proton exchange membrane, electrodes are integrated onto the PEM. Hence, suitable processes have been developed. In a conventional patterning process, acetone-based chemicals are used as photoresist

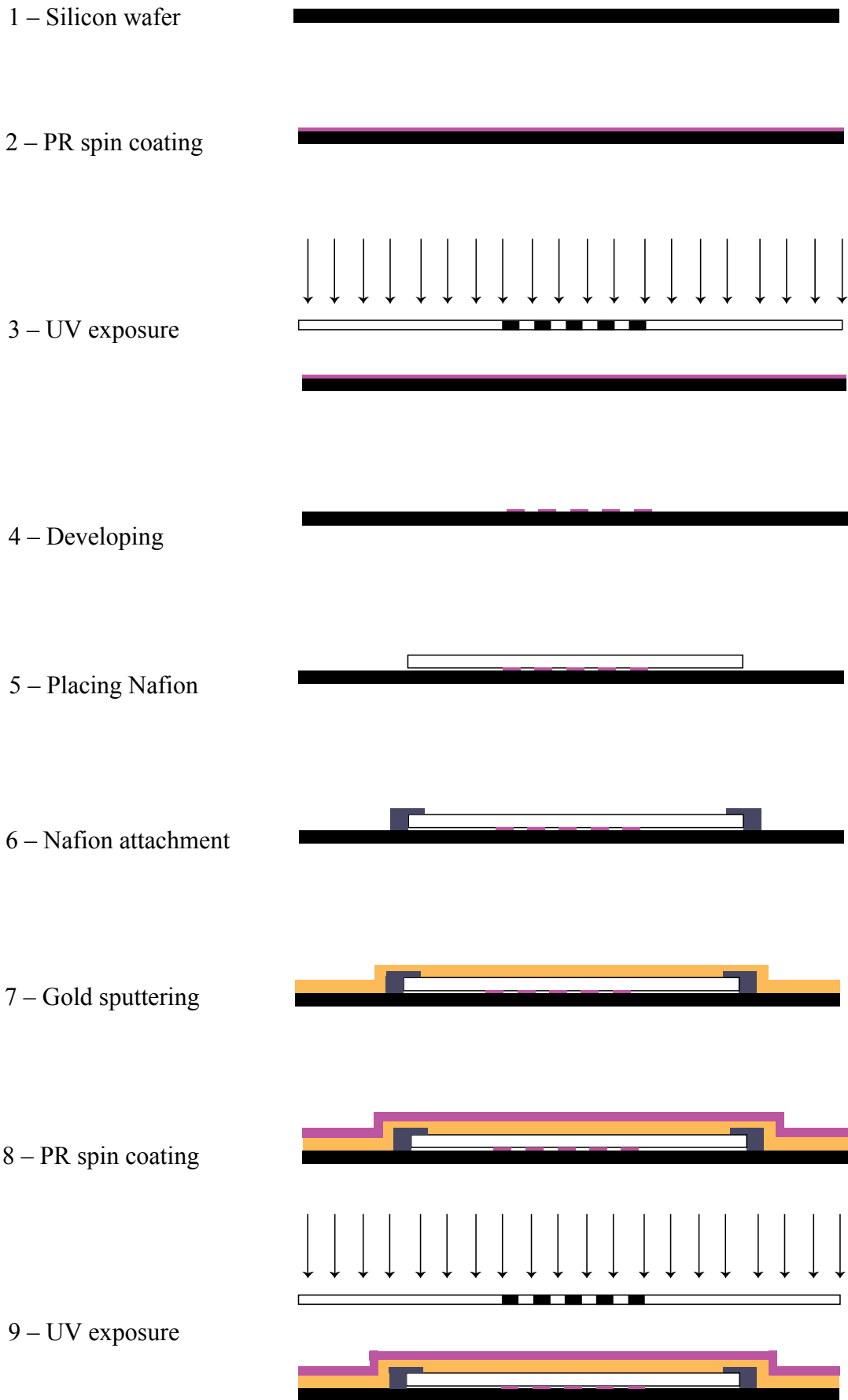
removers. These chemicals damage the Nafion<sup>®</sup> film. Hence, a new approach has been developed to integrate electrodes on the sides of the PEM. Typical electrode pattern design is shown in Figure 3-10. Instead of photoresist removers, developer solution was used to remove the photo-resist with the process introduced in Figure 3-11.



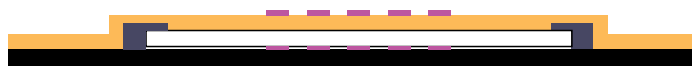
**Figure 3-10: Electrode pattern design**

Pore Density	D [ $\mu\text{m}$ ]	d [ $\mu\text{m}$ ]	L [ $\mu\text{m}$ ]	L/d Ratio	L/D Ratio
D1 – High	500	200	700	3.5	1.4
D2 – Med.		500	1000	2	2
D3 - Low		800	1300	1.62	2.6

**Table 3-2: Electrode design properties**



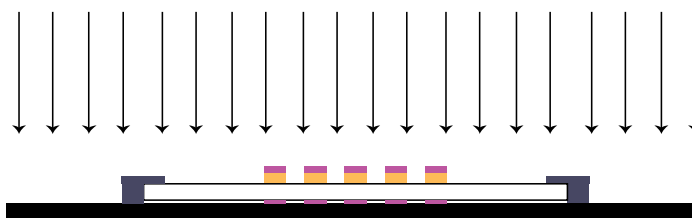
10 - Developing



11 - Gold etching



12 - Flood exposure



13 - Developing



14 - Nafion detachment



15 - Nafion flipping and reattachment



16 - Repeat steps 7-13

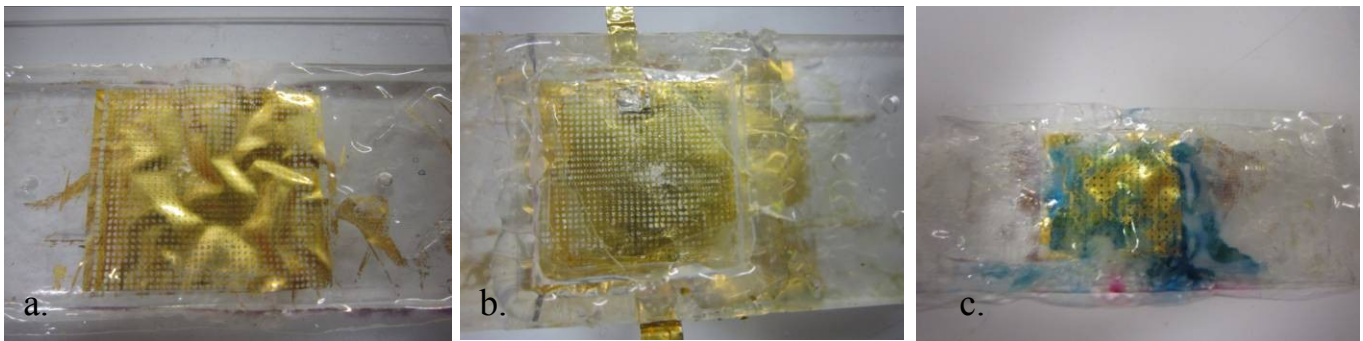
17 - Final detachment



Figure 3-11: Integrating electrodes on Nafion

During the fabrication process Nafion layer is attached to a silicon wafer which is used as a support. It has been noticed that pre-stressing the membrane prior to attachment to the silicon wafer results in a better stability of the layers during processing. Gold with a thickness of 100 nm is sputtered on the Nafion layer using Denton Sputtering machine. A layer of photoresist is then deposited on the gold using SITE Coater. A glass mask with the pattern shown in Figure 3-10, containing 3 patterns as shown in Table 3-2 is used for UV exposure. The sample is developed after exposure to UV, leaving a layer of photoresist which is the desired pattern on gold. Hence, this layer acts as a sacrificial layer during the gold etching process. At the end of gold patterning, the whole sample is exposed to UV radiation without any mask, in the “flood exposure” step which enables removing the remaining photoresist using the developing solution.

Figure 3-12 shows some electrode integrated PEM fabricated on Nafion. Resulting stresses from the mentioned developing processes can be observed in Figure 3-12-a. Figure 3-12-b presents a fairly good-quality sample whereas in Figure 3-12-c the stresses resulted in complete failure of the patterning process. Hence, in practice, fabrication process requires special care and considerations.



**Figure 3-12: Some electrode patterns on Nafion**

As mentioned earlier, pre tensile stressing of the membrane before attachment to the silicon wafer can reduce the wrinkles seen in the above figures. Attaching the membrane to the wafer such that any penetration under the membrane is avoided is also of a great importance. Moreover, special care should be taken not to over-etch the gold since the gold etching process is performed manually; a typical fabricated electrode is seen in Figure 3-12-b. After visual inspection of the samples, connectivity of the electrodes is checked in order to ensure their functionality.

After testing various methods for providing external connections to/from the electrodes, aluminum tape sputtered with gold on top, folded and attached to the electrodes using clear conductive overcoat pen was chosen as the final combination. Figure 3-13 shows the LOC packaged unit, with stress-free PEM integrated with electrodes between the two chambers.

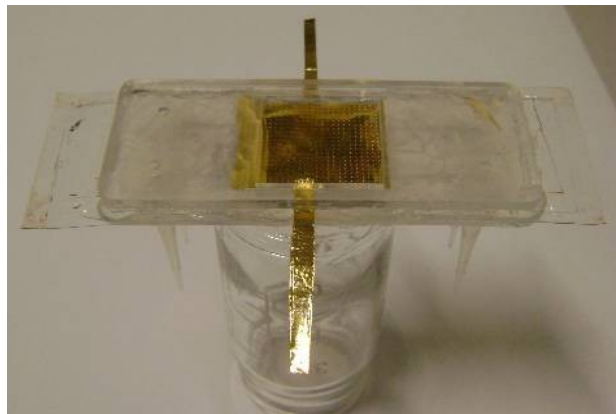


**Figure 3-13: External connection of the electrodes**

### 3.3.4 Assembly

After fabrication and preparation of all the components, assembly and bonding was performed. Exploded view of the unassembled model of  $\mu$ PSC developed in this work presented in Figure 3-14, followed by the assembled  $\mu$ PSC in Figure 3-15.

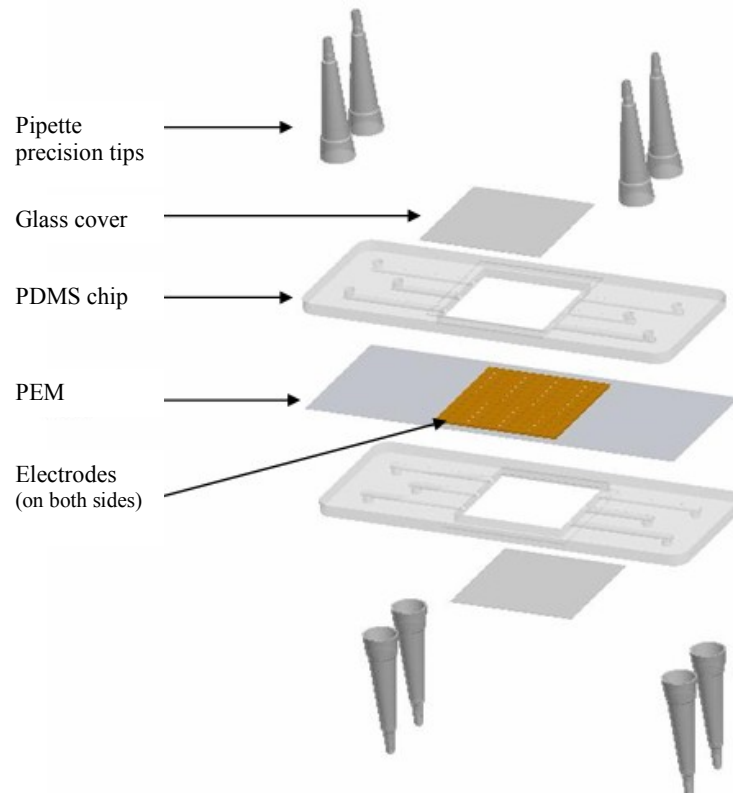


Figure 3-14: Exploded view of the  $\mu$ PSC

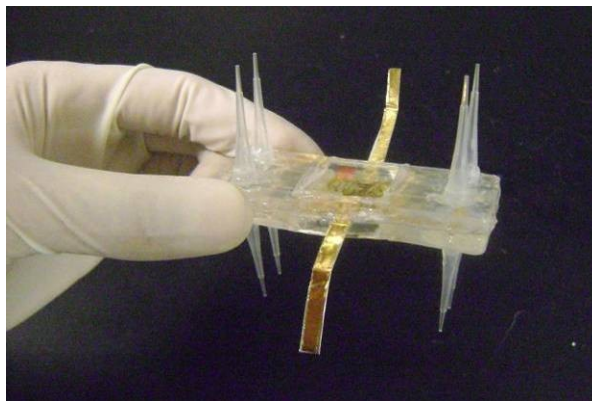


Figure 3-15: Assembled  $\mu$ PSC with fluid ports and external connections

Various bonding methods and materials have been used such as, RTV coating (DOW CORNING 3140 – Silicon rubber), PDMS glue (DOW CORNING – Silicon RTV), Pre-polymer (untreated or partially treated PDMS) and plasma treatment. As mentioned earlier, PDMS glue and plasma bonding are the two selected methods for the best performance.

### 3.3.5 External circuit

An external circuit is designed and fabricated to be used as the load. Considering the  $\mu$ PSC as the power source, the external load is the resistance in the circuit. Any of the three resistors (1 k $\Omega$ , 20 k $\Omega$  and 100 k $\Omega$ ) can be selected as the load. The output from the photosynthetic cell is collected using a data acquisition system (DAS) consisting of Data Translation USB Acquisition Board, connected to a computer using Measure Foundry as the interface to collect, monitor and post-process the outputs. Reliability of the measuring system has been confirmed through various tests.

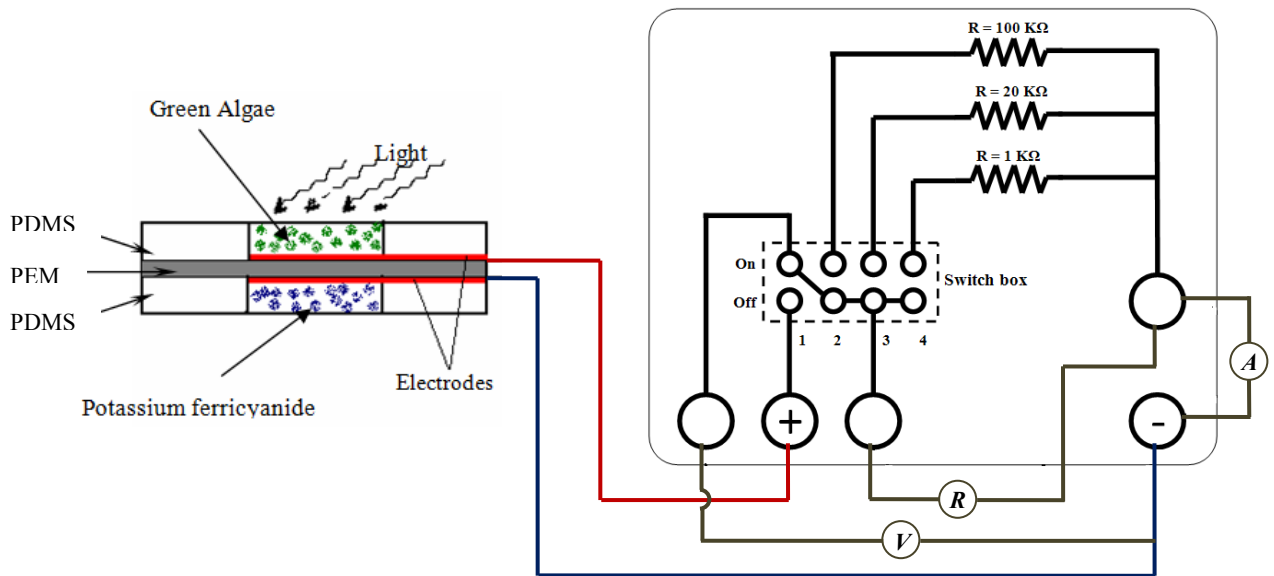


Figure 3-16: The external circuit

### 3.4 Results

$\mu$ PSC was tested by injecting green algae (*Chlamydomonas reinhardtii*, strain CC125) as a photosynthetic agent and potassium ferricyanide as an electron acceptor (catholyte) into the anodic and cathodic chambers, respectively. Numerous experiments have been conducted to examine the influence of different components and parameters. A sample experiment was performed for confirmation of functionality of the low stress electrode integrated PEM. Figure 3-17 illustrates the time varying output of the device in terms of voltage and current. For the first five minutes the voltage is monitored without any external load – open circuit voltage (OCV), therefore, no current was registered. This period of OCV monitoring is indicated on the graphs (Figure 3-17 and Figure 3-18). An external load of 1 k $\Omega$  was applied for the next 15 minutes of the experiment.

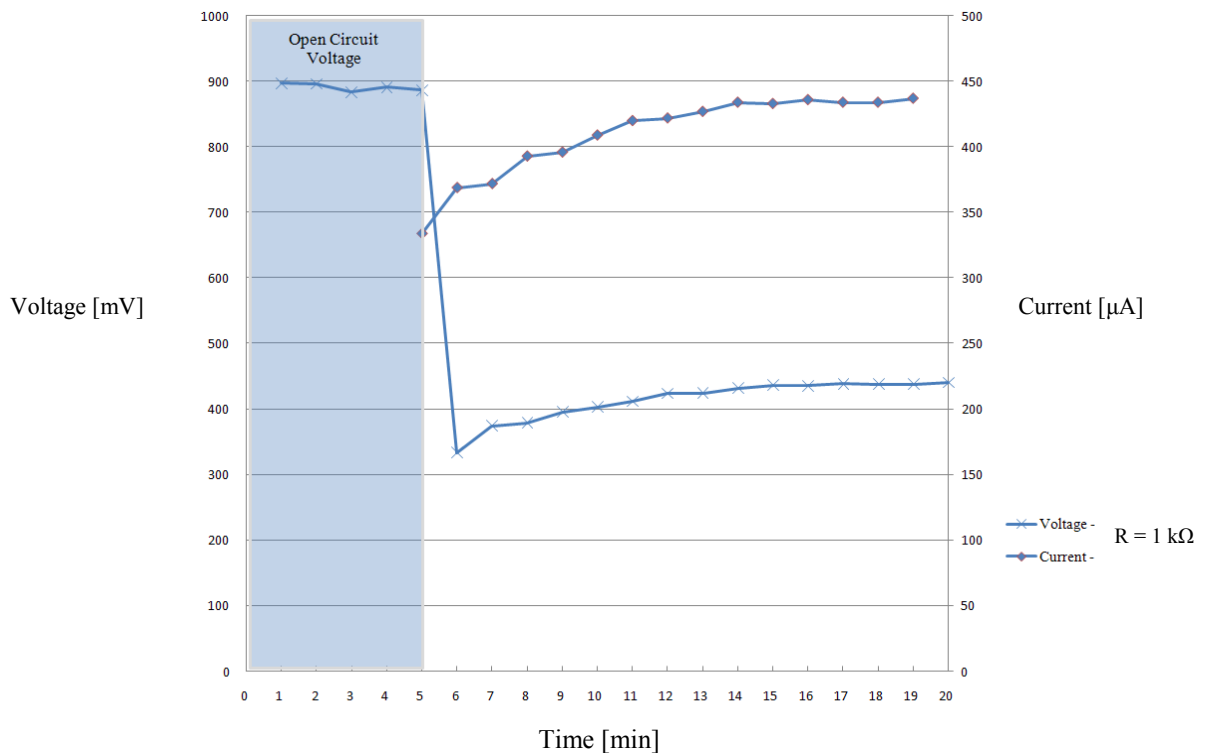


Figure 3-17: Output voltage and current

A sudden voltage drop is observed as soon as the external load is engaged. This voltage drop depends on the load being used such that the smaller the load, the more current and the lower voltage are observed. As the resistance is increased, electrons encounter more barriers to the flow. Hence, current will decrease and voltage increases and gets closer to the OCV value. In this experiment one can observe that the voltage is increasing before reaching a steady value. Increasing trend of the current is the consequence of this voltage increase under the constant external load being used.

Figure 3-18 illustrates the corresponding current and power densities. These parameters can be used for comparison purposes, expressing the output in terms of unit electrode area.

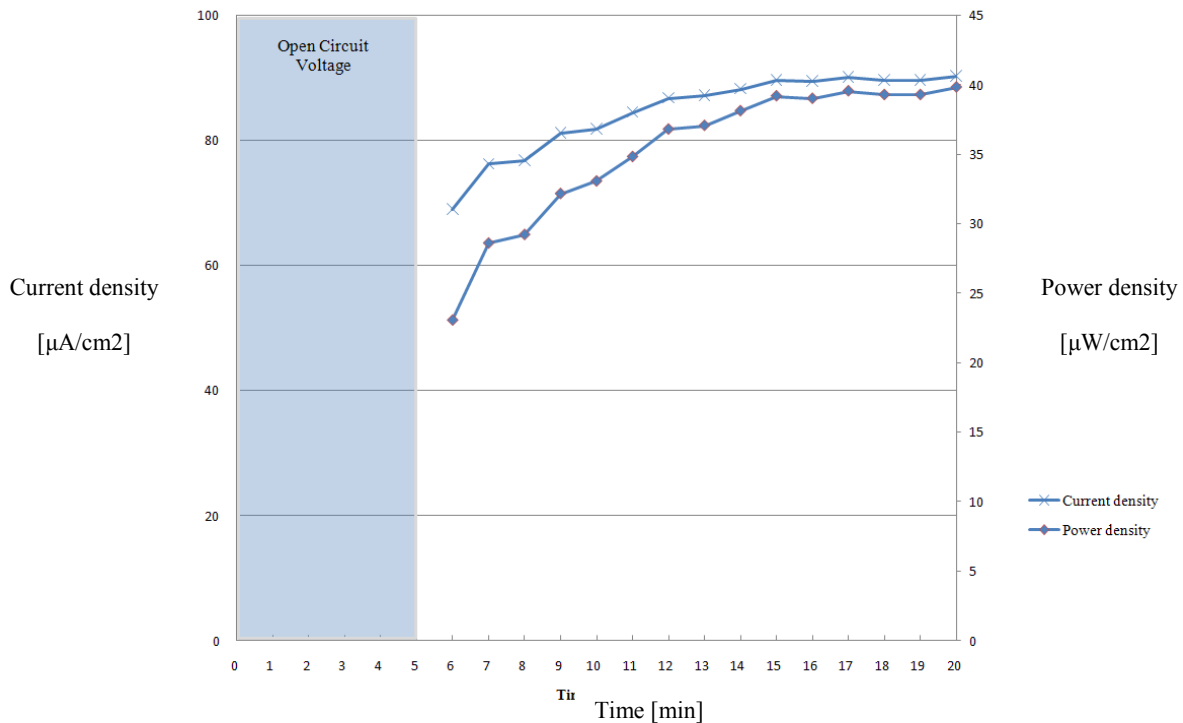


Figure 3-18: Current and power densities

### 3.5 Conclusions

This paper demonstrated the feasibility of microfabricating stress-free electrodes integrated with proton exchange membrane and realizing power generation in microphotosynthetic power cell through simple integration and packaging technique.

A polymer based photosynthetic electrochemical cell using electrodes integrated proton exchange membrane was developed. Three-layer technique was used consisting of two PDMS chips on top and bottom, and Nafion as the proton exchange membrane integrated with the electrodes on either side. Each PDMS chip includes all the necessary inlets/outlets, fluid channels and the reaction chamber. Due to the fabrication method used, the fluid channels have a circular profile. The proton exchange membrane is a Nafion integrated with electrodes on two sides. The proposed fabrication method enabled less expensive, easier and faster  $\mu$ PSC fabrication with geometrical flexibilities and simple packaging.

The results from the experiments are noticeable and can be compared to the previously fabricated  $\mu$ PSCs. Open circuit voltage as high as 897 mV was measured and average closed circuit voltage of 414.06 mV was obtained under external resistance of 1 k $\Omega$ . Maximum voltage measured under the mentioned load was 441 mV. Average and maximum measured currents were 410 and 437  $\mu$ A accordingly. These values correspond to power generation of 195.654  $\mu$ W and current and power densities as high as 91.66  $\mu$ A/cm<sup>2</sup> and 40.42  $\mu$ W/cm<sup>2</sup>.

This Chapter presented the fabrication of the  $\mu$ PSC. Next chapter will detail the experimental setup developed.

# Chapter 4

## *Experimental Setup*

## 4 Experimental setup

This chapter covers the objective 3-d of the “Objective and scope of the thesis” in Section 1.6.

### 4.1 Setup

Fabrication of different components of the device and accessories was described in chapter 3. Figure 4-1 presents the setup to be used for the experiments.  $\mu$ PSC is filled with potassium ferricyanide in one chamber and a solution containing the photosynthetic micro-organisms in the other chamber.  $\mu$ PSC is connected to the external circuit which in turn is connected to the Data Acquisition Board. Using the interface prepared in Measure foundry, data is monitored and recorded in Excel spread sheet for post processing.

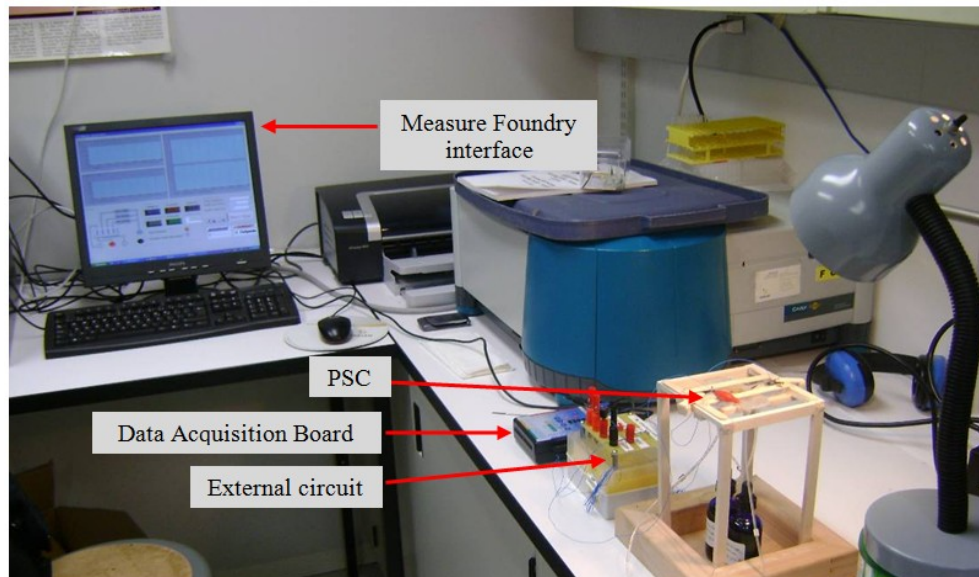


Figure 4-1: Experimental setup

In order to investigate different parameters and their influence on the performance of  $\mu$ PSC, various combinations and parameters were considered as mentioned below.

- Concentration of the catholyte solution: Potassium ferricyanide of different concentrations is studied
- Photosynthetic micro-organisms: Green algae (*Chlamydomonas reinhardtii*) is the main micro-organism used in the experiments. However, few experiments were performed using other organisms.
- Volume and concentration of the micro-organisms.
- Mediators such as Neutral Red, Thionin Acetate and Methylene Blue and their influence on the micro-organisms is studied.
- Glucose: Effect of addition of glucose to the anolyte solution is investigated.
- Proton exchange membrane: Three Nafion membranes with three different thicknesses were used as the PEM and the influence of PEM thickness on the  $\mu$ PSC operation was studied.
- Electrodes: Electrodes of different pore densities were patterned on each PEM.
- Other parameters such as light intensity, light/dark cycles and different external loads were studied as well.

Appendix A1 provides the summary of all the experiments performed in this work. Parameters of each experiment are given and the parameter under investigation is highlighted. Experiment numbers and indices found in A1 are used for identification purposes in the figures presented regarding each experiment.

## 4.2 Experimental verification

$\mu$ PSC is considered as a power source. Hence, the voltage and current are measured during the experiments. In order to make sure that the data obtained from the Data Acquisition System is reliable, a power supply of known parameters was employed. By comparing the outputs from the measuring system with the values set initially, reliability of the measuring system can be judged. In the first step a certain voltage is generated with the voltage generator. The output voltage is measured with both multi-meter and DAS and the readings are compared. In the next step the external circuit is also added to the system and voltage and current under certain load are measured. Other than the voltage generator, an AAA battery was also used as an alternate power source for these experiments.

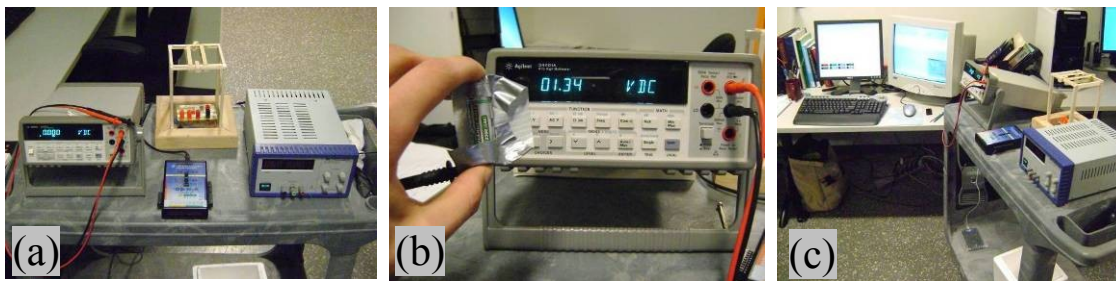


**Figure 4-2: Experimental verification with voltage generator (a) and AAA battery (b) using the external circuit and data acquisition system (c)**

In these experiments, initial reading from Measure Foundry interface was observed when there is no connection to the Data Acquisition Board, then the voltage generator was set to zero. Then it was connected to the Board and finally the voltage was increased up to a certain level. Readings from different devices were compared for verification purposes.

It should be mentioned that precision of the voltage generator used was one digit after decimal point (displayed on the voltage generator). However, precision of the multi meter used was 3 digits after decimal. The latter was also set as the precision for voltage readings from the DAS.

It was observed that when there was no connection to the Data acquisition Board (no input-channel in use); there was some random noise in all channels on the Measure Foundry interface (which is due to the passive components). However, as soon as the connection was made to a source, the displayed value matched the one on the multi-meter and voltage generator. This was true even when the voltage generator was set to zero volts.

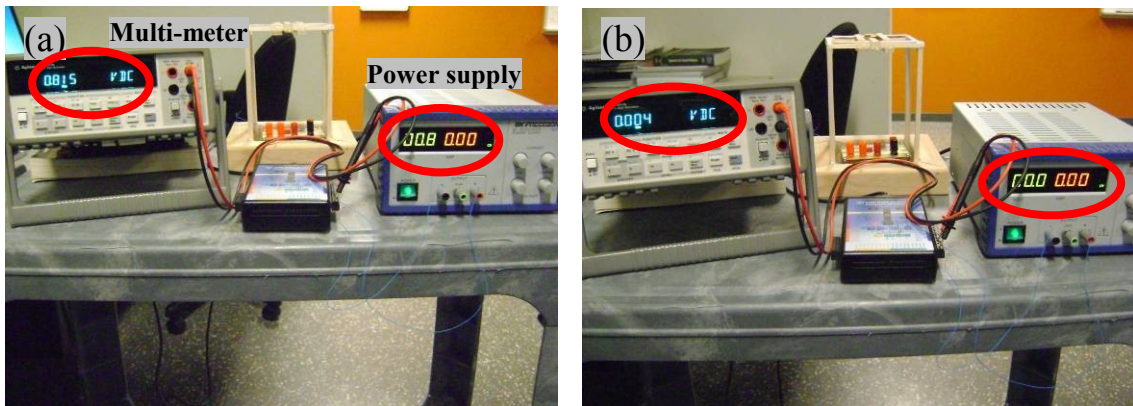


Figure 4-3: Experimental setup using power supply, multi meter and DAS

Figure 4-3 (a) shows the voltage generator set to 0.8 volts and (b) zero volts. It can be observed that the displayed values on the multi-meter were slightly different. That is due to the difference in the precisions of the devices mentioned earlier. It should also be noted that the values observed from the DAS matched those of the multi-meter (which used the same precision as the multi-meter).

From these experiments it is concluded that readings from DAS are reliable only if the channels are connected and there exists a potential difference between the channel under investigation and the ground channel.

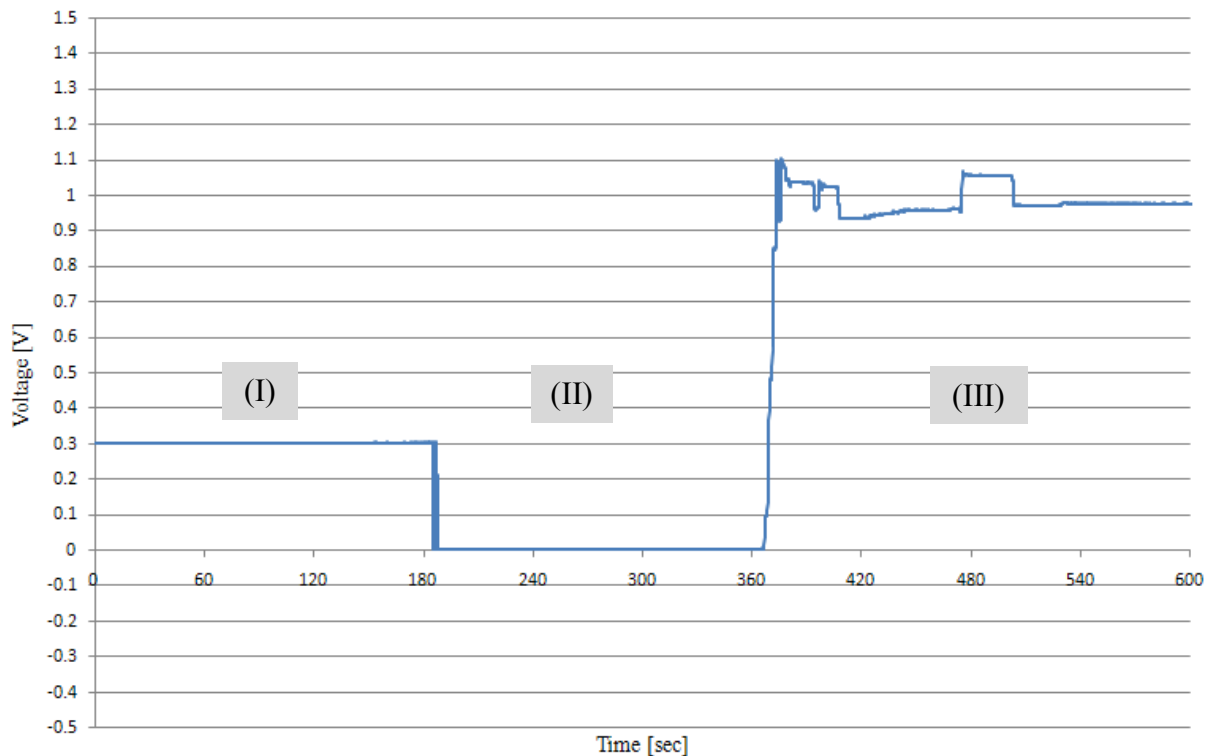
Hence, some other experiments were suggested which include the  $\mu$ PSC as well. The idea was to connect the outputs of the  $\mu$ PSC to the DAS without having the chambers filled and observing the readings. Apparently DAS should not display a generated voltage in order to rely on the obtained data. Table 4-1 enables better understanding of these experimental verifications.

Figure Number	DAS	Chamber 1	Chamber 2	Duration [min]
Figure 4-4	Not connected	N/A	N/A	3 (I)
	Connected to the voltage generator	N/A	N/A	3 (II)
		N/A	N/A	4 (III)
Figure 4-5	Not connected	N/A	N/A	3 (I)
	Connected to $\mu$ PSC. Anode to channel 0, cathode to channels 17 and 18	Empty	Empty	4 (II)
		Water	Empty	4 (III)
		$K_3[Fe(CN)_6]$ - 2 %	Empty	4 (IV)
		$K_3[Fe(CN)_6]$ - 5 %	Empty	5 (V)
Figure 4-6	Not connected	N/A	N/A	3 (I)
	Connected to $\mu$ PSC. Anode to channel 0, cathode to channels 17 and 18	Empty	Empty	4 (II)
		Empty	Water	4 (III)
		Water	Water	4 (IV)
		Water	$K_3[Fe(CN)_6]$ - 5 %	3 (V)
		Connected to voltage generator ( $V = 0$ v)	N/A	N/A

Table 4-1: Experimental verification using  $\mu$ PSC

Figure 4-4 demonstrates the results for the first set of experiments. First there is no connection to the data acquisition board and acquisition is done for 3 minutes. The error obtained here is due to the noise explained earlier ( $V = 0.2906$  volt). Voltage generator is set to zero volt and connections are made from the voltage generator to the data acquisition board for another 3 minutes. Finally the voltage on the power source is increased to 1 volt and acquisition is performed for another 4 minutes. The obtained voltages from Measure Foundry in the last two steps are 0.0041 and 0.9770 volt. The overall test time is 10 minutes and both chambers are empty during the three steps mentioned above.



**Figure 4-4: Experimental verification – DAS Vs voltage generator**

The next experiment contained five steps. In order to compare and assure the consistency of the results, the first step is similar to the previous test: no connection to the data acquisition board and apparently a false obtained reading. Then the electrodes (from  $\mu$ PSC) were connected to the channels of the data acquisition board while the two chambers are still empty. Then, chamber 2 was kept empty while water and potassium ferricyanide of 2% and 5% concentration were filled in chamber 1 in the next three steps (Table 4-1). No voltage generation was expected in these steps. Hence, a constant reading is observed as seen in Figure 4-5.

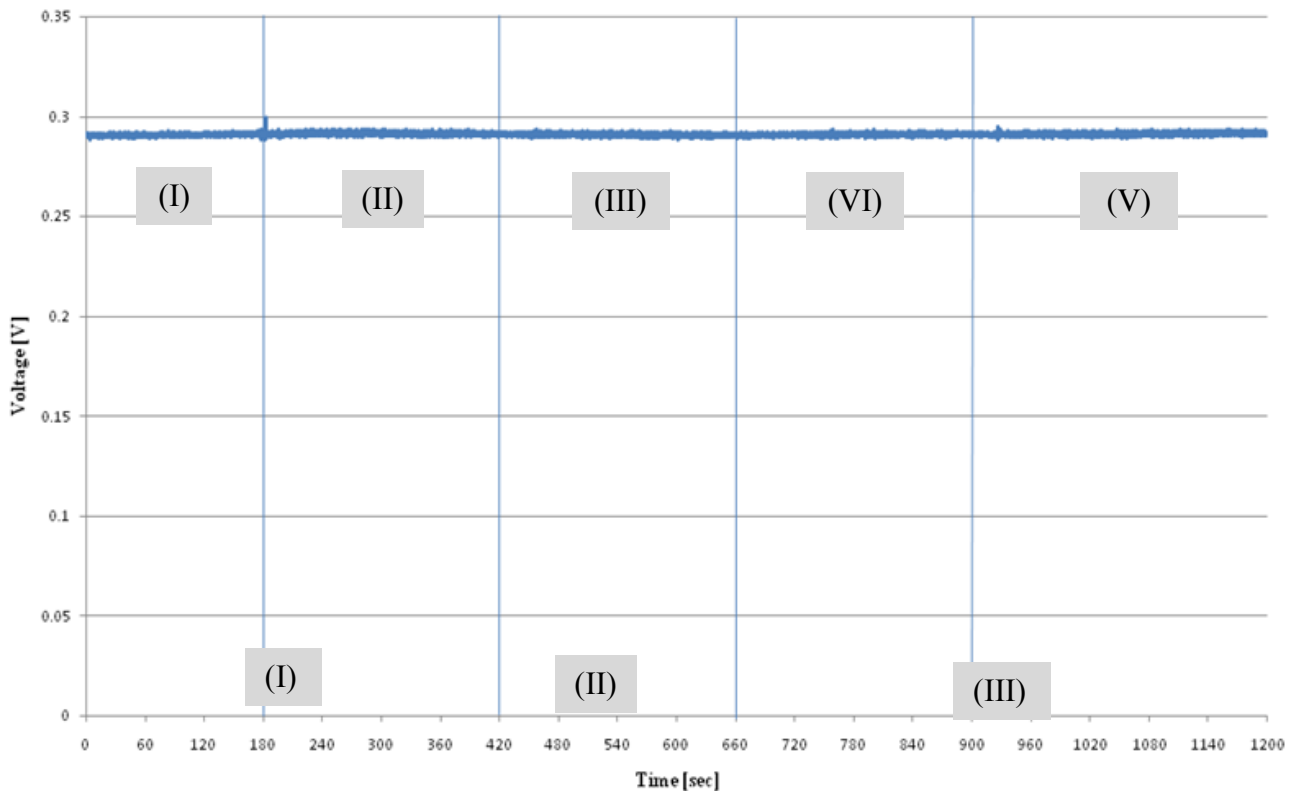


Figure 4-5: Experimental verification with  $\mu$ PSC

In the previous experiment one chamber was empty at all times. The aim of the next experiment was to confirm that there was no voltage generation being shown by the DAS when both of the chambers were filled with water and potassium ferricyanide

(different solutions not containing photosynthetic micro-organisms). The experiment included six steps. The first was the same as in the previous two experiments. In the 2<sup>nd</sup> step  $\mu$ PSC was connected to the DAS while the chambers were empty. Then water was filled into the 2<sup>nd</sup> chamber. After four minutes of acquisition, the other chamber is also filled with water. Then the content of chamber 1 was replaced with potassium ferricyanide. At the end in order to make sure if the readings are reliable, once again the voltage generator was set to zero and the connections were made to the power source. Immediate response after replacing the connections can be observed in Figure 4-6.

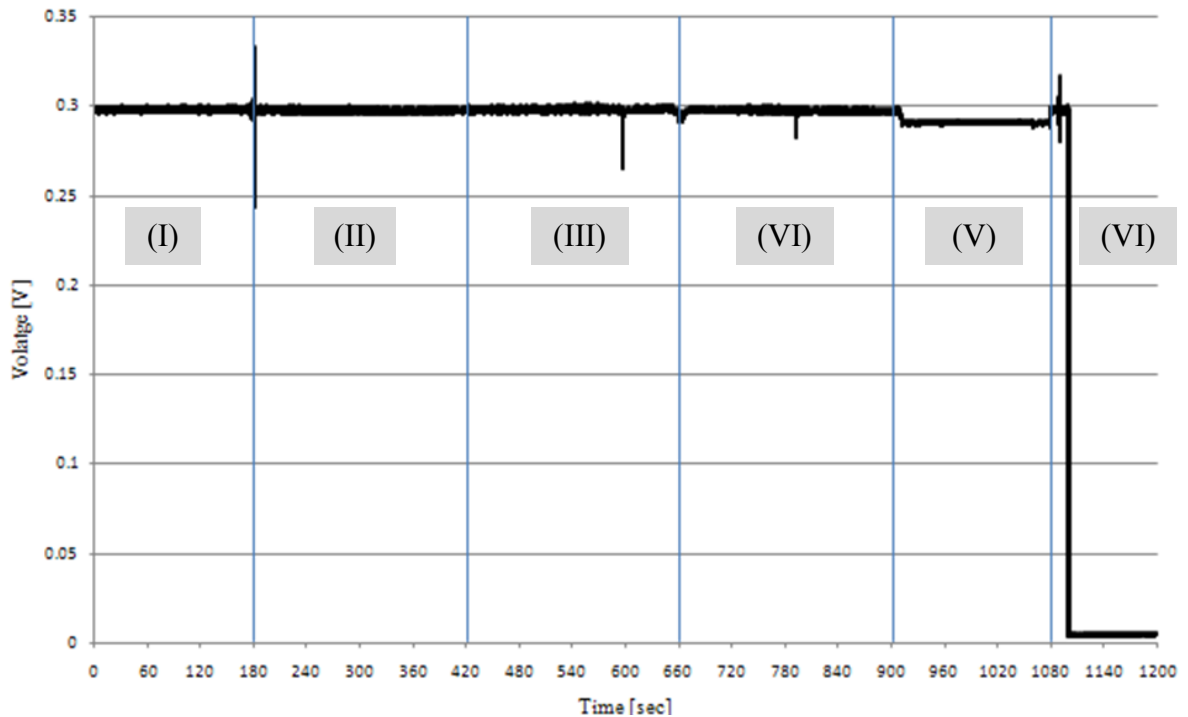


Figure 4-6: Experimental verification with  $\mu$ PSC – Cont'd

### 4.3 Calculations

As mentioned earlier, USB Data Acquisition Module (DT 9800 series) is used to collect data. Channel scan is performed with the following parameters and stored in Excel spreadsheet integrated in the Measure Foundry.

Clock frequency: 100 Hz

Buffer size: 1024

Buffer count: 30

External load of known resistance  $R$  [ $\Omega$ ] is used (see Section 3.3.5). Electrical current and power can be then derived as:

$$I = V / R = Q \times t \quad (4.1)$$

$$P = I \times V \quad (4.2)$$

Where:

I: Current [A]

V: Voltage [v]

R: External resistance [ $\Omega$ ]

P: Power [Watt]

Q: Charge [C]

T: time [s]

The power calculated above is considered as the output of the device. The input power however is not as easy to be obtained. There has been different ways of defining the input efficiency. For photosynthesis, one can obtain the efficiency according to the power of the light source used. For respiration, one method is to measure the total sugar

content in milligrams and converting it to the corresponding molar amount. The chemical energy of one mol glucose is 164 kJ and hence, the difference between the initial and final sugar content is considered as the amount of chemical energy converted to electrical energy [35-37].

Another way of expressing the output of the device which is used in this study is with consideration of the electrodes area. Since different devices have been fabricated and investigated, the current and power can be expressed as  $[A/cm^2]$  and  $[W/cm^2]$  in order to compare the outputs with each other and with previously performed experiments from the literature.

The dimensions of the electrodes are  $22 \times 22 \text{ mm}^2$  as discussed earlier. Hence, dividing the output current or power by the electrode surface area, the power and current densities can be calculated. Same calculations can be performed considering the volume of the anodic chamber (amount of photosynthetic agents used). These calculations enable the comparison of the results of the current work with previous studies.

The details of the experimental setup were discussed in this chapter. Next chapter presents the parametric study on the performance of the  $\mu\text{PSC}$ .

# **Chapter 5**

## **Results**

## **5 Results: Effect of Proton Exchange Membrane Electrode Configuration and Other Design Parameters on the Performance of Micro Photosynthetic Power Cell ( $\mu$ PSC)**

This chapter is based on a manuscript prepared for publication in the IEEE/ASME journal of Microelectromechanical Systems (JMEMS). This chapter covers the objectives 3-e and 3-f of the “Objective and scope of the thesis” in Section 1.6.

### **5.1 Introduction**

#### **5.1.1 Energy harvesting devices**

Various compact power-generating devices have been developed in recent years among which fuel cells are the most promising systems. Advantages of fuel cells include usage of continuously replenished reactants, no moving parts and reduced thermal conversion. The key disadvantage of the fuel cells is insufficient ionic conductivity of the electrolyte. Micro-scale fuel cells are being investigated as a solution to improve the ionic conductivity [3-5].

Heat engines remain the primary choice for power conversion at most large scale power plants. Based on the generation scale, different energy sources are used ranging from natural gas to coal to nuclear. Hydrocarbon fuels containing chemical energy are used also in micro-scale heat engines. Although the second law of thermodynamics puts a limit on the conversion efficiency of the heat engines, larger energy densities are achieved compared to lithium-ion batteries [3]. The very first micro heat engine was developed at MIT in 1990s. Soon after, internal combustion engines and steam engines

on micro scale have been developed and tested [3]. Large viscous losses resulting from thin boundary layer were found as one of the main disadvantages of these micro heat engines [6].

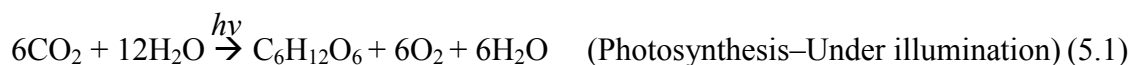
Thermophotovoltaics (TPV) is another class of energy conversion systems. Here, the power generation is based on a heated emitter radiating photons which are then absorbed by a photocell and converted to electricity. This concept is very close to the solar cells with one major difference which is the source of radiation [10]. Although the emitter can be heated by sunlight, extremely large beam concentrators are required in order to provide sufficient temperature for efficient operation which makes it less practical choice. Hence, the emitter is usually heated by combustion, providing a great deal of versatility in potential fuels. Higher power densities compared to solar cells are reported since the emitter and the photocell are in close proximity. The current challenges in TPV application on large scale are design, fabrication and material selection [11]. Solar cells are arguably the most thoroughly explored energy conversion systems. In a typical photovoltaic module, photons of longer wavelength do not generate electron-hole pairs. The respective portion of the light energy is converted to heat. Working temperature is increased and the cell efficiency is reduced. Structural damage might also occur due to overheating. Thus, combined systems such as photovoltaic/thermal hybrid solar systems were introduced, enabling production of both electricity and heat from one integrated system [14,19]. One example is a combination of TPV and solar-assisted heat pump systems with the TPV panel directly coupled to the heat pump [19].

Another promising category of small-scale power generating devices is Micro Photosynthetic Power Cell ( $\mu$ PSC) studied in this work. As appears from the name,  $\mu$ PSC

employs photosynthesis – a process of converting light energy to chemical energy, responsible for sustaining life on earth.  $\mu$ PSC is similar to fuel cells but no resupply of fuel is required. Hence, supply and exhaust are not considered as difficulties of design. Like solar cells,  $\mu$ PSC operates under illumination. However, absence of light not only does not stop the operation but also helps restoring the device. Thus, the device can be operated continuously both under illumination and in the dark. Moreover, it is environmental friendly and has no emission.

### **5.1.2 Photosynthesis**

Both photosynthesis and respiration form the basis of  $\mu$ PSC operation. Photosynthesis involves conversion of light energy to chemical energy by living organisms including plants, bacteria, algae, phytoplankton etc. Despite its complexity and variety, the fundamentals of photosynthesis are quite similar in all organisms, although there are differences in the reactants and the by-products. In higher plants and algae, photosynthesis splits water molecules to oxygen (liberated to the atmosphere) and hydrogen (protons). Carbon dioxide and hydrogen are combined into sugars (stored in the plants as a source of food). In the absence of light, the reverse process takes place called respiration, using oxygen and sugar, liberating carbon dioxide and energy. Both photosynthesis and respiration involve electron transport chains which are fundamental to  $\mu$ PSC. The electrons are released in one step and taken up in another. The idea is to interfere with the electron-transfer chain in such a way that the electrons get directed through an external load, resulting in electric current [43-50]. Equations 5.1 and 5.2 summarize the processes of photosynthesis and respiration.



### 5.1.3 Photosynthetic Power Cell

The schematic of the  $\mu\text{PSC}$  developed in this work is shown in **Figure 5-1**.

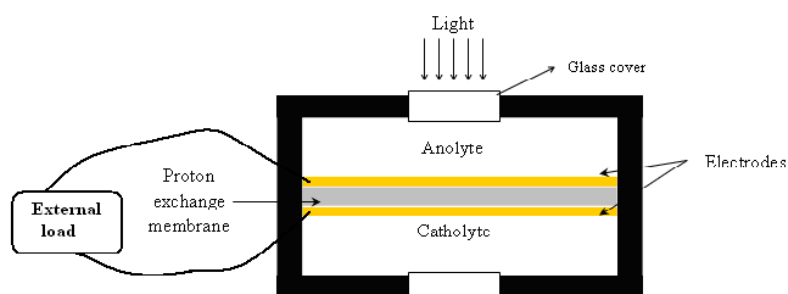


**Figure 5-1: Main components of PSC**

The electrolyte chamber is divided into two compartments by a Proton Exchange Membrane (PEM) which is made of a sulfonated polymer (Nafion). Electrodes are microfabricated on both sides of the PEM (See Chapter 3 for details). Anolyte compartment contains a media including live photosynthetic micro-organisms such as algae, cyanobacteria etc and a mediator. Ferrocyanide solution is used as the electron acceptor and is located in the catholyte compartment. Electrodes are connected to an external load. The top and optionally bottom sides of the chamber are covered with glass allowing light into the chambers. Since catholyte works as electron acceptor, it does not require to be exposed to light neither for photosynthesis nor for respiration.

Once electrons are released in the anolyte chamber, they are transferred through the external circuit to the other side of the chamber (catholyte). This transfer of electrons creates an ionic gradient which is balanced by the proton exchange membrane.

## **5.2 Fabrication**

### **5.2.1 Photosynthetic Power Cell**

Fabrication process of the  $\mu$ PSC studied in this work differs from previously fabricated photosynthetic electrochemical cells [42-20]. This design was introduced with the aim of improving the overall efficiency of the  $\mu$ PSC in terms of the output power. The influence of different parameters possibly affecting the output power was tested through various experiments. These results are the main focus of this Chapter. Hence, the fabrication process is just briefly mentioned below.

In contrast to the majority of the previous  $\mu$ PSCs, the current device is polymer based. PDMS (Polydimethylsiloxane) was used for the main body of the device. Figure 5-2 depicts the unassembled  $\mu$ PSC, followed by the fabricated device in Figure 5-3. The PEM is sandwiched between two identical half cells. The half cells are fabricated in single step and include the chamber, desired number of inlets/outlets and fluid ports. Glass covers are attached on both sides and precision tips are attached to the chip enabling usage of peristaltic pump for fluid circulation. Electrodes (100 nm thick gold) are directly patterned on the two sides of the PEM by a process that eliminates using of photoresist remover solution which is not compatible with the PEM. Moreover, no chrome is used as an auxiliary layer for gold electrode deposition and hence, the

electrode thickness is reduced by over 50% comparing to some previous works [42]. The final assembly of the PSC is achieved using oxygen plasma treatment and PDMS glue.

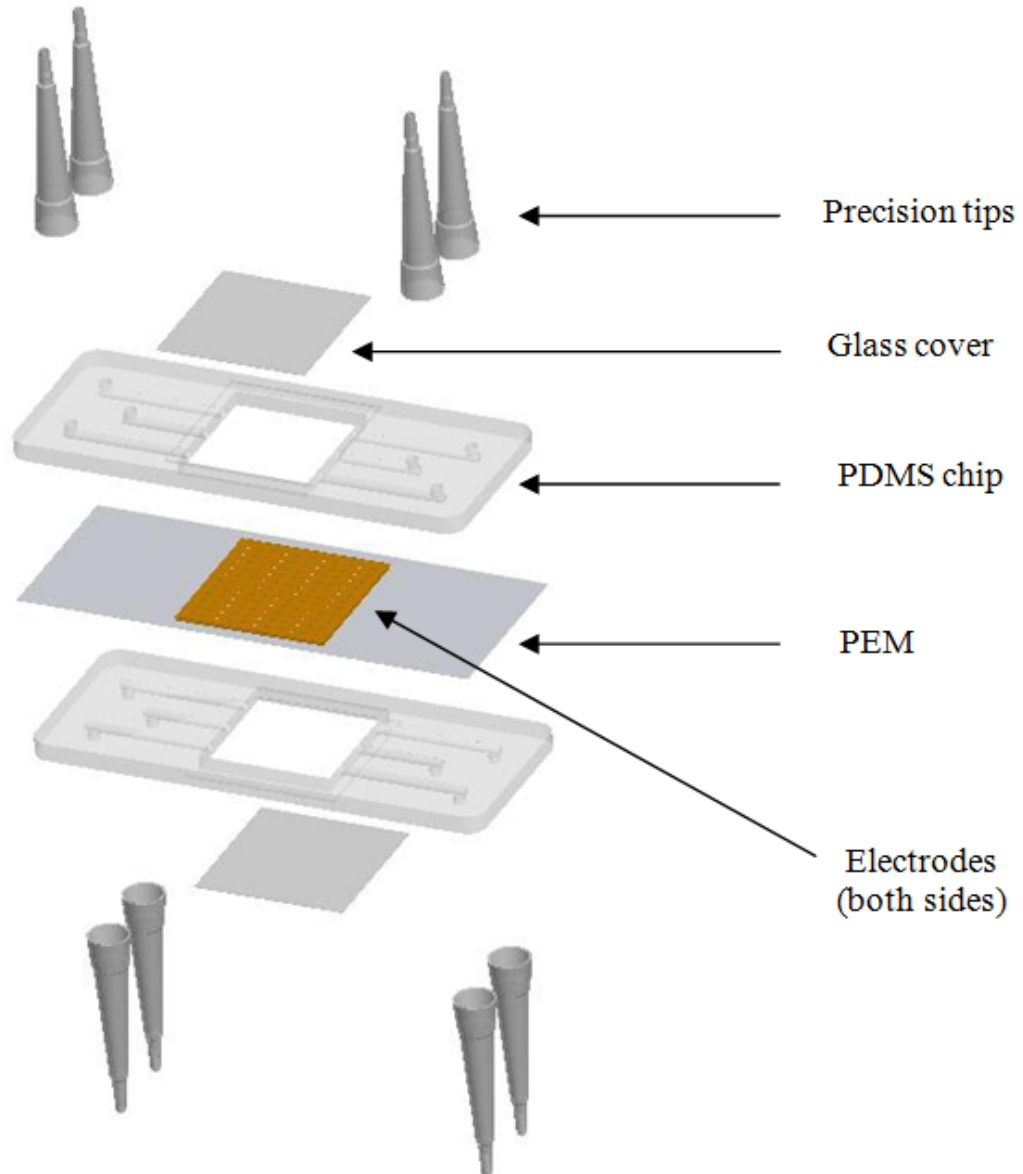


Figure 5-2: Unassembled  $\mu$ PSC model

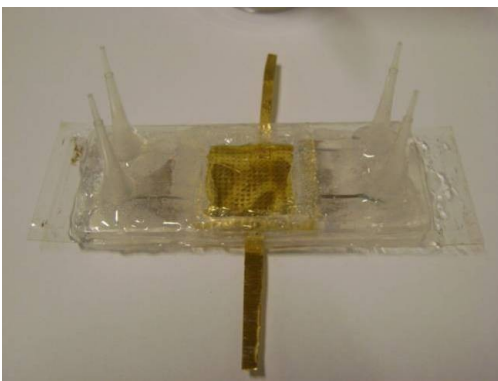


Figure 5-3: Assembled proposed  $\mu$ PSC

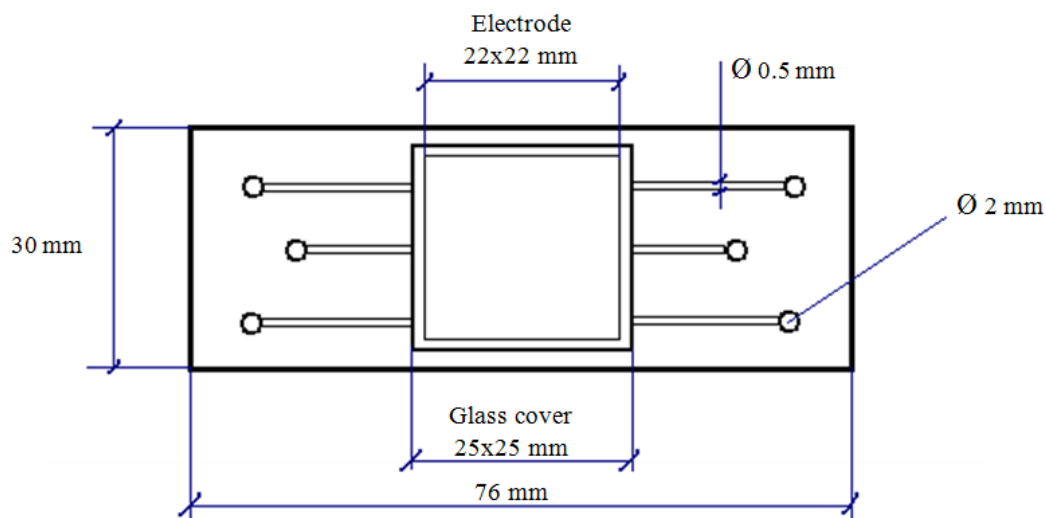


Figure 5-4: Schematics of the  $\mu$ PSC tested

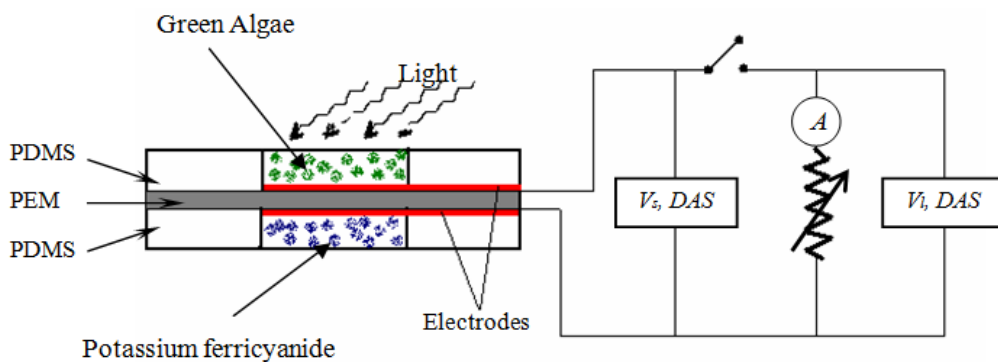


Figure 5-5: Schematics of the experiment setup

Some dimensions of the proposed PSC are presented in Figure 5-4. The rectangular PDMS chip is 76 by 30 mm<sup>2</sup> with thickness of 3 mm. Fluid ports include inlets/outlets of 2 mm in diameter and circular fluid channels of 0.5 mm in diameter and 12 to 18 mm in length. The designated electrode area is a square of 22 by 22 mm<sup>2</sup>. Green algae (*Chlamydomonas reinhardtii*) were used as the photosynthetic micro-organism in all experiments.

### 5.2.2 Measurement setup

A set of resistors was used as the external load with the  $\mu$ PSC. It contains three resistors with nominal values of 1 k $\Omega$ , 20 k $\Omega$  and 100 k $\Omega$ , switches to engage each resistor as desired, necessary ports for connections to the measuring system, a data acquisition system and a multi-meter. For some experiments where more resistance values within a certain range were required (such as V-I characteristics determination), a potentiometer was used.

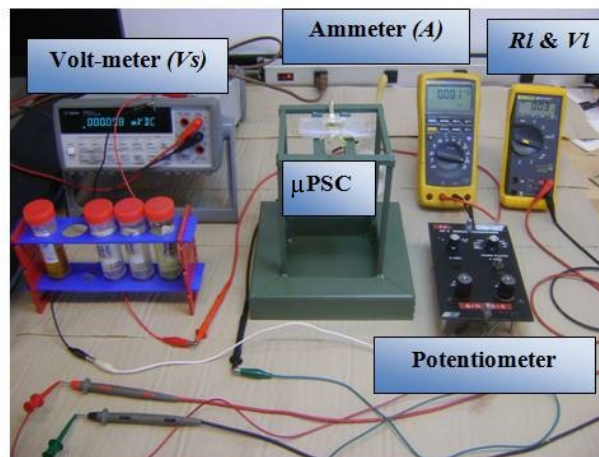


Figure 5-6: Experiment measurement setup

In the experimental setup, the electrodes from the  $\mu$ PSC were connected to the designated ports on the external circuit. A data acquisition system was used to measure the output voltages across the  $\mu$ PSC. Data Translator USB data acquisition module was used as the hardware and Measure Foundry was used as the interface between the module and computer.

The setup was designed such that one could continuously measure and monitor the Open Circuit Voltage (OCV) across the  $\mu$ PSC ( $V_s$ ) or measure current and voltage for a certain resistance of the external load. Theoretically, voltage in series configuration remains constant. The voltage ( $V_l$ ) across the load however, is slightly less than ( $V_s$ ). The difference between the two ( $V_s - V_l$ ) corresponds to the internal resistance of the  $\mu$ PSC which is an important parameter to be considered while designing power converters. In addition to current and voltage for certain loads, current and power densities based on the  $\mu$ PSC's electrode area were calculated in order to compare our results with those of previous works [22,42].

### **5.3 Experiments**

The performance of the  $\mu$ PSC may be affected by a multitude of parameters ranging from fabrication details to environmental conditions. The influence of several such parameters was explored in this paper by varying only one of the parameters at a time. The PEM separates the two chambers and directly affects the ionic transfer within the device. The electrodes are important components in the electron transport chain that affect the internal resistance of the  $\mu$ PSC. Photosynthetic agents are believed to be most effective at the vicinity of the PEM where the released electrons are absorbed by the electrodes. Hence, the present work discusses the following parameters: proton exchange

membrane properties, electrode pattern, volume and concentration of photosynthetic micro-organisms, illumination and external load.  $V-I$  characteristics as well as long term no-load performance were explored in order to understand the behavior of  $\mu$ PSC.

Green algae (*Chlamydomonas reinhardtii*) were used as the photosynthetic micro-organism in all the experiments. Using the experimental setup explained earlier, the Open Circuit Voltage (OCV) was measured. In addition to current and voltage under certain loadings, current and power densities based on the  $\mu$ PSC's electrode area were also calculated in order to compare our results with those of previous works [42-22].

### **5.3.1 Effect of proton exchange membrane and electrode configuration**

The ionic transfer in  $\mu$ PSC is a function of the photosynthetic samples, proton exchange membrane and electrode patterns. The ionic transfer across the membrane is strongly dependent on the thickness of the membrane and it was initially assumed that the thinner the PEM, the more efficient the ionic transfer would be. Electrodes having a high surface to volume ratio while providing proximity of the photosynthetic agents to the PEM are of great importance in the electron transfer. Hence, the electrode configuration becomes a critical parameter to be studied. All these might vary in relation to the species for instance the optimal shape, size and pitch of the pores in the electrodes might vary from one species to another.

In order to study the effect of PEM thickness and electrode configuration on ionic and electron transfer, three different configurations of electrodes on three different thicknesses of PEM are studied. In this study Nafion<sup>®</sup> was used as the proton exchange

membrane. Three types of Nafion<sup>®</sup> PEMs studied in this work and differing mainly in the thickness are summarized in Table 5-1.

PEM	Typical Thickness [ $\mu\text{m}$ ]	Basic weight [ $\text{g}/\text{m}^2$ ]
Nafion <sup>®</sup> NRE – 212	50.8	100
Nafion <sup>®</sup> N – 115	127	250
Nafion <sup>®</sup> N – 117	183	360

**Table 5-1: Nafion<sup>®</sup> properties**

Three patterns of electrodes are integrated on PEM on both sides. Design configurations of these electrodes are presented in Table 5-2. 100 nm gold is directly sputtered on PEM surface with no chrome used as an auxiliary layer. Consequently, the electrode thickness is reduced by more than 50% resulting in a higher surface to volume ratio. Table 5-2 presents the properties of the electrode configurations studied in this work.

Pore Density	$d_i$ [ $\mu\text{m}$ ]	$L_i$ [ $\mu\text{m}$ ]	pitch/diamter	$\Delta\sigma$ [%]	
D1 – High	200	700	1.4	56.849	
D2 – Med.	500	1000	2	19.545	
D3 - Low	800	1300	2.6	9.271	

**Table 5-2: Electrodes configuration**

$\sigma$  is introduced as the surface to volume ratio of the electrode. Number of pores in designs D1, D2 and D3 are 1024, 484 and 256 respectively. The changes in the electrode surface to volume ratio are calculated as follows and presented in Figure 5-7.

$$\sigma = \frac{A_{top} + A_{side}}{A_{top} \cdot t} \quad (5.3)$$

$$A_{top} = a^2 - \frac{D^2 \pi}{4} \cdot N \quad (5.4)$$

$$A_{side} = N \cdot \pi \cdot D \cdot t \quad (5.5)$$

Where:

$\sigma$ : Surface to volume ratio of the electrode

$A_{side}$ : side area of the pores

$A_{top}$ : top area of the electrode

N: Number of the pores in each design

D: Diameter of the pores = 500  $\mu\text{m}$

t: Electrode thickness = 100  $\mu\text{m}$

Substituting (5.4) and (5.5) into (5.3) and simplifying,

$$\sigma = \frac{1}{t} + \frac{N \cdot D \cdot \pi}{a^2 - \frac{D^2 \cdot \pi}{4} N} \quad (5.6)$$

Thus:  $\Delta\sigma$ , changes in the surface to volume ratio expressed in percentage is:

$$\Delta\sigma = \frac{\sigma_N - \sigma_0}{\sigma_0} \quad (5.7)$$

Where:

$\sigma_N$ : Electrode surface to volume ratio corresponding to “N” number of pores

$\sigma_0$ : Electrode surface to volume ratio with no pores (N=0)

As mentioned earlier, the electrode thickness in this work is 100 nm.

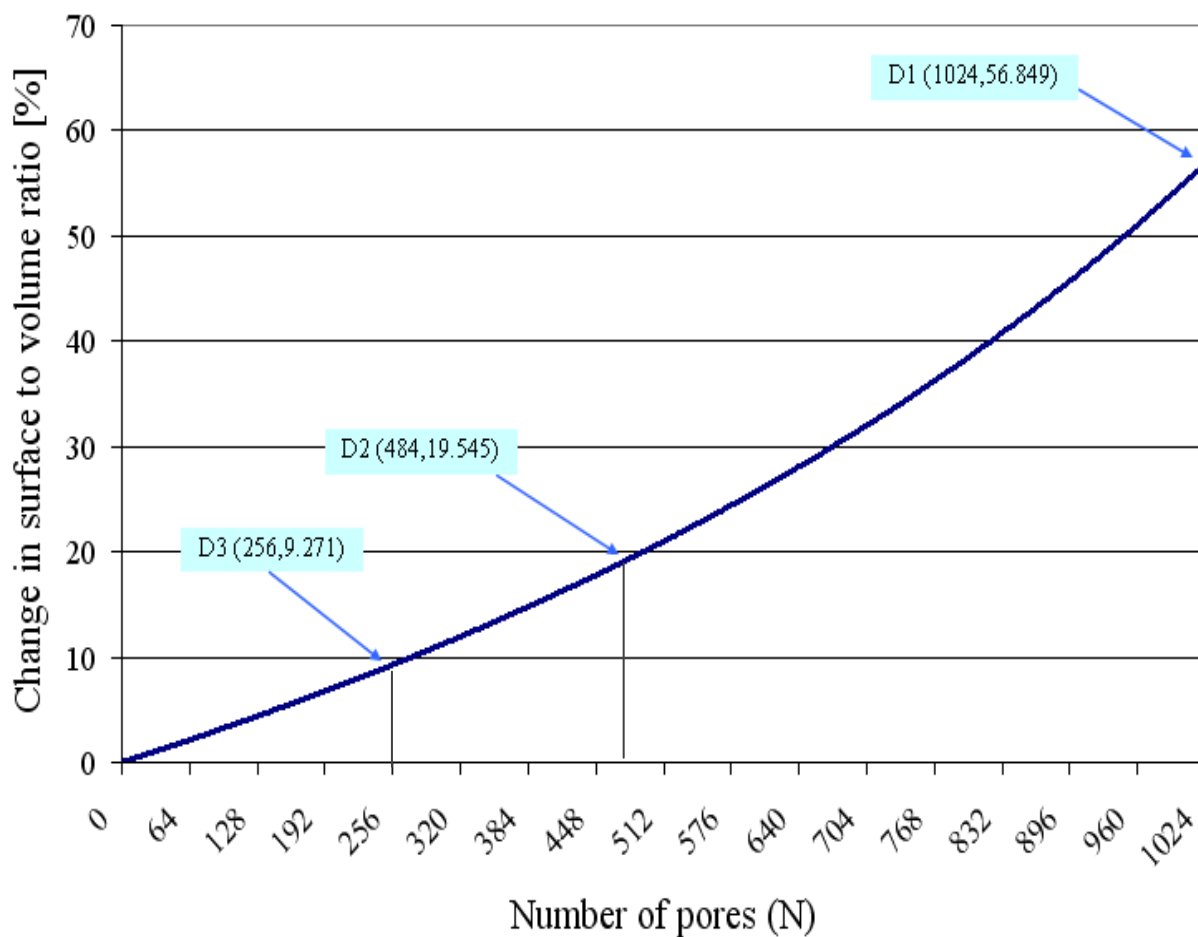


**Figure 5-7: Changes in the electrode surface to volume ratio with number of pores**

Thus, nine  $\mu$ PSC with three different combinations of PEM and three electrode patterns were fabricated and tested for performance. For each configuration two devices have been fabricated and the average output of the two measurements was used to plot the following graphs. 2% potassium ferricyanide solution was used as the catholyte and the OCV was monitored and compared in the following figures. Figure 5-8 represents a sample graph illustrating variations of the OCV with different electrode configurations on Nafion 212 as the PEM.

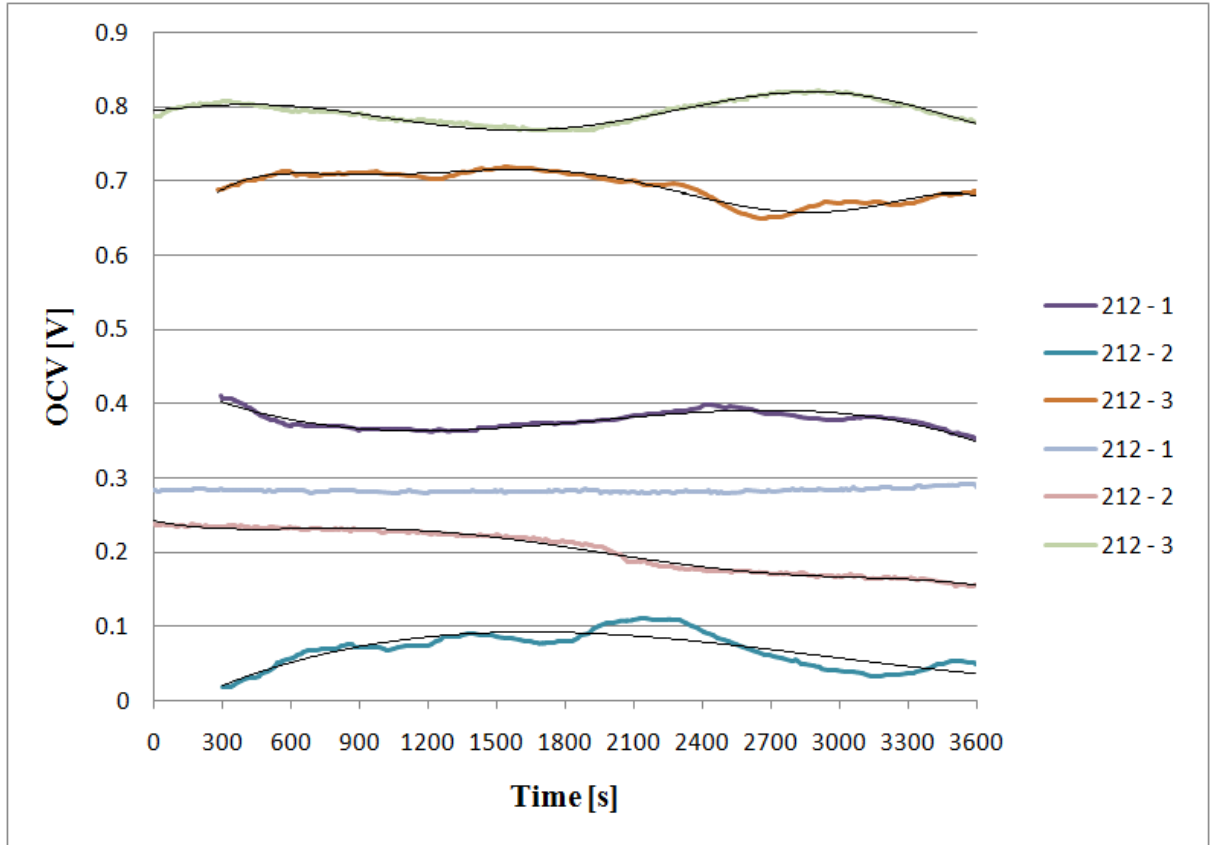


Figure 5-8: Variation of OCV with electrode configurations on Nafion 212

Average of the maximum OCVs for every combination is considered as the maximum OCV and the average of the mean values obtained over a range is considered as the mean OCV in the following figures.

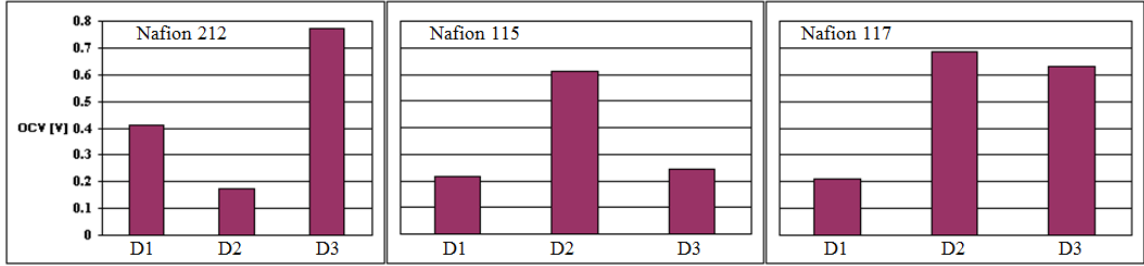


Figure 5-9: Variations of the maximum OCV with various electrode configurations on different PEMs

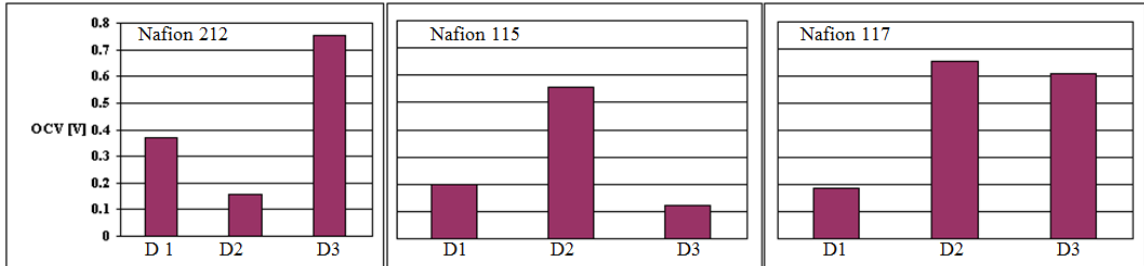


Figure 5-10: Variations of the mean OCV with various electrode configurations on different PEMs

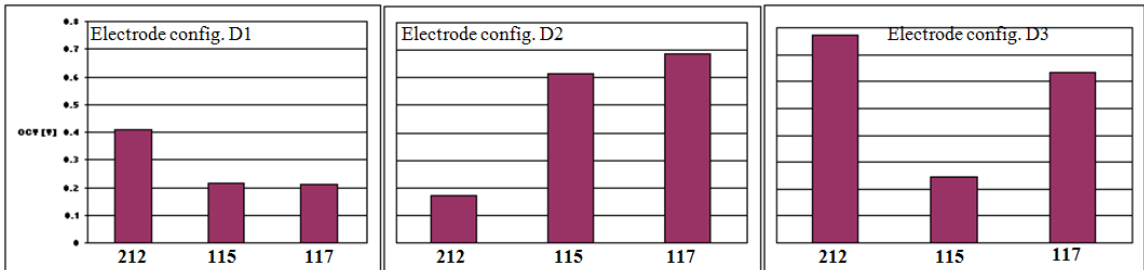


Figure 5-11: Variations of the maximum OCV with PEMs having the same electrode configuration

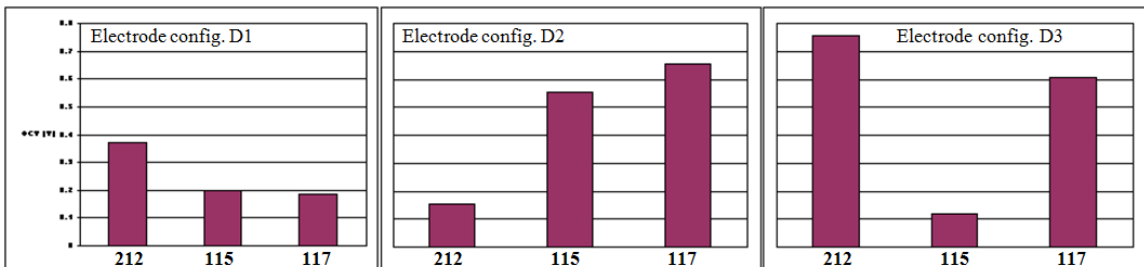


Figure 5-12: Variations of the mean OCV with PEMs having the same electrode configuration

It is observed that both the maximum and average OCV follow the same trend. In case of the thinnest membrane the highest output was observed with the electrode configuration D3 whereas for the other two membranes D2 and D3 outperformed D1. As seen from the above figures, the thinnest PEM did not produce high OCV. These results indicate that one has to select thickness of the membrane and associated pattern design depending upon the fabrication and other design parameters.

### 5.3.2 Effect of potassium ferricyanide concentration

As mentioned earlier, potassium ferricyanide is used as the catholyte solution in this study as the electron acceptor. Potassium ferricyanide ( $K_3[Fe(CN)_6]$ ) is a salt, bright red in color and shows greenish yellow once solved in water. Its redox potential is such that it is easily reduced to its related ferrocyanide making it a suitable to be used as the electron acceptor in many power cells. General oxidation-reduction of ferricyanide is mentioned below.



Since catholyte is directly involved in the electron transfer in the  $\mu$ PSC, it is believed that its concentration plays an important role and can affect the outputs. A  $\mu$ PSC with Nafion 117 and electrode D2 was used in studying the OCV with various potassium ferricyanide concentrations. The concentrations studied are 2, 5, 10, 15, 20 and 25 %. Figure 5-13 illustrates the no-load performance of the mentioned  $\mu$ PSC with various concentrations of catholyte followed by Figure 5-14 presenting a comparison of these concentrations and their effects on the maximum and mean open circuit voltage.

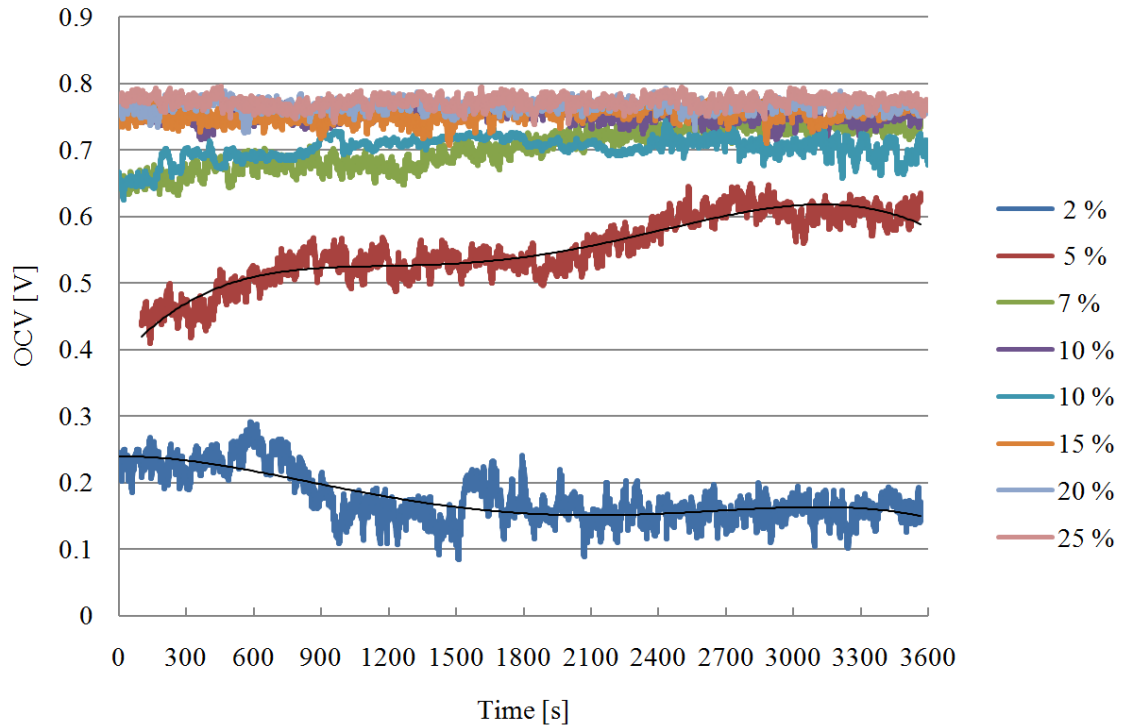


**Figure 5-13: OCV variations with different catholyte concentrations in a  $\mu$ PSC with Nafion 117 and electrode configuration D2**

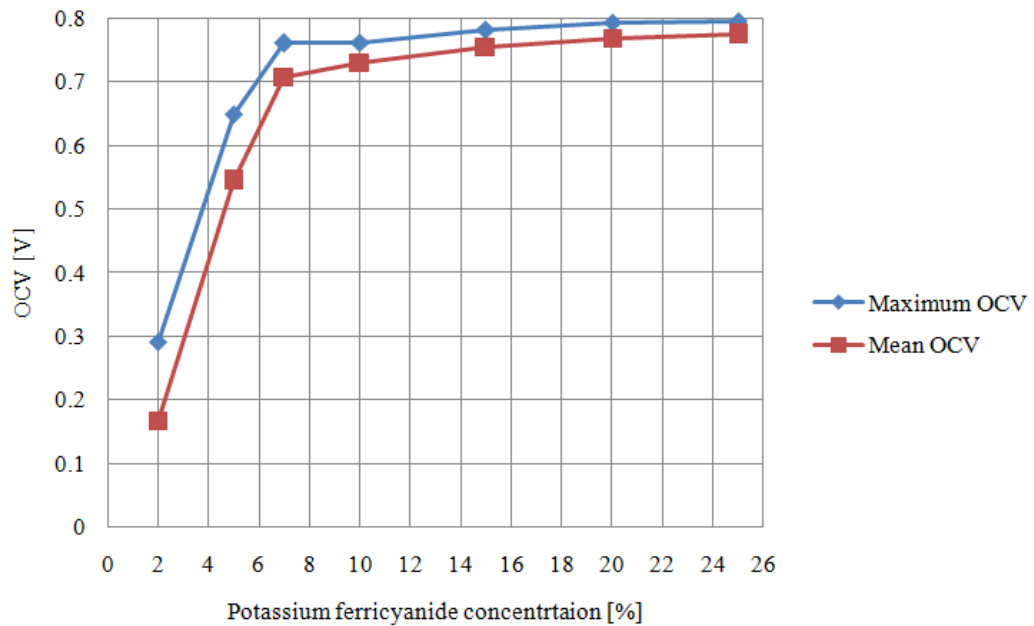


**Figure 5-14: Maximum and mean OCV with different concentrations of potassium ferricyanide with Nafion 117 and electrode configuration D2**

It can be seen that concentration of potassium ferricyanide directly affects the output voltage. Both the maximum and mean open circuit voltages show an increasing trend with using more concentrated solutions. The changes are very significant for the first few studied concentrations. For the higher concentrations (above 10%) these changes are still noticeable. Eventually the OCV tends to stabilize at concentrations around 25 %. As the performance saturates above 25 %, this concentration (25%) is chosen for other experiments in this work.

### **5.3.3 Effect of volume and concentration of algae**

Another parameter possibly affecting the efficiency of the electron transfer is proximity of the photosynthetic agents (algae in this study) to the PEM and the electrodes. For this study, 50 ml of green algae (*Chlamydomonas reinhardtii*) with an activity ratio of 0.742 and cell count of  $8 \times 10^5$  cells/ml was used as a stock solution. Different concentrations were prepared by diluting the stock solution with water. The concentrations used were  $\frac{1}{2}$ ,  $\frac{1}{4}$  and  $\frac{1}{8}$  of the stock concentration. In order to study the effect of proximity of the photosynthetic agents, four different volumes of algae were also studied. The volumes of 2 ml, 1.5 ml, 1 ml and 0.5 ml were used. Hence, sixteen experiments were performed by varying concentration and volume and with an external load of 20 k $\Omega$ . Potassium ferricyanide concentration of 25% was used as the catholyte in a  $\mu$ PSC with Nafion 117 membrane and the electrode pattern D3.

The the experiments with maximum volume or concentration were performed for 45 minutes including two periods of OCV observation (minutes 0-5 and 30-35). All other experiments were performed for 20. A sample result is shown in Figure 5-15 for the maximum volume with different concentrations. Two outputs (voltage and current) were

studied for each experiment. The period in which the OCV was monitored is indicated on the figure. As no load is being used during that period, no data for current is plotted during the OCV measurements. By normalizing the volume and concentration values and averaging the output voltage under the external load for each experiment, graphs similar to those presented in Figure 5-16 were obtained. Combining these results, an axonometric plot was obtained as presented in Figure 5-17.

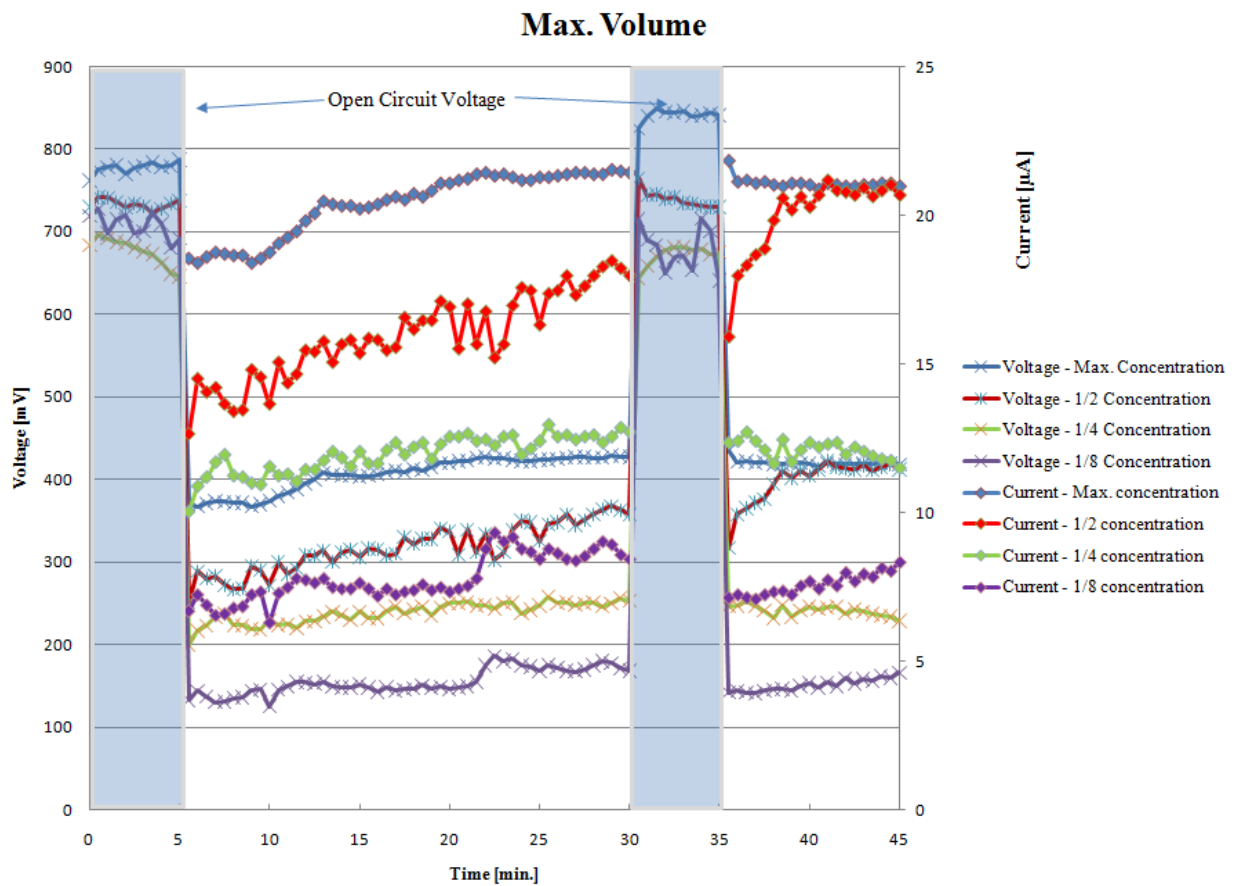


Figure 5-15: Effect of the algae concentration with maximum volume (2 ml)

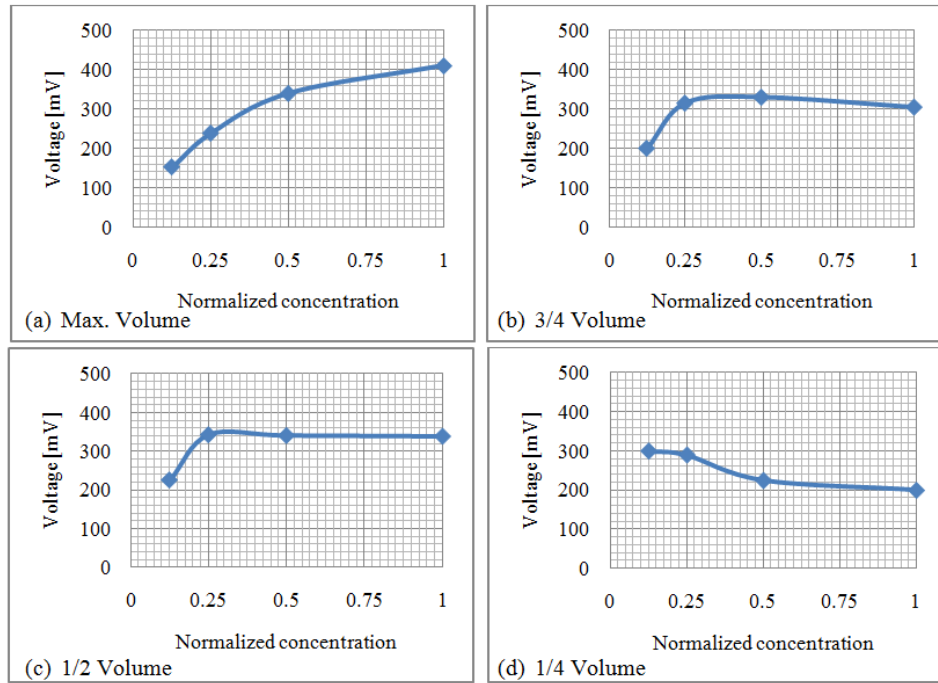


Figure 5-16: Variations of closed circuit voltage with normalized concentration for different chamber volumes

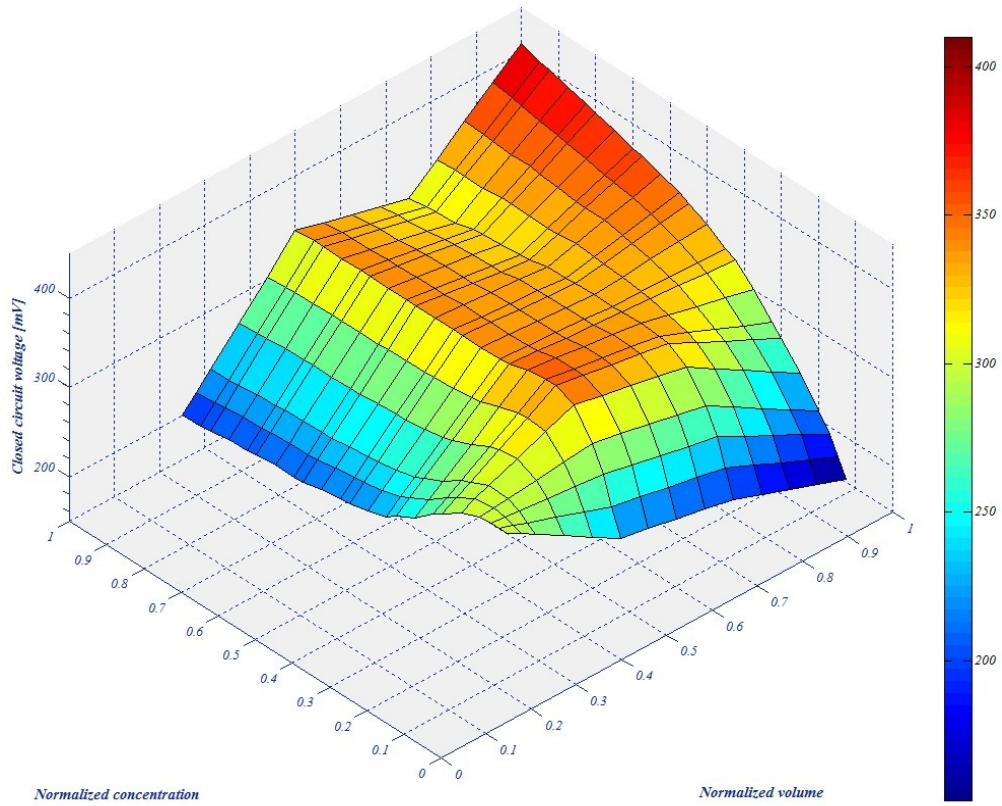
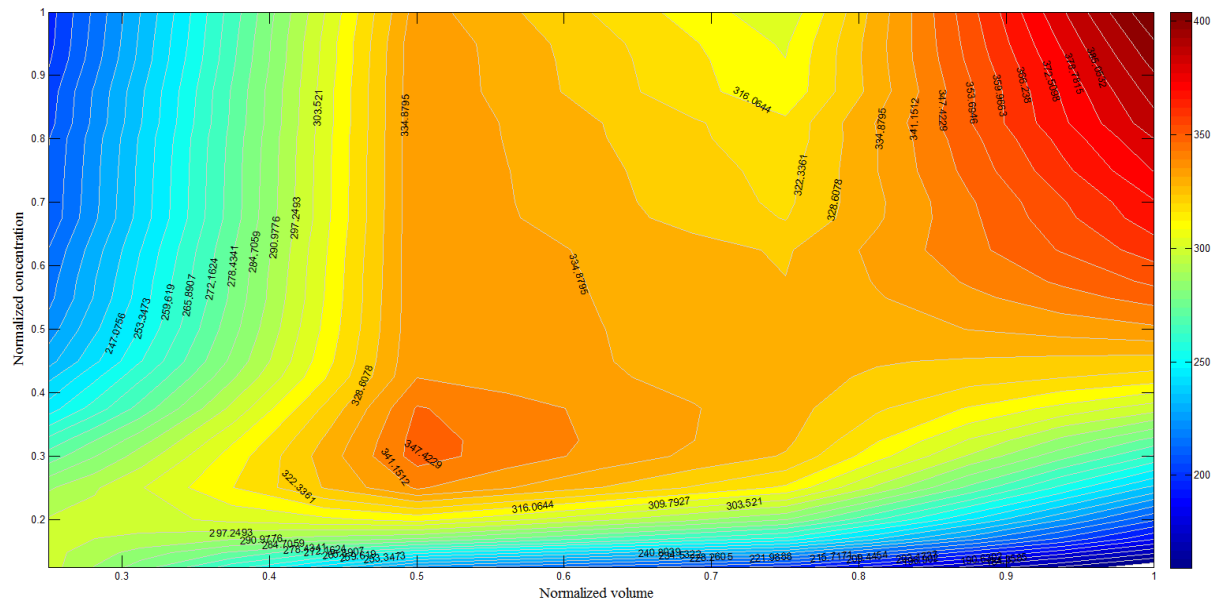


Figure 5-17: Axonometric plot of the closed circuit voltage variations with algae volume and concentration

It was found that there exists an optimal volume for each concentration used. Further experiments can provide the guidelines for determination of the optimal concentration given the volume of the  $\mu$ PSC, and vice versa. The existence of the phenomenon is due to the interplay between the following considerations: Photosynthesis is taking place only where algae are present. However, the zone which is of interest for ionic transfer is located in the vicinity of the PEM, as only those electrons released within this zone realistically diffuse to the electrode (gold). Increasing the volume of the media does not change this active zone; however, it increases the freedom of the cells to move away from it. As algae cells get further from the electrode, they contribute less to the electron transfer and even block some photons from reaching the cells present in the active area.



**Figure 5-18: Contour plot of the output voltage variations with algae's volume and concentration**

Based on Figure 5-17, the contour plot in Figure 5-18 illustrates the correlations between volume and concentration of algae affecting the output voltage. It can be observed that in higher concentrations, volume of algae directly affects the output voltage whereas in lower concentrations, an increase in volume results in a decrease in the output.

In the cases of lower concentrations, the number of cells that are involved in the ionic transfer and are close to the PEM, decrease as volume increases leading to reduction in performance. As cells have a tendency to float away from the electrodes and near to the surface, lower volume is preferred for lower concentration. As the concentration increases, the number of cells that are involved in ionic transfer and close to the PEM also increases with volume leading to an increase in performance.

Considering the current configurations of the  $\mu$ PSC and the external load, the maximum measured voltage was 410 mV. Assuming 75% (300 mV) and more as the acceptable range of operation, Figure 5-19 presents region of suitable concentration and volume.

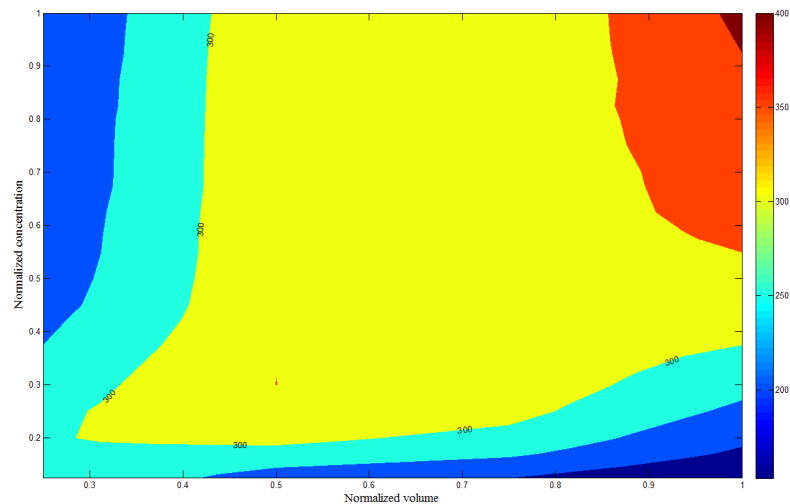


**Figure 5-19: Closed circuit voltage of 300 mV and more under 20 k $\Omega$  load**

#### 5.3.4 Effect of illumination

Illumination is also an important parameter for the photosynthetic cultures. During illumination photosynthesis is the major process (although respiration takes place with a very low rate). On the other hand, in the absence of light respiration would be the major process.

A  $\mu$ PSC with Nafion 117 as the PEM and electrode configuration D2 was used in an experiment for 80 minutes with 10 minute cycles of light and dark. The OCV was monitored in the last two cycles whereas in the other cycles  $1k\Omega$  resistance was used as the load. Very high value of the resistance selected in the previous experiments led to lower output current. In this experiment, it was decided to choose a lower resistance to increase the current and better observe the variations. Potassium ferricyanide with 25% of concentration was used as the catholyte.

Figure 5-20 shows the variations of voltage and current with light. In all the experiments so far the light intensity was 600-650 lux. In this experiment however, the measured photometric parameter of the illumination source reaching the surface of the  $\mu$ PSC was 1100-1200 lux.

In order to comment on the effect of illumination, a more comprehensive study and some new sets of experiments are suggested in the Future Works. The result of the experiment regarding the effects of illumination performed in this work is however shown in Figure 5-20.

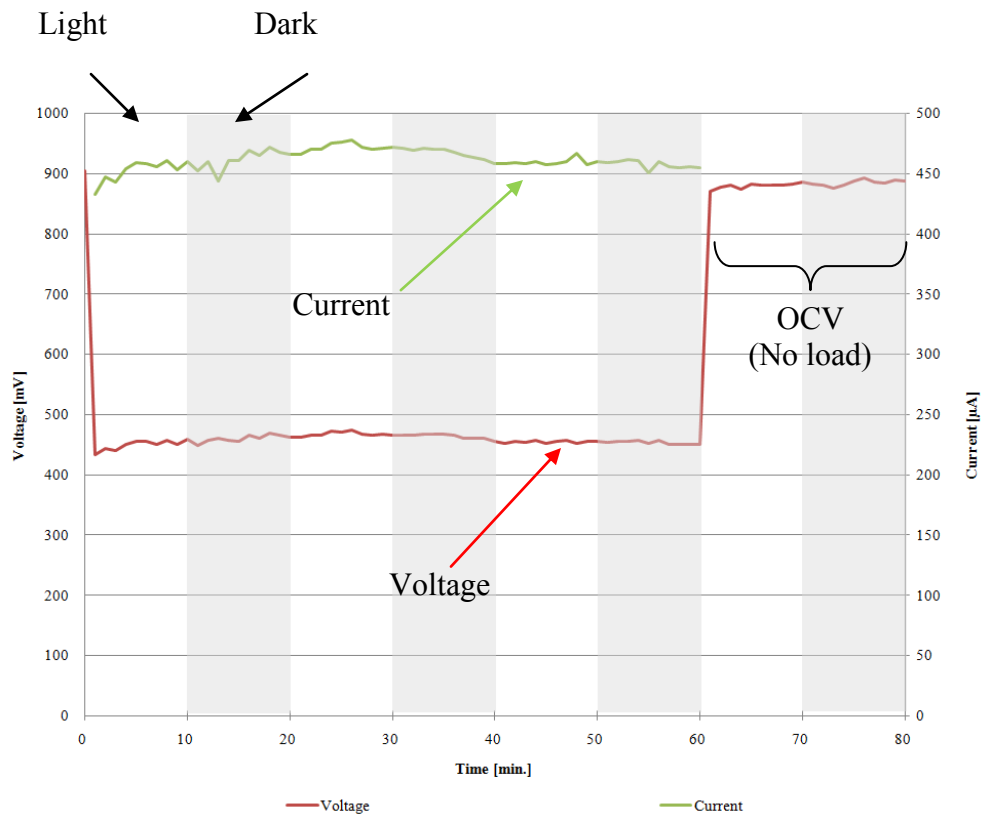


**Figure 5-20: Variations of voltage and current with illumination under load and no-load conditions**

Quality of the photosynthetic (PS) organism cultures and components of the  $\mu$ PSC are probably the most important factors in functionality of the  $\mu$ PSC. Both the PS sample and the  $\mu$ PSC used in this experiment were already optimized according to the results of the previously mentioned experiments. That is probably one of the reasons that the outputs do not change significantly. Little fluctuations in Figure 5-20 are also believed to be related to the fluctuations of the PS sample as observed in previous experiments. In some studies, the highest outputs were reported to be those in dark. Continuous illumination increases the temperature as well. Photosynthesis tends to flatten at about 25 °C. Respiration however, continues to rise above this temperature. The higher the temperature the more dominant respiration becomes. That is probably another reason that the highest outputs are not necessarily obtained under illumination. It should be noted, however, that these cycles help the  $\mu$ PSC and more precisely the PS culture to

restore itself and undoubtedly affect the life time of the device without refilling the analyte. Hence, illumination cycles are strongly recommended for extending the life of the photosynthetic elements and the device.

### 5.3.5 V-I Characteristics

Voltage-current ( $V-I$ ) characteristics are useful to understand the behavior of a power generating device. They are also useful for designing power converters and performing electrical modeling of the device.  $V-I$  characteristics of  $\mu$ PSC studied in this work were obtained by testing a  $\mu$ PSC with Nafion 117 and electrode pattern D2 which was found to be an optimal configuration among the previous experiments. Potassium ferricyanide solution with 25% concentration was used as the catholyte. Figure 5-21 shows variations of the output voltage and current while the resistance is increased.

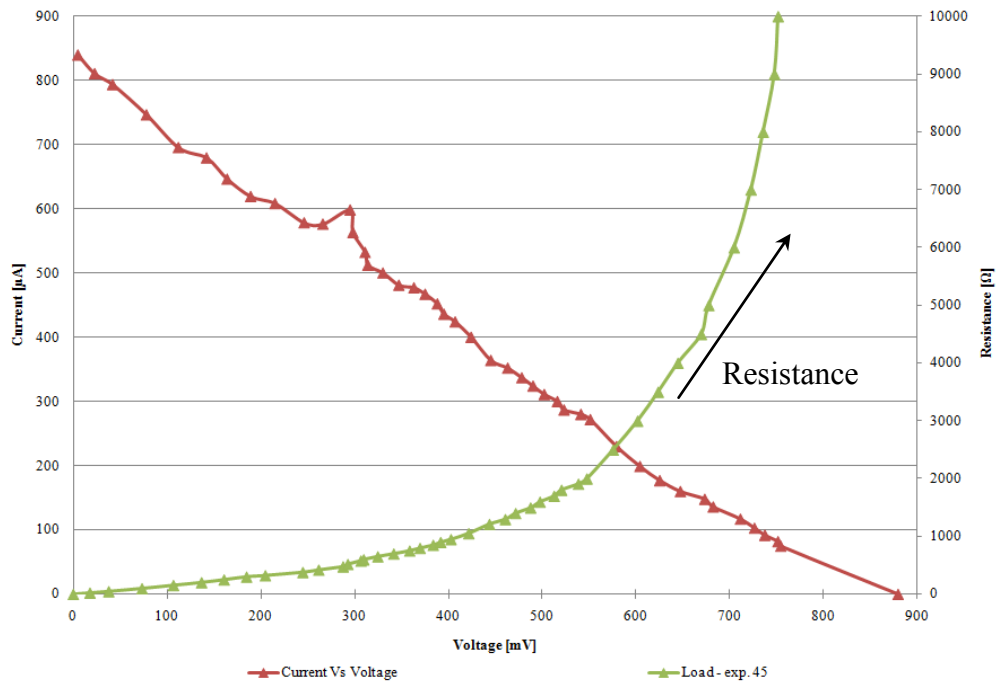
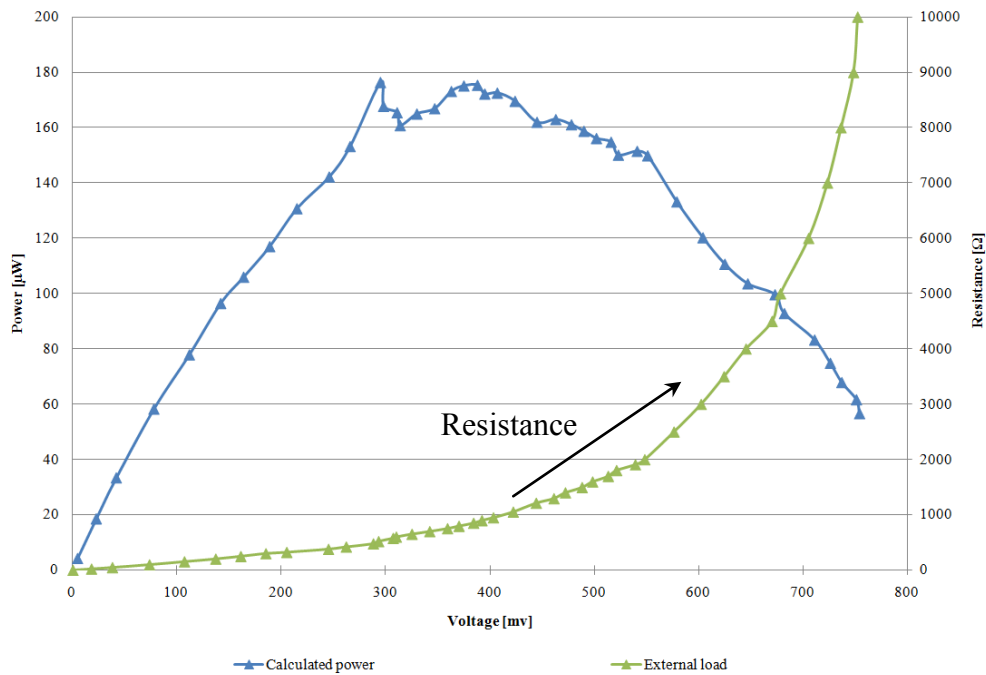


Figure 5-21: V-I characteristics of a  $\mu$ PSC with Nafion 117 and electrode pattern D2



**Figure 5-22: Power generation curve of a  $\mu$ PSC with Nafion 117 and electrode pattern D2**

As observed,  $V$ - $I$  characteristics show linear behavior with the change in resistance. As the resistance is increased there would be more barrier against flow of the electrons resulting in a decrease in current and an increase in voltage. Beyond a certain point of increase in the resistance, even though the voltage still increases, the resulting current significantly decreases, causing the output power to decrease as well. Hence, studying the power generation curve (Figure 5-22) enables defining a meaningful operational working range for  $\mu$ PSC. With current configurations, the operational range of the device is suggested between 300–500 mV, providing the highest generated power (approximately 175.37  $\mu$ W corresponding to 36.23  $\mu$ W/cm<sup>2</sup>).

Electrical power was calculated according to equations below. Combining Equation 5.9 with the Ohm's law (Equation 5.10) results in an alternate expression for electrical power (Equation 5.11).

$$P = V \times I \text{ [w]} \quad (5.9)$$

$$I = \frac{V}{R} \text{ [A]} \quad (5.10)$$

$$P = I^2 \times R = \frac{V^2}{R} \text{ [w]} \quad (5.11)$$

### 5.3.6 Long-term Behavior Analysis

Two  $\mu$ PSCs were used for the long term analysis, one for open circuit voltage measurements and the other for closed circuit voltage measurements with 20k $\Omega$  resistance. For the OCV, a  $\mu$ PSC with Nafion 115 and electrode pattern D3 was used whereas the  $\mu$ PSC with Nafion 117 and electrode pattern D2 was used for the closed circuit voltage observations. Both experiments have been performed for 25 hours and 25% potassium ferricyanide was used as the catholyte. The results of the experiments are shown in Figure 5-23.

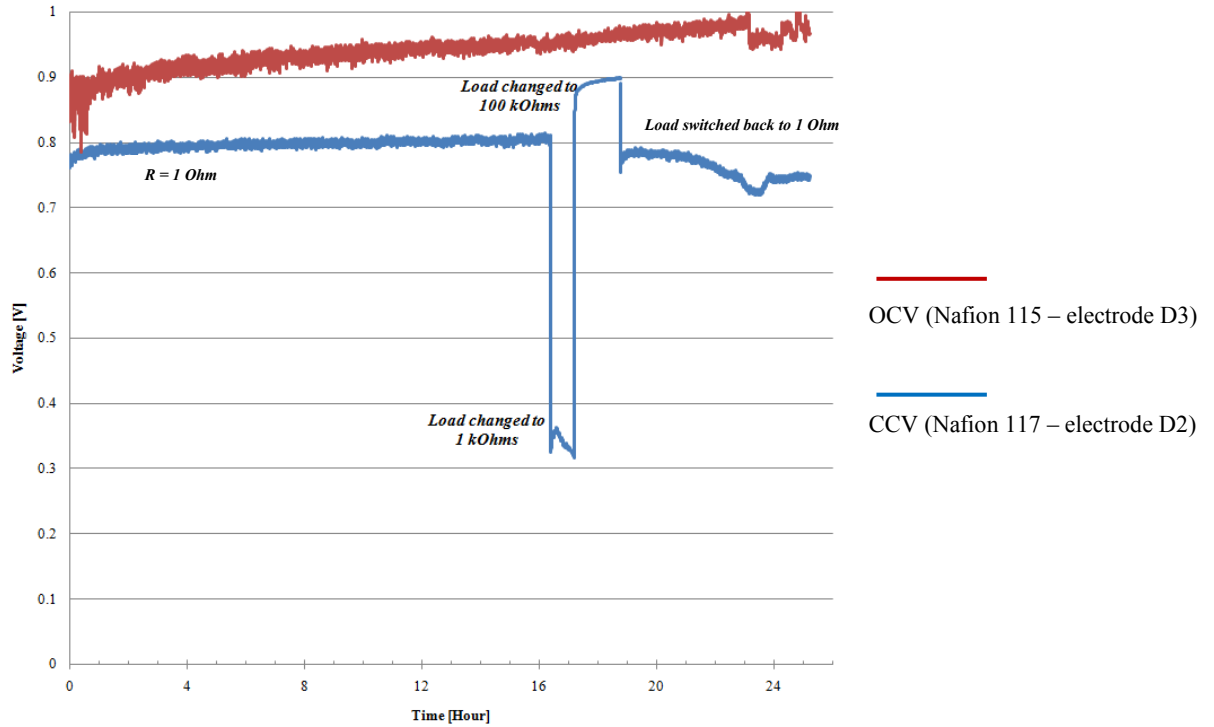


**Figure 5-23: long-term behavior of PSC**

The long-term behavior of the device showed an increasing trend for the OCV. Since open chamber (anodic chamber without glass cover)  $\mu$ PSC was used for these experiments, evaporation of the media was faster. The maximal OCV of more than 0.9 volts was observed and after significant fraction of the media has evaporated the increasing trend changed to a decreasing one (Figure 5-23). For the long-term behavior with external load (with Nafion 117 and electrode D2), the 20 k $\Omega$  resistor was used initially. Due to the scale used to plot results in Figure 5-23, some minor fluctuations are not visible, however, enlarging a portion of the results (Figure 5-23) shows some periodic fluctuation in the output similar to those observed in other experiments. Using this load, the output voltage tended to stabilize around 0.8 volts. After approximately 17 hours of continuous operation, the load was changed to 1 k $\Omega$  and the output voltage dropped as

expected. For verification, a load of greater resistance was used as well. Current decreased and the voltage increased and got closer to the OCV when a 100 k $\Omega$  resistor was used. Eventually after about 20 hours, considerable evaporation of the media resulted in a decreasing trend.

## 5.4 Conclusion

A novel polymer-based photosynthetic power cell was designed and fabricated. After verifying the functionality of the device, a series of experiments were conducted to obtain the most stable  $\mu$ PSC, given the proposed fabrication method. Some parameters affecting the performance of the device were studied; long-term behavior and  $V$ - $I$  characteristics were observed. Decreasing the thickness of the PEM and increasing the surface to volume ratio of the electrodes in general results in more efficient ion transfer. This is, however, limited by the imperfections of the fabrication method as in this study the thinnest PEM and electrodes with highest pore density did not provide the most stable  $\mu$ PSC and resulted in a relatively poor performance of the device. Hence Nafion<sup>®</sup> 115 / 117 and the electrode pattern with medium pore density (Table 4) were suggested for the future experiments.

The performance of the  $\mu$ PSC was found to be strongly dependent on the concentration of catholyte solution. Up to certain limit (around 25%), increasing the concentration of the potassium ferricyanide increased the OCV significantly; as 25% concentration was reached the performance became saturated.

For every concentration of the photosynthetic agent used, there exists an optimal volume of the media to be used in the  $\mu$ PSC. Using smaller volume might not provide the

maximum power generation capacity while using more might be non influential. Therefore, one has to select right combination of volume and concentration for better performance.

The long-term behavior of PSC showed an increasing trend for the output voltage for almost 20 hours after which evaporation of the media resulted in a decrease in the output. Hence continuous circulation of media into the chamber maintaining fixed desired volume at all time is suggested for efficient operation.

*V-I* characteristics of the device indicate the optimal operation range to be 300 to 500 mV, resulting in power generation of more than 175.37  $\mu\text{W}$  corresponding to power density of 36.23  $\mu\text{W}/\text{cm}^2$ .

This chapter studied the influence of design and operating conditions on the performance of the  $\mu\text{PSC}$  with green algae. Next chapter presents results with other photosynthetic organisms.

# **Chapter 6**

## **Experiments with other photosynthetic organisms**

## **6 Experiments with other photosynthetic organisms**

This chapter covers the objectives 3-e and 3-f of the “Objective and scope of the thesis” in Section 1.6.

### **6.1 Introduction**

As was mentioned in previous chapters, there are many parameters which might affect the efficiency of the device. These parameters vary from fabrication parameters to biological and environmental parameters. The parameters studied in this chapter are: glucose addition, different photosynthetic samples and mediators.

Photosynthesis (P), respiration (R) and P/R ratio were discussed earlier in Chapter 2. Glucose is a direct indication of cellular respiration. Hence, addition of glucose increases respiration rate. Consequently, changing the P/R ratio by adding glucose to the anodic compartment is expected to affect the performance of the  $\mu$ PSC. Addition of mediators to growth media to facilitate the electron transfer in  $\mu$ PSC while keeping the cultures intact is another promising study performed partially in this work.

#### **6.1.1 Glucose addition**

Glucose ( $C_6H_{12}O_6$ ), a monosaccharide, is an important carbohydrate which is used by cells as a source of energy. It is one of the main products of photosynthesis and an initial reactant in cellular respiration. Solubility of glucose in water (25 °C) is equal to 91g/100ml. Glucose solutions with six different concentrations (5%, 10%, 20%, 30%, 50% and 70 % of that maximal concentration) were prepared (Figure 6-1).

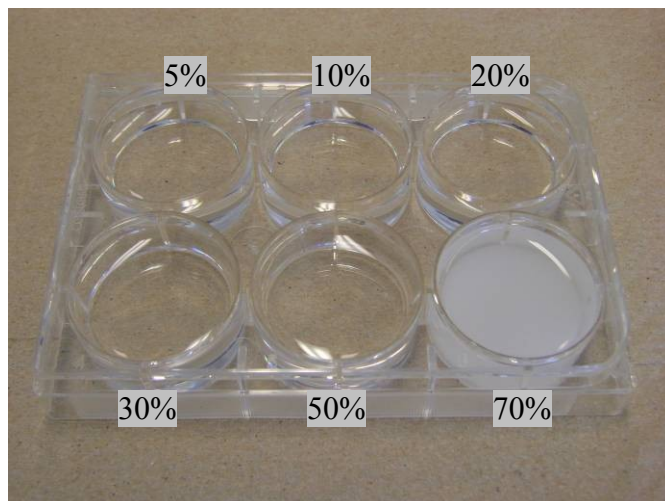


**Figure 6-1: Glucose solutions of different concentrations**

Green algae (*Chlamydomonas reinhardtii*) with cell count of 1,300,000 cells/ml and activity ratio ( $\Phi_m$ ) of 0.680 were used as the photosynthetic agent. Potassium ferricyanide with 10% concentration was used as the catholyte.

A  $\mu$ PSC with Nafion 115 as PEM and electrode D2 was used in three experiments comparing the no load performance with no glucose, 5% and 10% glucose solution. The experiment was performed for one hour and a lot of fluctuation was observed (Figure 6-2). Acquisition was started right after adding 0.5 ml of glucose solution to the anolyte. Higher concentrations of glucose were studied later with the same  $\mu$ PSC and the results were summarized in Figure 6-2.

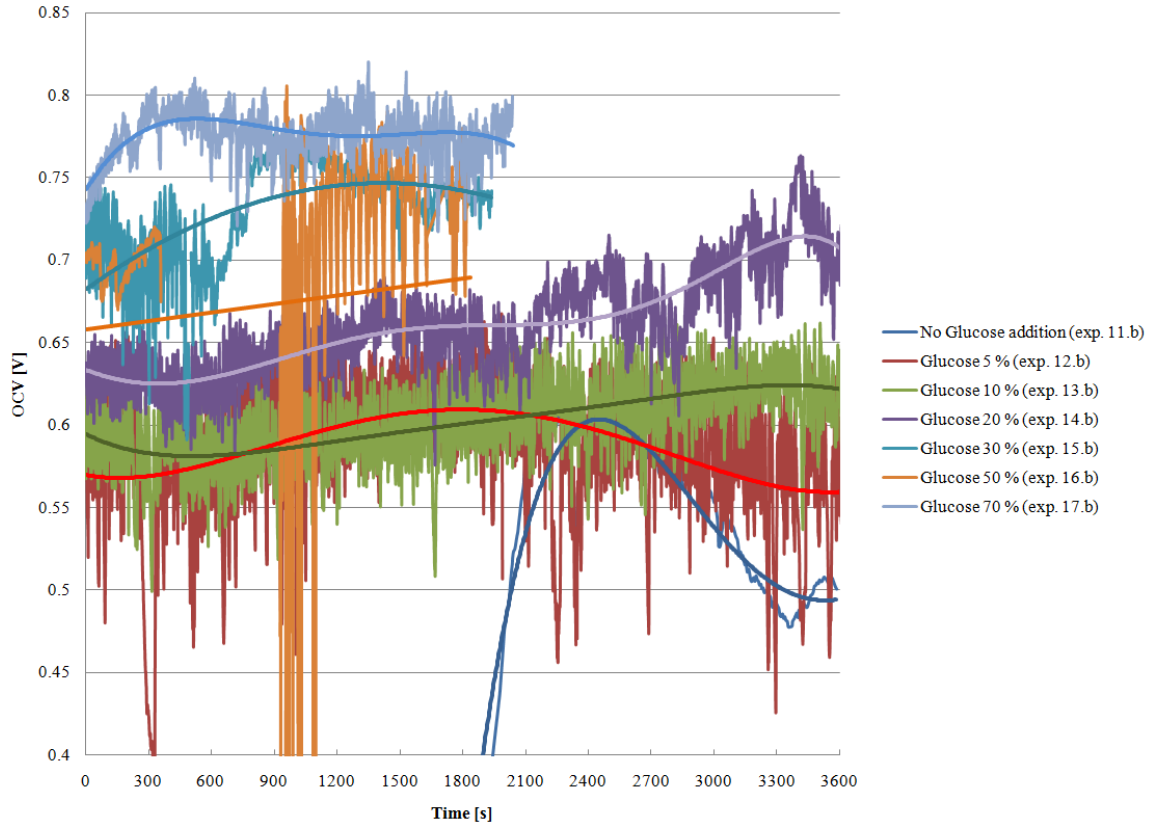
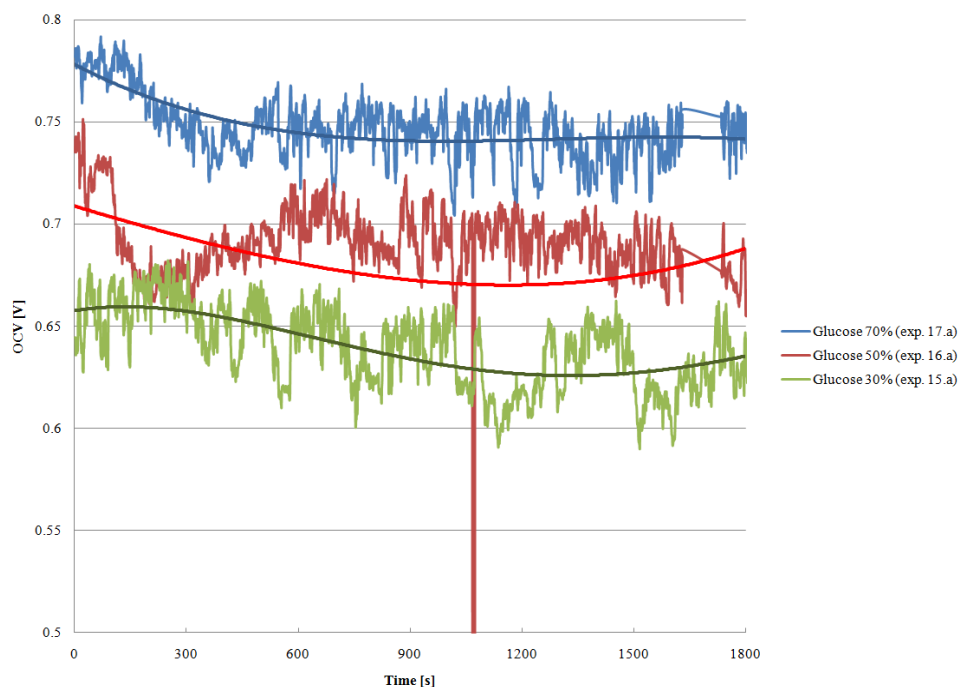


**Figure 6-2: Effect of glucose addition with  $\mu$ PSC with Nafion 115 and electrode D2**

The higher concentrations as well as the experiments with no glucose were only monitored for thirty minutes as seen in Figure 6-2.

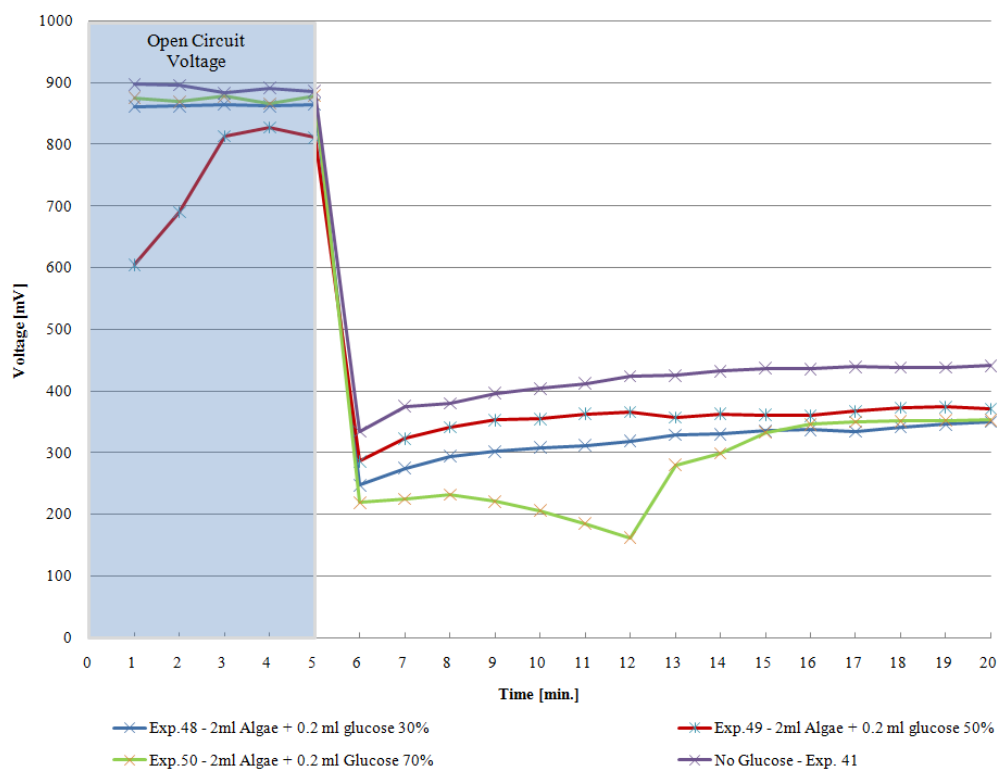
The higher concentrations of glucose were tested once more with another  $\mu$ PSC. In another set of experiments, a  $\mu$ PSC with Nafion 117 and electrode D2 was used. 0.5 ml glucose solution of 30%, 50% and 70% was added in each experiment, acquisition was started, and no load performance was monitored for thirty minutes.

Figure 6-3 presents the results of glucose addition with  $\mu$ PSC with Nafion 117 and electrode D2. Less fluctuations were observed when higher concentrations of glucose were used.



**Figure 6-3: Effect of glucose addition with  $\mu$ PSC with Nafion 117 and electrode D2**

Later on, it was decided to explore the combined influence of two parameters: effect of illumination and addition of glucose. The purpose was to study not only the effect of glucose addition but also to study the addition time and its effect on the performance. Ten-minute cycles of dark/light were used. Same amount of glucose (0.5 ml) was added at time  $T=0$  and  $T=10$  [min] to investigate the variations. It was also decided to reduce the amount of glucose added to the anolyte. Hence, an experiment was performed with a  $\mu$ PSC with Nafion 115 and electrode D3 in which acquisition was started one minute after addition of 0.2 ml glucose of 30%, 50% and 70% of concentration to the anolyte.  $1\text{k}\Omega$  resistance and potassium ferricyanide with 25% concentration were used for the experiment.



**Figure 6-4: Effect of glucose addition on performance of a  $\mu$ PSC with Nafion 115 and electrode D3 and external load of  $1k\Omega$**

In the previous experiments higher concentrations of glucose showed higher outputs. In this experiment however, it was observed that addition of glucose does not necessarily increase the performance. As seen in Figure 6-5, after engaging the external load, the variations became more significant as compared to the no load performance period. Performance with no added glucose showed the highest outputs and the voltage from  $\mu$ PSCs with glucose tended to stabilize around 350 mV for  $1k\Omega$  resistance.

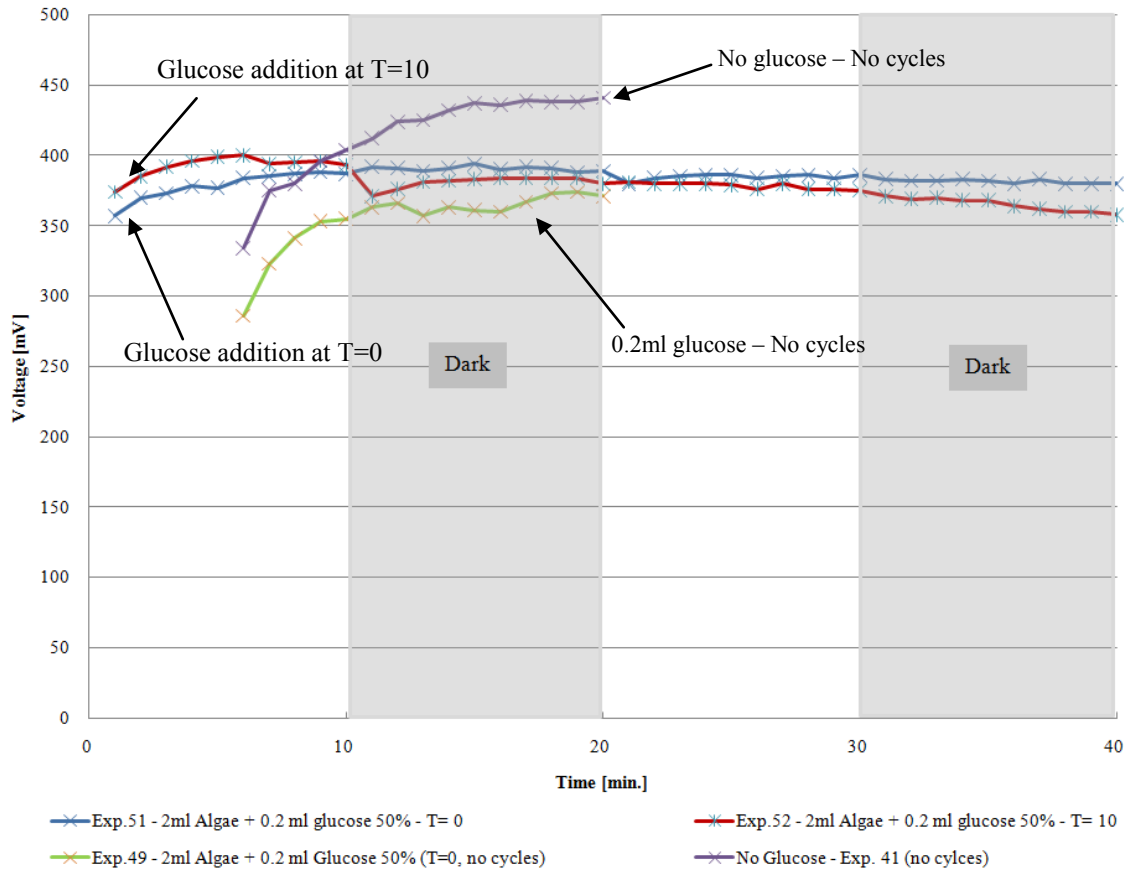


**Figure 6-5: Effect of glucose addition and injection time on the closed circuit voltage under 1kΩ resistance and μPSC with Nafion 115 and electrode D3**

It was concluded that glucose addition can affect the performance of the device since it changes the P/R ratio however; addition of glucose has another inevitable consequence which is the increase in volume and decrease in concentration of the photosynthetic sample used in the anodic chamber. This engages another affecting parameter which was studied earlier in chapter 5, effect of volume and concentration of the photosynthetic agents. Hence, once using glucose, proper considerations should be taken into account.

### 6.1.2 Photosynthetic organisms

All the experiments mentioned so far have been performed using one type of green algae (*Chlamydomonas reinhardtii*) as the photosynthetic agent. Two additional organisms were tested in the following experiments. Table 6-1 includes the parameters and conditions of the cultures used in this experiment.

A  $\mu$ PSC with Nafion 115 and electrode D3 was used and the V-I characteristics were obtained for each sample. Potassium ferricyanide with 25% of concentration was used as the catholyte.

<b>Experiment No.</b>	<b>Organisms name</b>	<b>Species</b>	<b>Activity (<math>\Phi</math>)</b>	<b>Cell count [cells/ml]</b>
<b>Experiment 53</b>	Green algae	<i>Chlamydomonas reinhardtii</i> CC125	0.647	835 200
<b>Experiment 54</b>	Diatom	Navicula Pelliculosa	0.392	637 200
<b>Experiment 55</b>	Cyanobacteria	632	0.659	1 025 000

**Table 6-1: Parameters of the cultures used**

Figure 6-6 presents the V-I characteristics of the  $\mu$ PSC containing mentioned photosynthetic organism. The experiment performed was similar to the V-I characteristics mentions in Chapter 3. The resistance was increased gradually and the voltage and current were measured as the outputs. These results were used to obtain power generation curve presented in Figure 6-7.

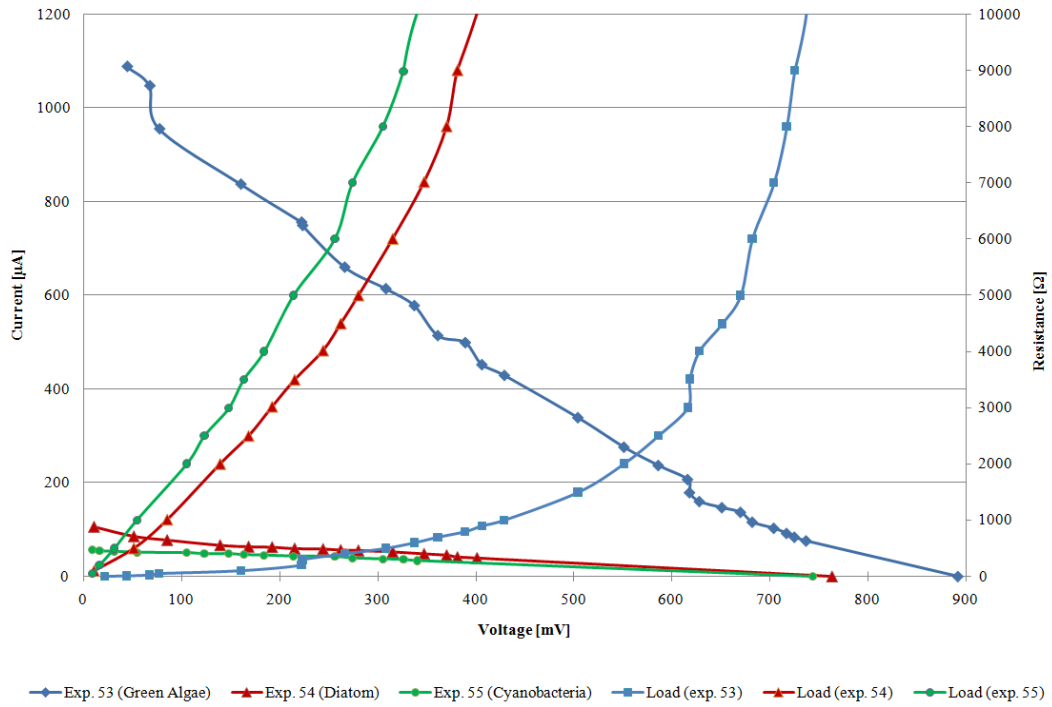


Figure 6-6: Comparison of V-I characteristics of  $\mu$ PSCs with different photosynthetic samples

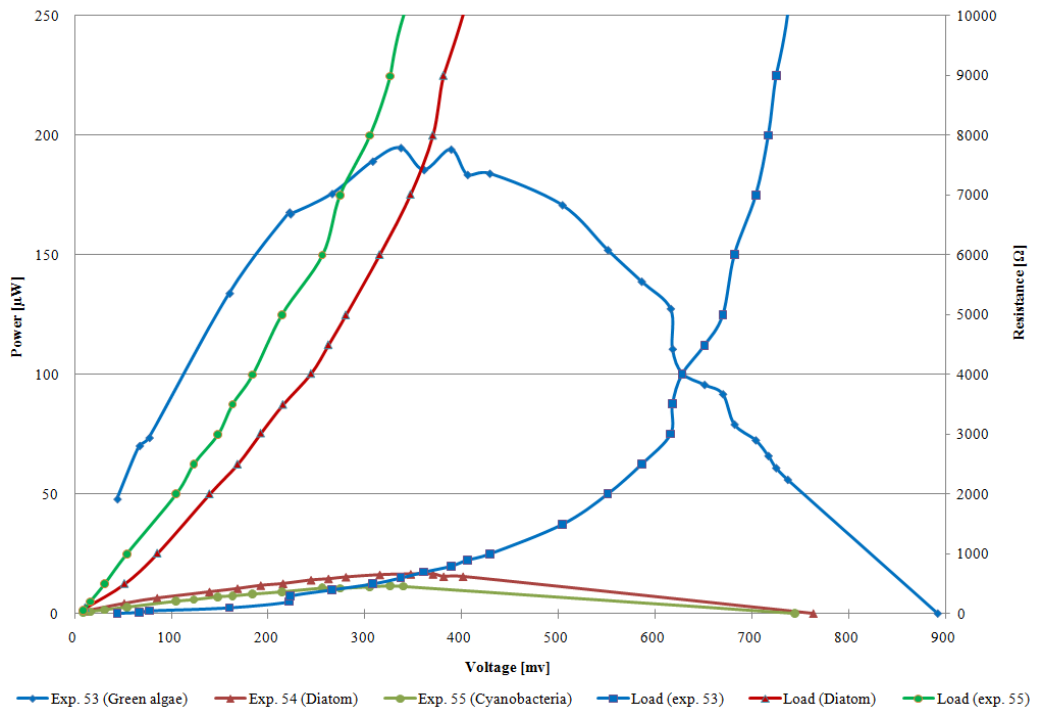


Figure 6-7: Power generation of different photosynthetic samples

According to Figure 6-7, the highest outputs correspond to green algae. However, we believe that commenting on the mentioned graph in fact requires more investigation and consideration due to the following: Same device was used for all the three experiments, with photosynthetic agent being changed. Compared to other power generation curves obtained earlier, it is clearly observed that the  $\mu$ PSC was not in as good conditions as those tested earlier. Moreover, during the experiment some leakage was observed which just verifies the mentioned comment. These conditions were deteriorating over time. Hence, the  $\mu$ PSC was found to be relatively in better conditions when used with Algae comparing the last two experiments with Cyanobacteria and Diatom. Hence, for future works it is suggested to test more samples for verification purposes. An important observation however was that the  $\mu$ PSC is able to produce electricity with different samples. This adds to performance diversity of  $\mu$ PSC and brings new topics to be investigated such as optimizing the parameters and conditions relative to the photosynthetic sample used.

### **6.1.3 Mediators**

Mediators are chemical solutions used to strain living cells and added to some growth media of bacteria and cell cultures. This section is only a brief study to investigate the effect of addition of mediators to the growth media. Experiments with each sample used below in  $\mu$ PSC and obtaining V-I characteristics is suggested for future works.

Algae or any other photosynthetic sample is grown in a media. The media used to grow green algae and cyanobacteria are namely HSM and CHU respectively.

In this study three mediators are used (Methylene blue (MB), Thionine acetate (TA) and Neutral red (NR)). Two photosynthetic samples (Green algae (CC125) and Cyanobacteria (632)) with known density (cell count [cells/ml]) are used as well. Hence, 24 samples are prepared details of which are included in Table 6-2.

Combining, photosynthetic agents, media and mediators mentioned earlier, various combinations can be considered. The following presents the investigations in this work.

- Cell count of cultures with no mediators added, defining the natural growth rate
- Cell count of the cultures with mediators added, defining the modified growth rate
- Absorption spectrum of the media with no mediator, monitored for 4 day
- Absorption spectrum of media with mediators added and monitored for 4 days

Sample No.	Mediator (5µl in 3ml)	Cell count [cells/ml]	
		Green algae	Cyanobacteria
A1 – C1	No mediator	32000	37333
A2 – C2		32500	30000
A3 – C3		40500	46000
A4 – C4	Methylene blue	68000	43000
A5 – C5		50000	52000
A6 – C6		48000	63600
A7 – C7	Thionine acetate	49000	52000
A8 – C8		33000	51500
A9 – C9		42500	40000
A10 – C10	Neutral red	38000	40000
A11 – C11		425000	64000
A12 – C12		41500	50000

**Table 6-2: Samples used for studying the effect of mediators**

The values measured above are considered as the reading at time T=0 [days]. Cell count measurements are performed in 1, 2 and 4 days after addition of mediator and the effect of mediators on growth of the cultures is shown in Figure 6-8 and Figure 6-9.

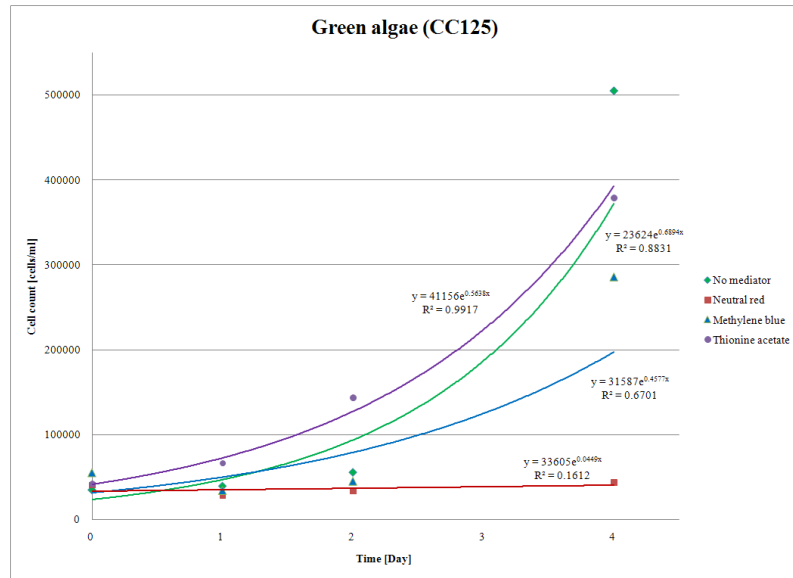


**Figure 6-8: Effect of mediators on growth rate of green algae**

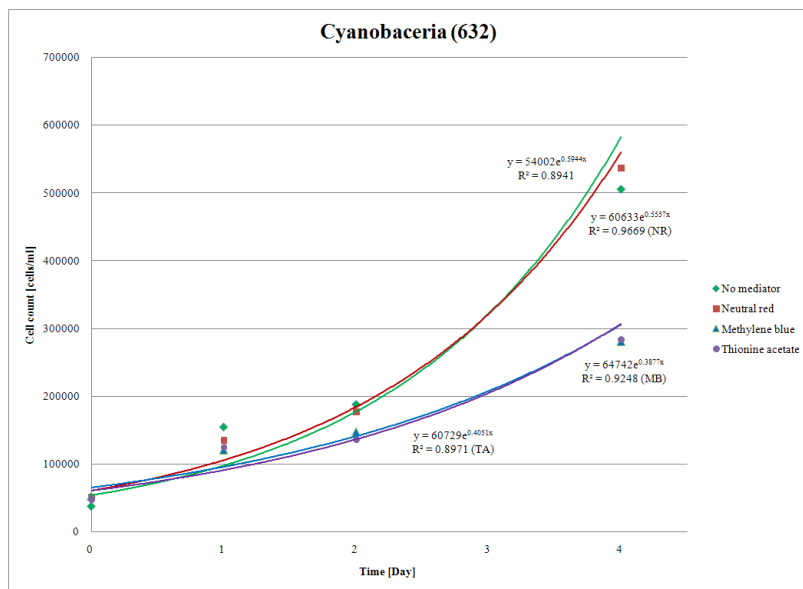


**Figure 6-9: Effect of mediators on growth rate of cyanobacteria**

Considering the growth period of the cultures thionine acetate provided the closest growth comparing the neutral conditions in case of green algae cc125. In case of cyanobacteria the same statement is true using neutral red. This implies that some cells couldn't survive due to addition of other mediators.

It was also decided to study the absorption spectrum of these samples to see which ones stay intact. Incubator light spectrum, room light spectrum as well as absorption spectrum of the green algae, cyanobacteria and media were obtained as references.

The light intensity used for the growth period (preparation of samples in the incubator) used in all experiment (both this section and other experiments mentioned earlier) is equal to 10 klux. Figure 6-10 presents the incubator light spectrum followed by the room light spectrum in Figure 6-11.

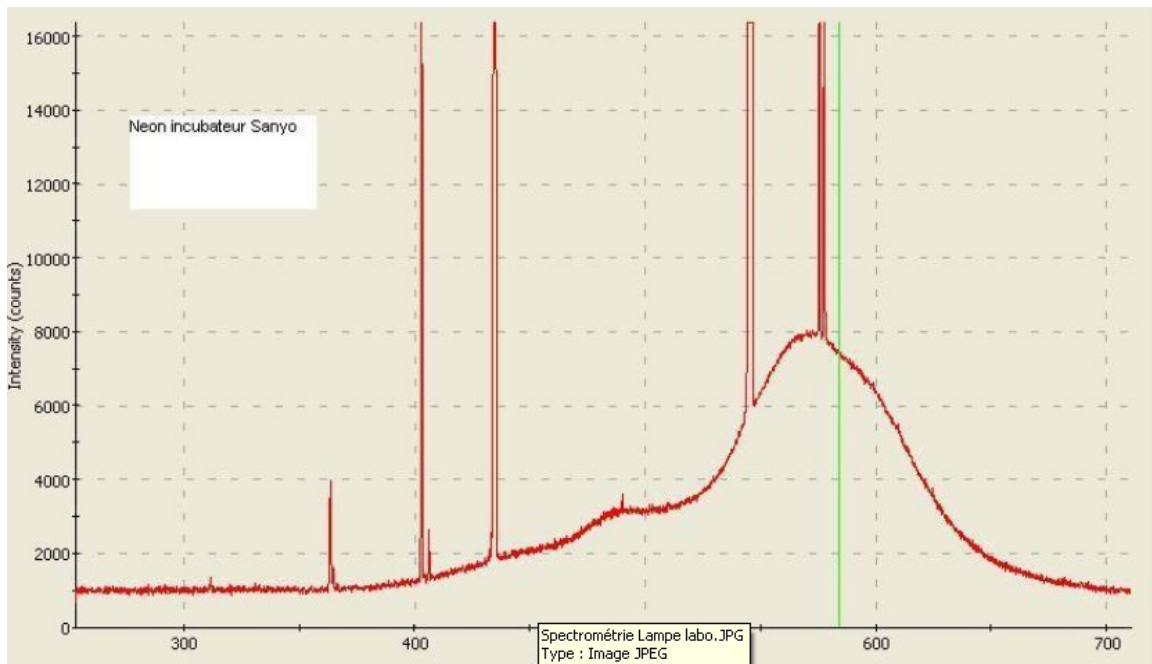


**Figure 6-10: Incubator's light spectrum**

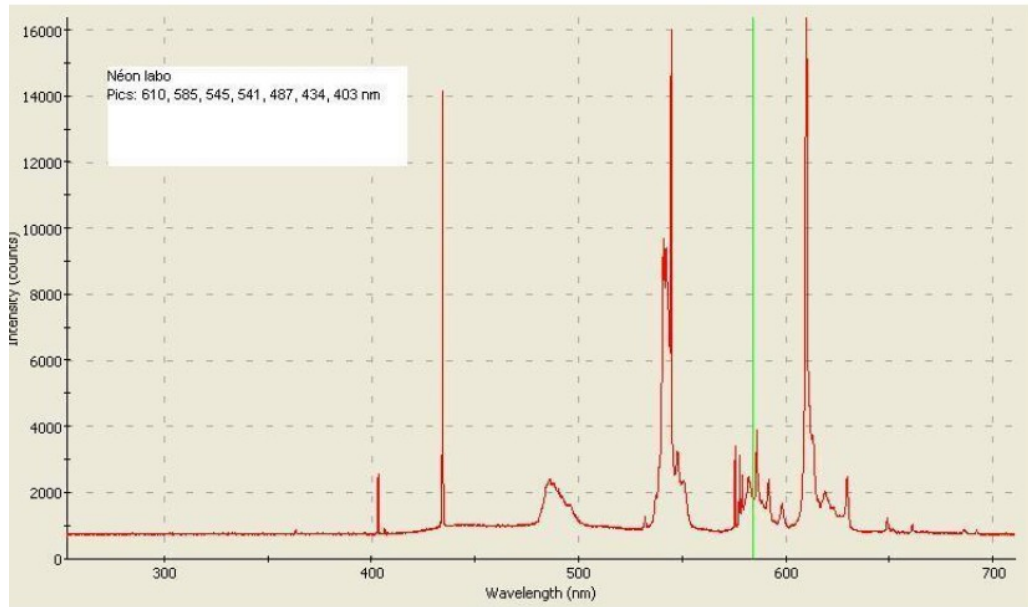


Figure 6-11: Room light spectrum used for the experiments

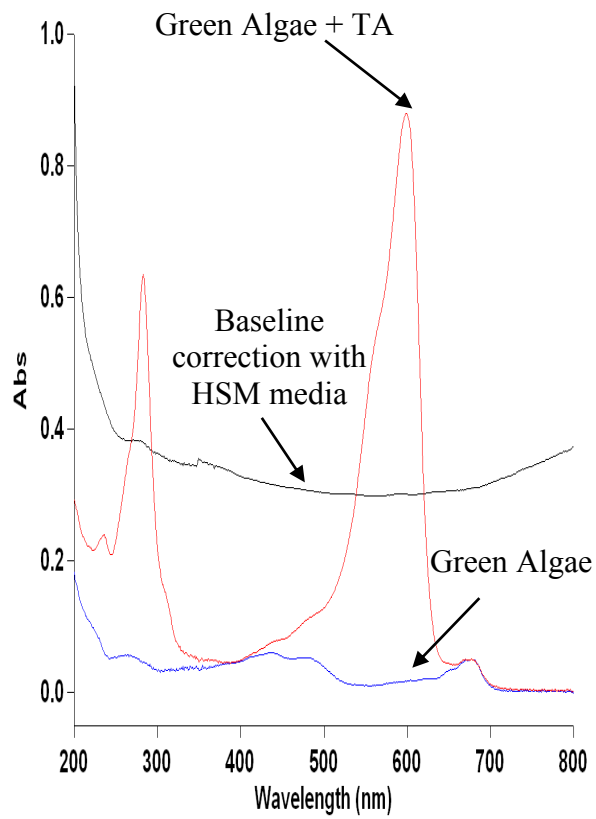
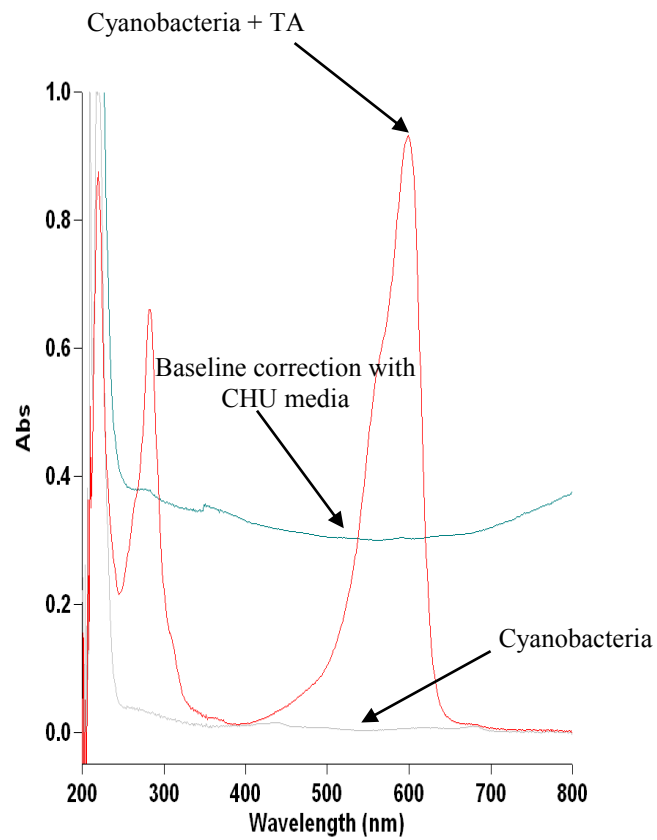


Figure 6-12: Absorption spectrum of Algae with mediators



**Figure 6-13: Absorption spectrum of cyanobacteria with mediators**

Each media is combined with different mediators and the absorption spectrum is monitored for four days. The results are presented in the following figures.

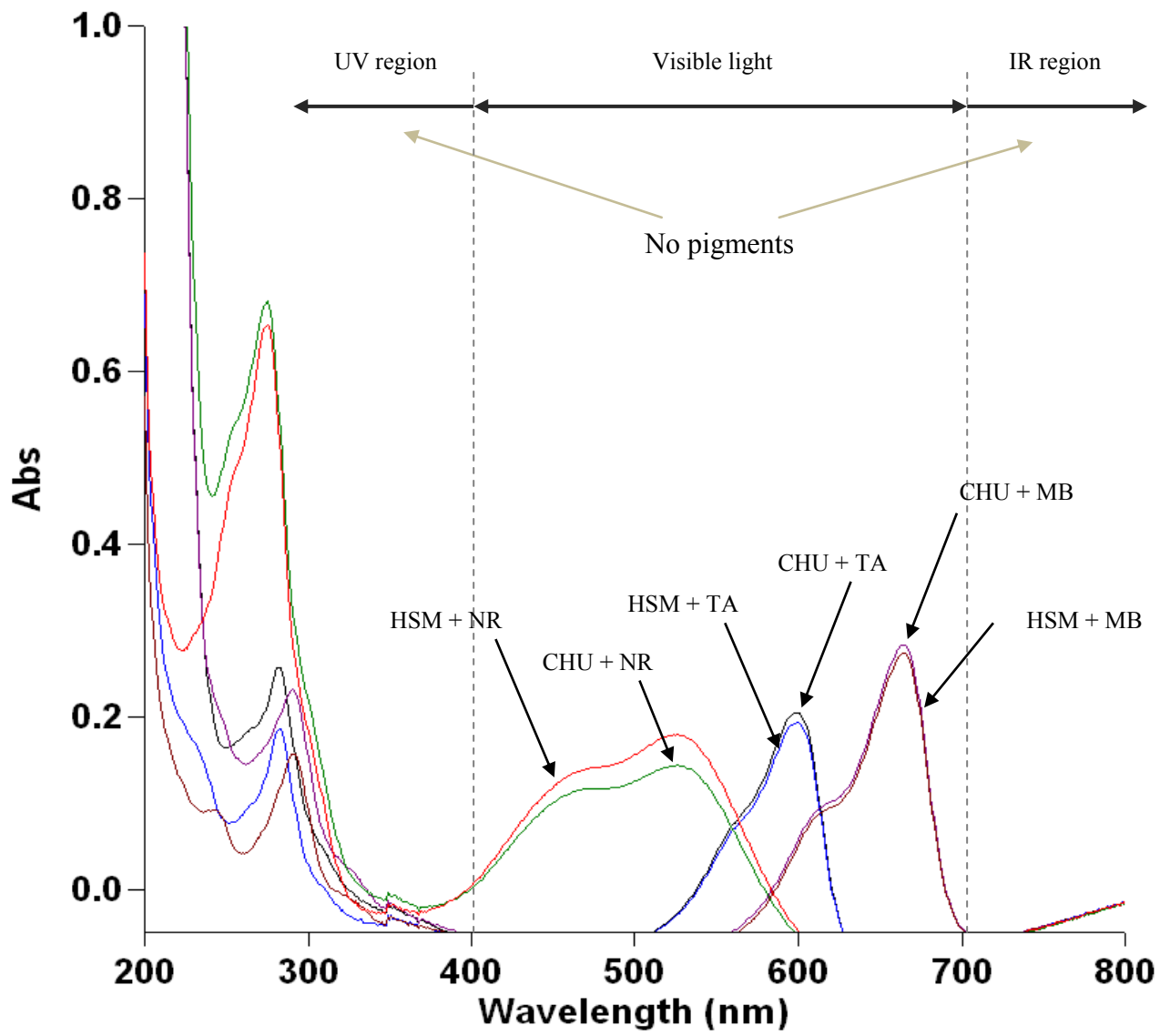


Figure 6-14 Absorption spectrum of media with mediators - T = 0

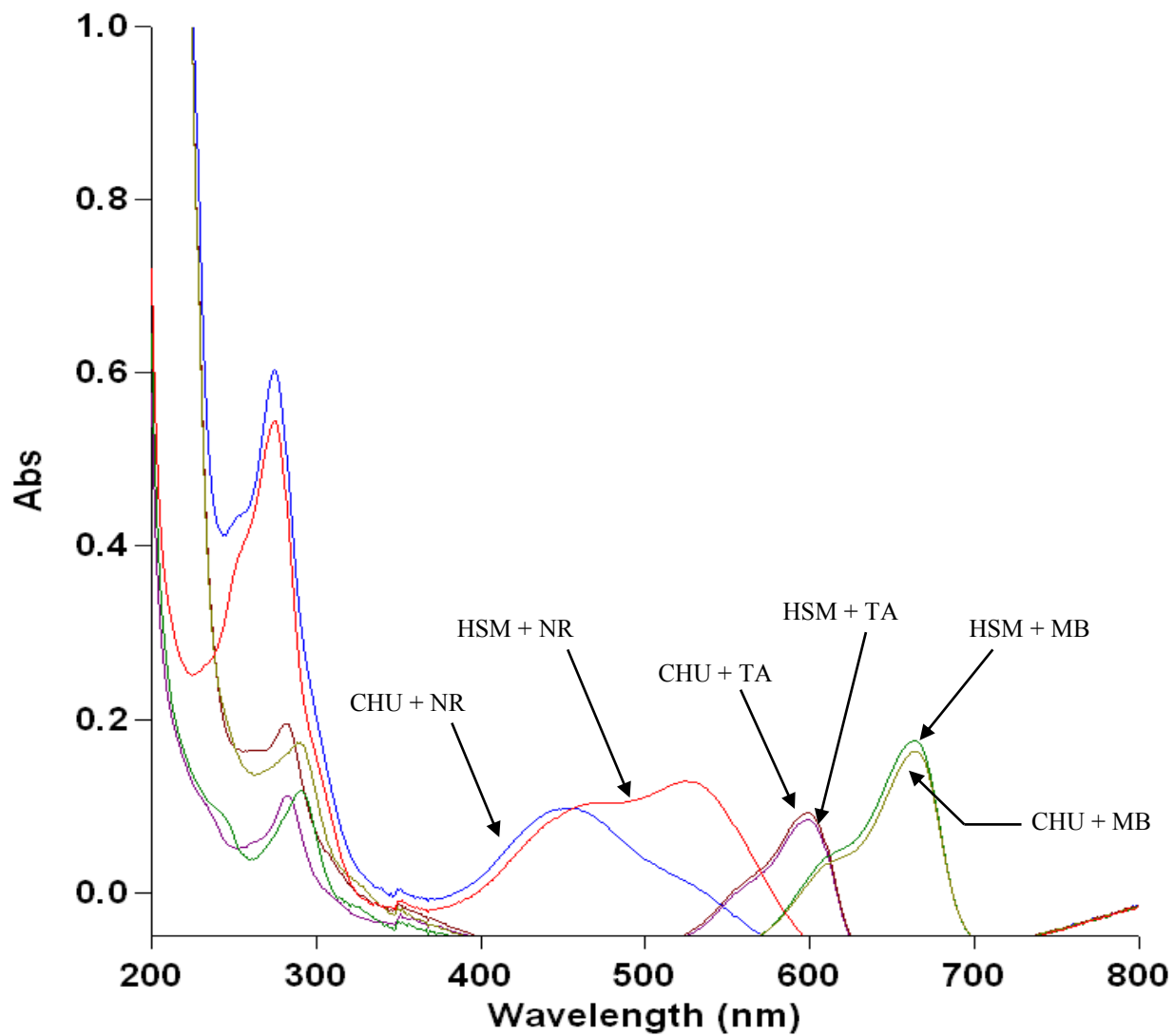


Figure 6-15 Absorption spectrum of media with mediators - T = 1 [Day]

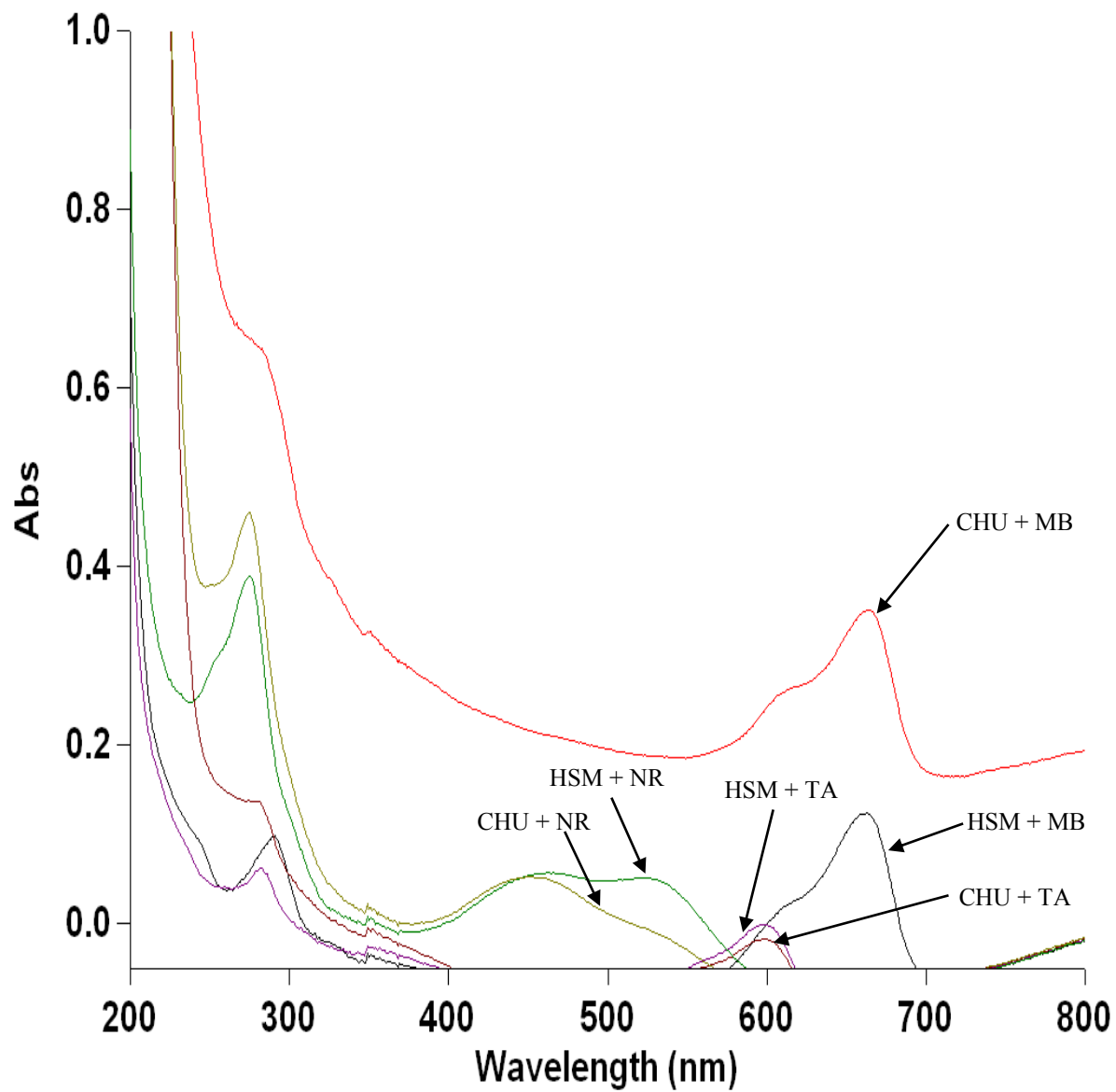


Figure 6-16 Absorption spectrum of media with mediators - T = 2 [Day]

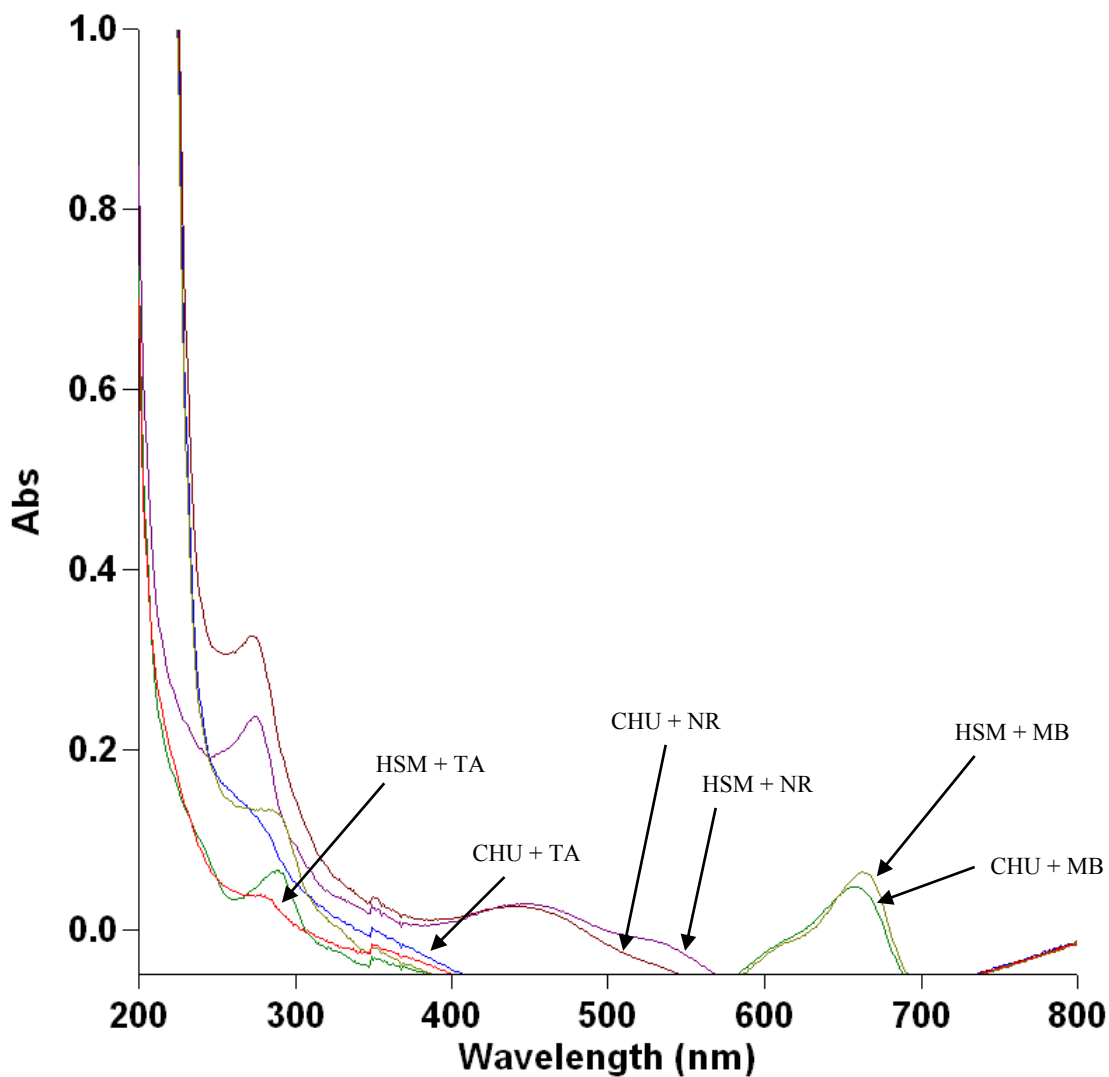


Figure 6-17 Absorption spectrum of media with mediators - T = 4 [Day]

A shift in the absorption spectrum of the media is obtained by addition of the mediators. For all the mediators absorption is decreased over time as seen in Figure 6-14 to Figure 6-17. Decrease in absorption corresponds to photo destruction or change of the mediators. Reaction between the media and mediator can be one of the reasons of this change. This is most obvious in case of thionine acetate which is completely destroyed after 4 days in both HSM and CHU. Studying these graphs, methylene blue seemed to be the most intact mediator.

In our case methylene blue stayed intact with the two media (HSM and CHU) however, it decreased the growth rate of the cultures. Thionine acetate however, did not make a considerable change in the growth rate but had strong reaction with the media and caused a significant shift in the absorption spectrum.

Thionine acetate is an amine compound widely used in biological staining. It's also used to mediate electron transfer in microbial fuel cells [74]. Neutral red comes as a chloride salt and is generally used for staining in histology. It can be used as a pH indicator since it changes from red to yellow between pH 9.8 – 8. It can be used to stain living cells and is added to some growth media for bacteria and cell cultures [75]. In analytical chemistry, methylene blue is widely used as a redox mediator. MB is blue when in an oxidizing environment and turns colorless once exposed to a reducing agent. For instance in case of yeast and in presence of active enzymes MB turns colorless thus indicating living cells. Hence it is also used as an indicator to determine if the cells are live [76].

The final decision for using the mediators still stays a question depending on the future experiments with the  $\mu$ PSC. Once again mentioning that electron transfer and affecting the live cells are two separate important topics. Effect of mediators on the cells and the absorption spectrum was studied here however, in order to better understand the effect of the mediators on the electron transfer each sample is suggested to be tested with  $\mu$ PSC as well. Due to the limited time and insufficient materials to fabricate new  $\mu$ PSCs, this part was not performed in this work and is mentioned as a suggestion for the future works.

This chapter dealt with testing different micro-organisms and mediators. The next chapter presents conclusions and suggestions to be forwarded for future works.

*Chapter 7*

*Conclusions &*

*Future works*

## 7 Conclusions and future works

### 7.1 Conclusions

A photosynthetic power cell is presented, including its operational principle and fabrication process. The developed device is polymer based (PDMS instead of silicon) which provides a cheaper device with easier and faster fabrication and more flexible geometry. Different bonding methods for the assembly of the device were tested and a neat and reliable assembly was achieved by combining plasma bonding and PDMS glue.

After various tests on the components of  $\mu$ PSC and experiments to verify the reliability of the measurement setup, different sets of experiments were performed to study the parameters affecting the performance of the cell. In the first step, fabrication parameters were investigated to find optimal PEM and electrode configuration. Then, influence of other parameters such as concentrations of electrolytes, addition of glucose and illumination cycles were studied.

In contrast to the theoretical prediction, devices using Nafion 212 as the PEM did not provide the highest outputs due to lack of stability due to the current technology and fabrication process. The same thing was observed with the first pattern of electrode used (D1). Hence, Nafion 115 or 117 with D2 or D3 patterns are suggested to be used for future  $\mu$ PSCs.

Instead of depositing chrome (auxiliary layer) and gold as the electrodes with overall thickness of 2500 Å on silicon, gold with a thickness of only 1000 Å was deposited and patterned directly on the Nafion (PEM). This provided the following benefits:

- Thickness of the electrodes was decreased by half compared to previously fabricated devices. Consequently the surface to volume ratio of the electrodes was increased and the internal resistance of the electrodes was decreased which contributed to higher performance of the electrodes and consequently the  $\mu$ PSC.
- Fabrication of the electrodes and patterns of gold on Nafion resulted in a proposed process by modifying the traditional MEMS processes. This was considered as an achievement in the current work.
- Electrodes being patterned on the PEM provides a better electron transfer and facilitates the assembly of the device.

Concentration of catholyte (potassium ferricyanide in this study) proved to be a significant parameter. Potassium ferricyanide solution with concentration of 25 % is suggested to be used for future experiments.

Studying the effects of volume and concentration of the anolyte (algae culture in this study) led to interesting results. It was found that there exists an optimal volume for each concentration. Hence, knowing the concentration (cells count) of the culture can specify the optimal amount to be injected and circulated in the chamber.

By varying the external load, the V-I characteristics of the  $\mu$ PSC were obtained which showed a linear behavior. Voltage was increased by increasing the resistance and current was decreased. The power generation curve was found to be parabolic and an operational range for  $\mu$ PSC was established. It is suggested to operate the  $\mu$ PSC with external loads varying from 800 to 2000 Ohms which provides a voltage of 300 to 500 mV and a power generation over 160  $\mu$ W corresponding to power density of 36.23  $\mu$ W/cm<sup>2</sup>.

Long-term behavior of the  $\mu$ PSC was also explored. The  $\mu$ PSC showed a quite stable behavior over time until evaporation of the anolyte solution started to affect the volume and concentration of the solution.

In contrast to the literature data, addition of glucose did not have a very significant effect (probably not as significant as other parameters studied in this work). Moreover, addition of glucose increases the volume of anolyte and decreases the concentration of the photosynthetic culture. Small addition of glucose of 50% of concentration provides more stable outputs. Hence, lot of care should be taken into consideration for adding glucose to the anolyte.

The variation of the output voltage in dark and light was not very significant however illumination cycles are found to be very beneficial for the  $\mu$ PSC by restoring the living cultures and increasing the lifetime of the cells and the device consequently.

## **7.2 Future works**

After conducting various experiments, some points are suggested to be considered and briefly mentioned for future works:

- Finding optimal parameters for plasma bonding leading to improved final assembly of the  $\mu$ PSC
- More accurate inspection of the electrodes by comparing resistance of the electrodes to the theoretical prediction for a perfect mesh.
- Conducting more experiments to investigate the effects of changing volume and concentration of the photosynthetic agents. This can lead to a reference chart to be

used such that by knowing the concentration of the photosynthetic organism, the optimal amount to be injected and circulated in the chamber can be obtained.

- A more comprehensive set of experiments in order to determine the affects of illumination and illumination cycles.
- Connecting a couple of  $\mu$ PSCs in different combinations: series, parallel or combined and studying the V-I characteristics.
- More experiments are suggested to be performed using mediators. Different photosynthetic cultures with and without mediators are to be used with  $\mu$ PSC and the outputs are to be monitored and variations are to be discussed.
- Environmental conditions and the catholyte used in this study might not be (and most probably they are not as in case of cyanobacteria) most suitable for all photosynthetic cultures. Hence, different cultures are to be studied in order to find the corresponding optimal growth and media conditions. Then, they can be used with  $\mu$ PSC and the outputs can be compared.
- Mathematical modeling to be performed and matched with the experimental results.
- Finding the equivalent electrical circuit (model) for  $\mu$ PSC for every application.
- Designing power converter for  $\mu$ PSC.
- Storing and utilizing the energy from  $\mu$ PSC.

## 8 References

1. L. M. Roylance and J. B. Angell, "A batch fabricated silicon accelerometer", IEEE, Trans. Electron Devices, Vol. 29, Issue 12, 1979, pp. 1911 – 1917
2. N. Maluf and K. Williams, "An introduction to microelectromechanical systems engineering", 2<sup>nd</sup> edition, Chapters 1 – 3, 2004
3. "Microfabricated Power Generation Devices: Design and Technology", Edited by A. Mitsos and P. Barton.
4. W. R. Grove, "On voltaic series and combination of gases by platinum", Philosophical magazine, Vol. 14, 1839, pp. 127 – 130
5. B. C. Steel and A. Heinzl, "Materials for fuel cell technologies", Nature, 414, 2001, pp. 345 – 352
6. Epstein, A. H. and S. D. Senturia, "Macro Power from Micro Machinery", Science. Vol. 276, 1997, 1211
7. L. G. Frechette, S. A. Jacobson, K. S. Breuer, F. F. Ehrich, R. Khanna, C. W. Wong, X. Zhang, M. A. Schmidt and A. H. Epstein, "High-speed microfabricated silicon turbomachinery and fluid and fluid film bearings", Journal of microelectromechanical systems, Vol. 14, 2005, pp. 141 – 152
8. W. A. Dahm, J. Ni, K. Mijit, R. Mayor, G. Qiao, A. Benjamin, Y. Gu, Y. Lei and M. Papke, "Internal combustion swing engine for portable power generation systems", 40<sup>th</sup> AIAA, 2002, 722
9. J. L. Steyn, S. H. Kendig, R. Khanna, T. M. Lyszczarz and C. Livermore, "Generating electric power with a MEMS electroquasistatic induction turbine-generator", Proceeding of the 18<sup>th</sup> IEEE international conference on Micro Electro Mechanical Systems, 2005, pp. 614 – 617
10. H. H. Kolm, Quarterly progress report, solid state research, group 35, Technical report, MIT Lincoln Laboratory, Lexington, MA, 1956.
11. L. M. Fraas, J. E. Avery and H. X. Huang, "Thermophotovoltaics: heat and electric power from low bandgap solar cell around gas fired radiant tube burners", 29 IEEE PVSC Conference, New Orleans, USA
12. O. M. Nielson, L. R. Arana, C. D. Baertsch, K. F. Jensen and M. A. Schmidt, "A Thermophotovoltaic micro-generator for portable power applications", Transducers, 3, Boston, USA, 2003
13. W. Yang, "A prototype microthermophotovoltaic power generator", Applied Physics letters, 84, Vol. 19, 2004, pp. 3864 – 3866

14. H. Gerischer, "Electrochemical Photo and Solar Cells Principles and Some Experiments", *Electroanalytical chemistry and interfacial electrochemistry*, Vol. 58, 1975, pp. 263 – 274
15. E. Becquerel, *C. R. Academy of Science*, Vol. 9, pp. 561 – 567, 1839
16. A. Fujishima and K. Honda, *Bull.Chem. Soc. Jap.* 44 (1971) 1184, *Nature* 238 (1972) 37
17. "Solar energy to electricity", UNCTC Publications, United Nations, New York, 1992
18. A. M. Hermann, "Polycrystalline thin-film solar cells – A review", *Solar Energy Materials and Solar Cells*, Vol. 55, 1998, pp. 75 – 81
19. T. T. Chow, "A. review on photovoltaic/ thermal hybrid solar technology", *Applied energy*, Vol. 87, 2010, pp. 365 – 379
20. D. Park and J. Zeikus, "Electricity generation in microbial fuel cells using neutral red as electronophore", *Applied and Environmental Microbiology*, Vol. 66, Issue 4, 2000, pp. 1292 - 1297
21. K. B. Lam, E. A. Johnson, M. Chiao and L. Lin, "A MEMS Photosynthetic Electrochemical Cell Powered by Subcellular Plant Photosystems", *Journal of Microelectromechanical Systems*, Vol. 15, Issue 5, 2006, pp. 1243 -1250
22. M. Chiao, K. B. Lam and L. Lin, "Micromachined Microbial And Photosynthetic Fuel Cells", *Journal of Micromechanics And Microengineering*, Vol. 16, 2006, pp. 2547 – 2553
23. D. L. Nelson and M. M. Cox, "Lehninger Principles of Biochemistry", 3<sup>rd</sup> edition, 2000, pp. 691 – 714
24. I. Ieropoulos, J. Greenman, C. Melhish and J. Hart, "Comparative study of three types of microbial fuel cell", *Enzyme and microbial technology*, Vol. 37, 2005, pp. 238 – 245
25. R. M. Allen and H. P. Bennetto, "Microbial fuel cells: electricity production from carbohydrates", *Applied Biochemistry Biotechnology*, Vol. 39, Issue 40, 1993, pp. 27-40
26. M. Allen and A. Crane, "Null Potential Voltammetry – An approach to the study of the plant photo system", *Bioelectrochemistry and Bioenergetics*, Vol. 3, 1976, pp. 84 – 91
27. M. Aizawa, M. Hirano and S. Suzuki, "Photoelectrochemical energy conversion system modeled on the photosynthetic process", *Electrochimica Acta*, Vol. 23, 1978, pp. 1185 – 1190

28. L. A. Drachev, A. A. Kondrashin, V. D. Samuilov, and V. P. Skulachev, "Generation of electric potential by reaction center complexes from *Rhodospirillum rubrum*", FEBS Letters, Vol. 50, 1975, pp. 219 – 222
29. L. A. Drachev, A. A. Jasaitis, A. D. Kaulen, A. A. Kondrashin, L. V. Chu, A. Y. Semenov, I. I. Severina and V. P. Skulachev, "Reconstitution of biological molecular generators of electric current: Cytochrome oxidase", Journal of Biological Chemistry, Vol.251, 1976, pp. 7072 – 7076
30. N. K. Packham, D. M. Tiede, P. Mueller and P. L. Dutton, "Construction of a flash – activated cyclic electron transport system by using bacterial reaction centers and the ubiquinone-cytochrome b-c1/c segment of mitochondria", Proceedings of the National Academy of Science, Vol. 77, 1980, pp. 6339 - 6343
31. N. K. Packham, C. Packham, P. Mueller, D. M. Tiede and P. L. Dutton, "Reconstitution of photochemically active reaction centers in planar phospholipid membranes", FEBS Letters, Vol. 110, 1980, pp. 101 – 106
32. A. F. Janzen, "Photoelectrochemical conversion using reaction-center electrodes", Nature, Vol. 286, 1980, pp. 584 – 585
33. K. Tanaka, R. Tamamushi and T. Ogawa, "Bioelectrochemical fuel cells operated by cyanobacterium *anabaena variabilis*", Journal of Chemical Technology & Biotechnology, Vol. 35, 1985, pp. 191 – 197
34. K. Tanaka, N. Kashiwagi and T. Ogawa, "Effects of light on the electrical output of bioelectrochemical fuel-cells containing *anabaena variabilis* M-2 mechanisms of the post-illumination burst", Biotechnology, Vol. 42, 1988, pp. 235 – 240
35. T. Yagishita, S. Sawayama, K. Tsukahara and T. Ogi, "Photosynthetic bio-fuel cell using cyanobacteria", Renewable Energy, Vol.9, 1996, pp. 958 – 961
36. T. Yagishita, T. Horigome and K. Tanaka, "Effect of light, CO<sup>2</sup> and inhibitors on the current output of bio-fuel cells containing the photosynthetic organism *synechococcus* sp. ", Journal of Chemical Technology & Biotechnology, Vol. 56, 1993, pp. 393 – 399
37. T. Yagishita, T. Horigome and K. Tanaka, "Bio-fuel cells containing photosynthetic microorganisms", Journal of the electrochemical society, Vol. 61, 1993, pp. 687 – 688
38. T. Yagishita, S. Sawayama, K. Tsukahara and T. Ogi, "Effects of intensity of incident light and concentration of *synechococcus* sp. and 2-hydroxy-1,4-naphthoquinone on the current output of photosynthetic electrochemical cell ", Solar Energy, Vol. 61, 1997, pp. 347 – 353

39. T. Yagishita, S. Sawayama, K. Tsukahara and T. Ogi, "Effects of glucose addition and light on current outputs in photosynthetic electrochemical cell using *synechocystis* sp. Pcc6714", *Journal of bioscience and bioengineering*, Vol. 99, 1999, pp. 210 – 214
40. R. Bhardwaj, R. Pan and E. Gross, "Solar energy conversion by chloroplast photochemical cells", *Nature*, Vol. 289, 1981, pp. 396 – 398
41. W. Haehnel and H. Hockheimer, "On the current generated by a galvanic cell driven by photosynthetic electron transport", *Bioelectrochem. Bioeng.*, Vol. 6, 1979, pp. 563 – 574
42. K. B. Lam, M. Chiao and L. Lin, "A Micro Photosynthetic Electrochemical Cell", *IEEE The sixteen annual international conference on micro electromechanical systems*, 2003, pp. 391-394
43. B. Ke, "Photosynthesis Photobiology and Photobiophysics", *Advances in Photosynthesis*, Volume 10, 2001
44. The World Bank, "Electrical power consumption per capita", <http://data.worldbank.org>, last visited: Sept. 02, 2011
45. The biology place, [www.phschool.com/science](http://www.phschool.com/science), last visited: July 28, 2011
46. G. Putumbaka, S. Bingham, "Differential gene expression of *Chlamydomonas* during State1 to State2 Transitions", Internship report, Computational Biosciences Program, Arizona State University, 2008
47. "Probing Photosynthesis – mechanisms, regulation and adaptation", Edited by: M. Yunus, U. Pathre and P. Mohanty, 2000
48. "Molecular to global photosynthesis", Edited by: M. Archer and J. Barber, Series of photoconversion of solar energy, Vol. 2, Imperial College Press, 2004
49. E. Rabinowitch, "Photosynthesis and energy transfer", photosynthesis laboratory, botany department, University of Illinois, Urbana, Vol. 61, pp. 870 – 878, 1957
50. D. Aron, D. Knaff, B. McSwain, R. Chain and H. Tsujimoto, "Three light reactions and two photosystems of plant photosynthesis", *Photochemistry and photobiology*, Vol. 14, pp. 397 – 425, 1971
51. Wikipedia, Last visited: Feb. 10, 2010, <http://en.wikipedia.org>
52. N. Krauß, "Mechanisms for photosystem I and II", *Current opinion in chemical biology*, Vol. 7, pp. 540 – 550, 2003
53. M. Blomberg, "Proton coupled electron transfer in respiration-oxygen reduction and proton pumping", Presentation, Stockholm University, March 2011
54. V. Robert, J. Cavanaugh, "Human Development: A Life-span View (4, illustrated ed.)", Cengage Learning, pp. 58, 2006

55. J. P. Decker, "Effect of temperature on photosynthesis and respiration in red and loblolly pines", *Plant Physiology*, Vol. 4, pp. 679 – 688, 1944
56. J. P. Decker, "Some effects of temperature and carbon dioxide concentration on photosynthesis of *Mimulus*", Carnegie institution of Washington, Stanford, California, June 1958
57. J. Servaites and D. Geiger, "Effects of light intensity and oxygen on photosynthesis and translocation in sugar beet", *Plant physiology*, Vol. 54, pp. 575 – 578, 1974
58. T. Yagishita, S. Sawayama, K. Tsukahara and T. Ogi, "Effects of glucose addition and light on current outputs in photosynthetic electrochemical cells using *synechocystis* sp. PCC6714", *Journal of bioscience and bioengineering*, Vol. 88, No. 2, pp. 210-214, 1999
59. P. Kramer and J. Decker, "Relation between light intensity and rate of photosynthesis of loblolly pine and certain hardwoods", *Plant physiology*, Vol. 19, pp. 350 – 358, 1944
60. G. Rechtsteiner and J. Ganske, "Using natural and artificial light sources to illustrate quantum mechanical concepts", *The chemical educator*, Springer Berlin, Vol. 3, No. 4, pp. 1-12, 1998
61. Introduction to atmospheric sciences, Handouts, [www.atmos.washington.edu](http://www.atmos.washington.edu), Last visited June 16, 2010
62. M. Stomp, J. Huisman, L. Stal and H. Matthijs, "Colorful niches of phototrophic microorganisms shaped by vibrations of the water molecule", *The ISME Journal* (2007) 1, 271–282, July 2007
63. R. Govindjee, "The absorption of light in photosynthesis", *Scientific American*, Vol. 23, pp. 64-82, 1974
64. K. Sauer, "Photosynthetic light reactions - Physical aspects. Photoynthesis III: Photosynthetic membranes and light systems", Springer-Verlag, Vol. 19, pp. 85-97, 1986
65. Product data sheets, DuPont Fuel Cells, <http://www2.dupont.com>, last visited: Feb. 22, 2010
66. Technical Notes, "Nafion: Physical and chemical properties background", DuPont, <http://www.permapure.com/TechNotes>
67. P. Beattie, F. Orfino, V. Basura, K. Zychowska, J. Ding, C. Chuy, J. Schmeisser, S. Holdcroft, "Ionic conductivity of proton exchange membranes", *Journal of Electroanalytical Chemistry*, Vol. 503, pp. 46-56, 2001

68. A. Bayrakceken, S. Erkan, L. Turker, I. Eroglu, "Effects of membrane electrode assembly components on proton exchange membrane fuel cell performance", *International Journal of Hydrogen Energy*, Vol. 33, pp. 165-170, 2008
69. Y. Sato, K. Fujii, N. Mitani, A. Matsuura, T. Kakigi, F. Muto, J. Li, A. Oshima, M. Washio, "Development of sulfonated FEP-NAfion hybrid proton exchange membranes for PEMFC", *Nuclear Instruments and Methods in Physics Research, B* 265, pp. 213-216, 2007
70. U. Pal, J. Sánchez-Ramírez<sup>2</sup>, S. Gamboa, P. Sebastian and R. Pérez, "Drastic improvement of electrical properties of Nafion® 112 membrane on impregnation of bimetallic Au/Pd nanocluster", *Physica status solidi, (c)* 0, No. 8, pp. 2944-2948, 2003
71. S. Banerjee, D. Curtin, "Nafion perfluorinated membranes in fuel cells", *Journal of Fluorine Chemistry*, Vol. 125, pp. 1211-1216, 2004
72. W. Pyle, A. Spivak, R. Cortez and J. Healy, "Making electricity with hydrogen", *Home Power*, Vol. 35, June/July 1993
73. K. Rabaey, G. Lissens, S. Siciliano and W. Verstraete, "A microbial fuel cell capable of converting glucose at high rate and efficiency", *Biotechnology letters*, Vol. 25, pp. 1531 – 1535, 2003
74. J. A. Kiernan, "Classification and naming of dyes, stains and fluorochromes", *Biotech Histochem*, Vol. 76, pp. 261–78, 2001
75. J. Winckler, "Vital staining of lysosomes and other cell organelles of the rat with neutral red", *Prog. Histochem. Cytochem.*, Vol. 6, pp. 1-89, 1974
76. P. K. Gillman, K. W. Bradley, J. D. Andrew, W. Y. Liang, "Methylene blue is a potent monoamine oxidase inhibitor", *Canadian Journal of Anesthesia*, Vol. 55 (5), pp. 311–312, 2008

## Appendices

Appendix A1 contains the complete table of the parametric study performed in this work. Experiment numbers and indices are used for identification purposes in the appendices A2 to A11.

### A1: Parametric study of the performance of the micro photosynthetic power cell

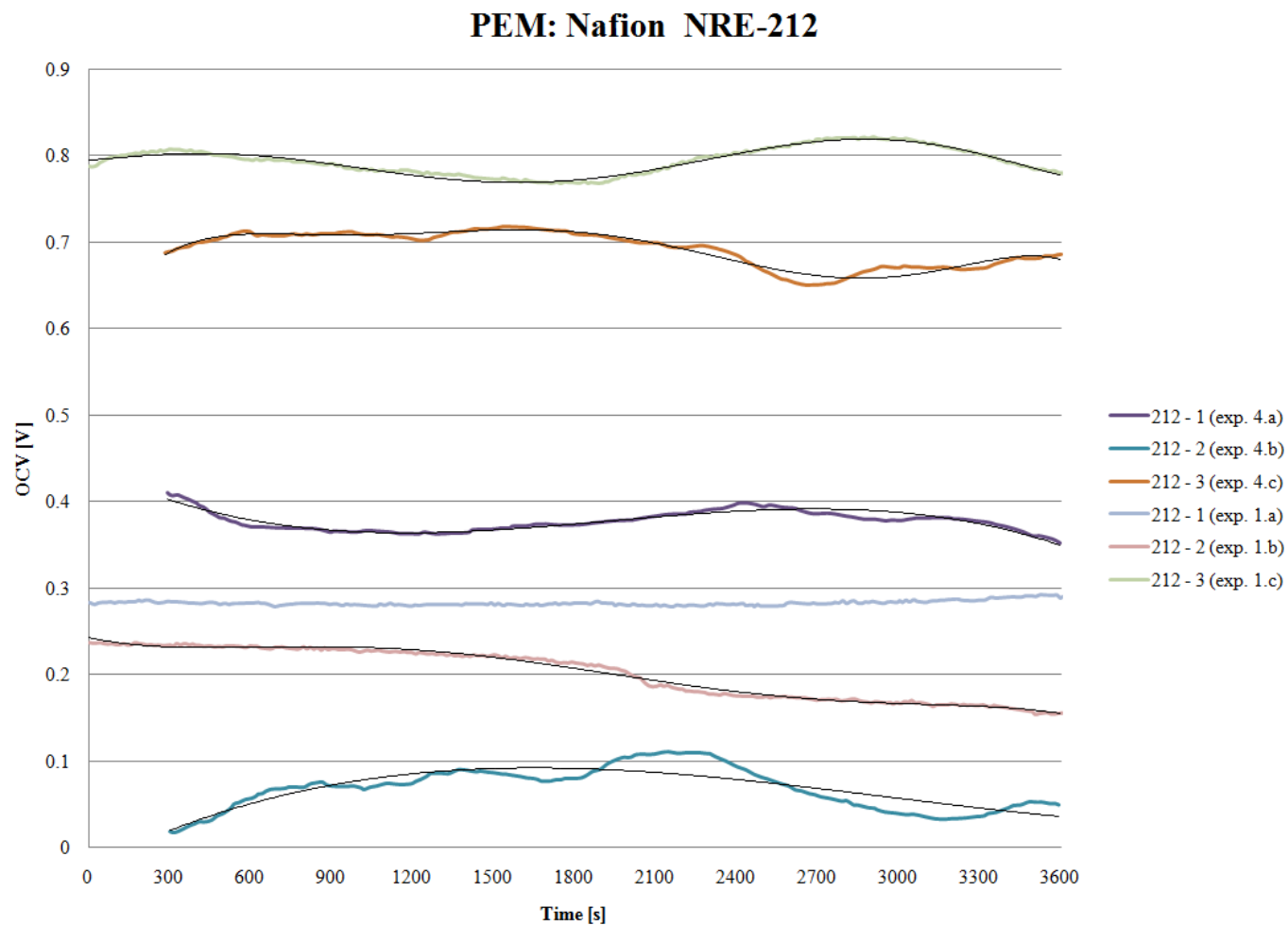
Experiment No.	Index	Device code	PEM (Nafion)	Electrode (Gold pattern)	Catholyte	Glucose addition	Voltage	Illumination	Comment
1	a	<i>A.I.N12.G1</i>	212	D1	2 %	N/A	OCV	600-650 lux	Proton exchange membrane And Electrode pattern
	b	<i>A.I.N12.G2</i>	212	D2					
	c	<i>A.I.N12.G3</i>	212	D3					
2	a	<i>A.II.N15.G1</i>	115	D1					
	b	<i>A.II.N15.G2</i>	115	D2					
	c	<i>A.II.N15.G3</i>	115	D3					
3	a	<i>A.III.N17.G1</i>	117	D1					
	b	<i>A.III.N17.G2</i>	117	D2					
	c	<i>A.III.N17.G3</i>	117	D3					
4	a	<i>A.I.N12.G1</i>	212	D1					
	b	<i>A.I.N12.G2</i>	212	D2					
	c	<i>A.I.N12.G3</i>	212	D3					
5	a	<i>A.II.N15.G1</i>	115	D1					
	b	<i>A.II.N15.G2</i>	115	D2					
	c	<i>A.II.N15.G3</i>	115	D3					
6	a	<i>A.III.N17.G1</i>	117	D1					
	b	<i>A.III.N17.G2</i>	117	D2					
	c	<i>A.III.N17.G3</i>	117	D3					

7	a	<i>A.III.NI7.G2</i>	117	D2	2 %	N/A	OCV	600-650 lux	Catholyte concentration				
	b	<i>B.I.NI7.G3</i>	117	D3	2 %								
8	a	<i>A.III.NI7.G2</i>	117	D2	5 %								
	b	<i>B.I.NI7.G3</i>	117	D3	5 %								
9	a	<i>A.III.NI7.G2</i>	117	D2	7 %								
	b	<i>B.I.NI7.G3</i>	117	D3	7 %								
10	a	<i>A.III.NI7.G2</i>	117	D2	10 %								
	b	<i>B.I.NI7.G3</i>	117	D3	10 %								
11	a	<i>A.III.NI7.G2</i>	117	D2	10 %					N/A	OCV	600-650 lux	Catholyte concentration & Glucose addition
	b	<i>B.I.NI5.G2</i>	115	D2	10 %					N/A			
12	a	<i>A.III.NI7.G2</i>	117	D2	15 %	N/A							
	b	<i>B.I.NI5.G2</i>	115	D2	10 %	5ml – 5%							
13	a	<i>A.III.NI7.G2</i>	117	D2	20 %	N/A							
	b	<i>B.I.NI5.G2</i>	115	D2	10 %	5ml – 10%							
14	a	<i>A.III.NI7.G2</i>	117	D2	25 %	N/A							
	b	<i>B.I.NI5.G2</i>	115	D2	10 %	5ml – 20%							
15	a	<i>A.III.NI7.G2</i>	117	D2		5ml – 30%							
	b	<i>B.I.NI5.G2</i>	115	D2		5ml – 30%							
16	a	<i>A.III.NI7.G2</i>	117	D2		5ml – 50%							
	b	<i>B.I.NI5.G2</i>	115	D2		5ml – 50%							
17	a	<i>A.III.NI7.G2</i>	117	D2		5ml – 70%							
	b	<i>B.I.NI5.G2</i>	115	D2		5ml – 70%							
18	a	<i>A.III.NI7.G2</i>	117	D2		20 %	N/A	R=1 kΩ	600-650 lux	Trial power generation			
19	a	<i>A.III.NI7.G2</i>	117	D2	25 %	N/A	R=20 kΩ	600-650 lux	Volume and concentration of anolyte				
20	a	<i>A.III.NI7.G2</i>											
21	a	<i>(m)A.III.NI7.G2</i>											
22	a	<i>(m)A.III.NI7.G2</i>											
23	a	<i>(m)A.III.NI7.G2</i>											
24	a	<i>(m)A.III.NI7.G2</i>											
25	a	<i>(m)A.III.NI7.G2</i>											
26	a	<i>(m)A.III.NI7.G2</i>											

27	a	(m)A.III.N17.G2												
28	a	(m)A.III.N17.G2												
29	a	(m)A.III.N17.G2												
30	a	(m)A.III.N17.G2												
31	a	(m)A.III.N17.G2												
32	a	(m)A.III.N17.G2	117	D2		N/A	R=20 k $\Omega$	600-650 lux						
33	a	(m)A.III.N17.G2	117	D2	25 %	N/A	R=20 k $\Omega$							
34	a	(m)A.III.N17.G2	117	D2	25 %	N/A	R=20 k $\Omega$							
35	a	(m)A.I.N12.G3	212	D3	25 %	N/A	R= 1 k $\Omega$			600-650 lux	Resistances			
36	a	(m)A.I.N12.G3					R=20 k $\Omega$							
37	a	(m)A.I.N12.G3					R=100 k $\Omega$							
38	a	C.II.N15.G3	115				D3	25 %	N/A			R= 1 k $\Omega$	600-650 lux	Resistances
39	a	C.II.N15.G3										R=20 k $\Omega$		
40	a	C.II.N15.G3										R=100 k $\Omega$		
41	a	C.I.N15.G3										R= 1 k $\Omega$		
42	a	C.I.N15.G3										R=20 k $\Omega$		
43	a	C.I.N15.G3										R=100 k $\Omega$		
44	a	C.II.N15.G3	115	D3	25 %	N/A	Variable R	600-650 lux	V-I Charac.					
45	a	C.I.N17.G2	117	D2			Variable R							
46	a	C.I.N15.G3	115	D3	25 %	N/A	OCV	600-650 lux	Steady state					
	b	C.II.N15.G3					R=20 k $\Omega$							
47	a	C.A.N17.G2	117	D2	25 %	N/A	R = 1 k $\Omega$	1100-1200 lux	Dark/light					
48	a	C.I.N15.G3	115	D3	25 %	R = 1 k $\Omega$	30 %	600-650 lux	Glucose addition					
49	a	C.I.N15.G3					50 %							
50	a	C.I.N15.G3					70 %							
51	a	C.I.N15.G3					50 %		Glucose addition time					
52	a	C.I.N15.G3					50 %							
53	a	C.I.N15.G3	115	D3	25 %	N/A	Variable R	600-650 lux	Different PS Samples					
54	a	C.I.N15.G3												
55	a	C.I.N15.G3												

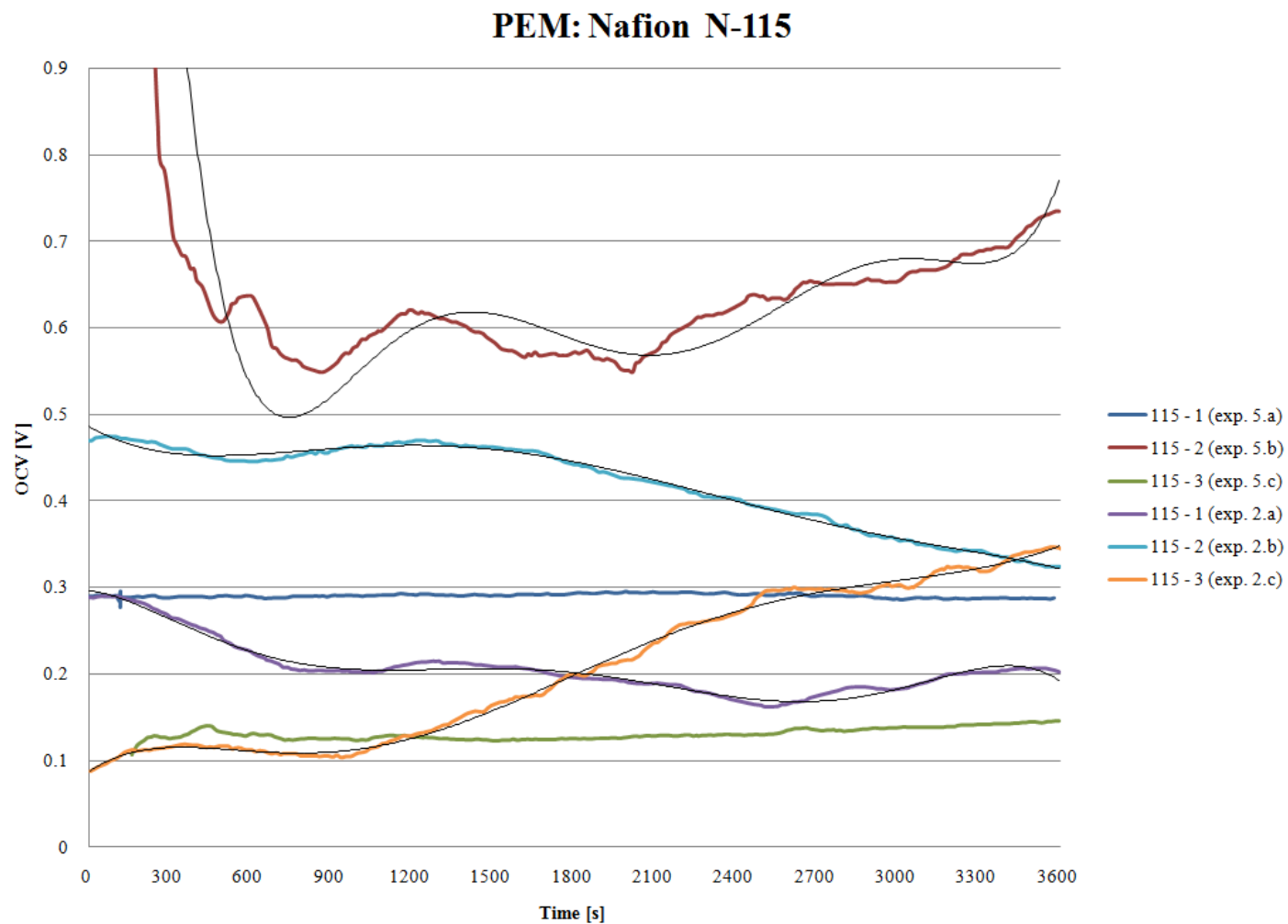
## A2: No-load performance of $\mu$ PSCs with Nafion 212 and various electrode configurations

(Discussed in Chapter 5 - Refer to Appendix A1 for details and parameters of the experiments)



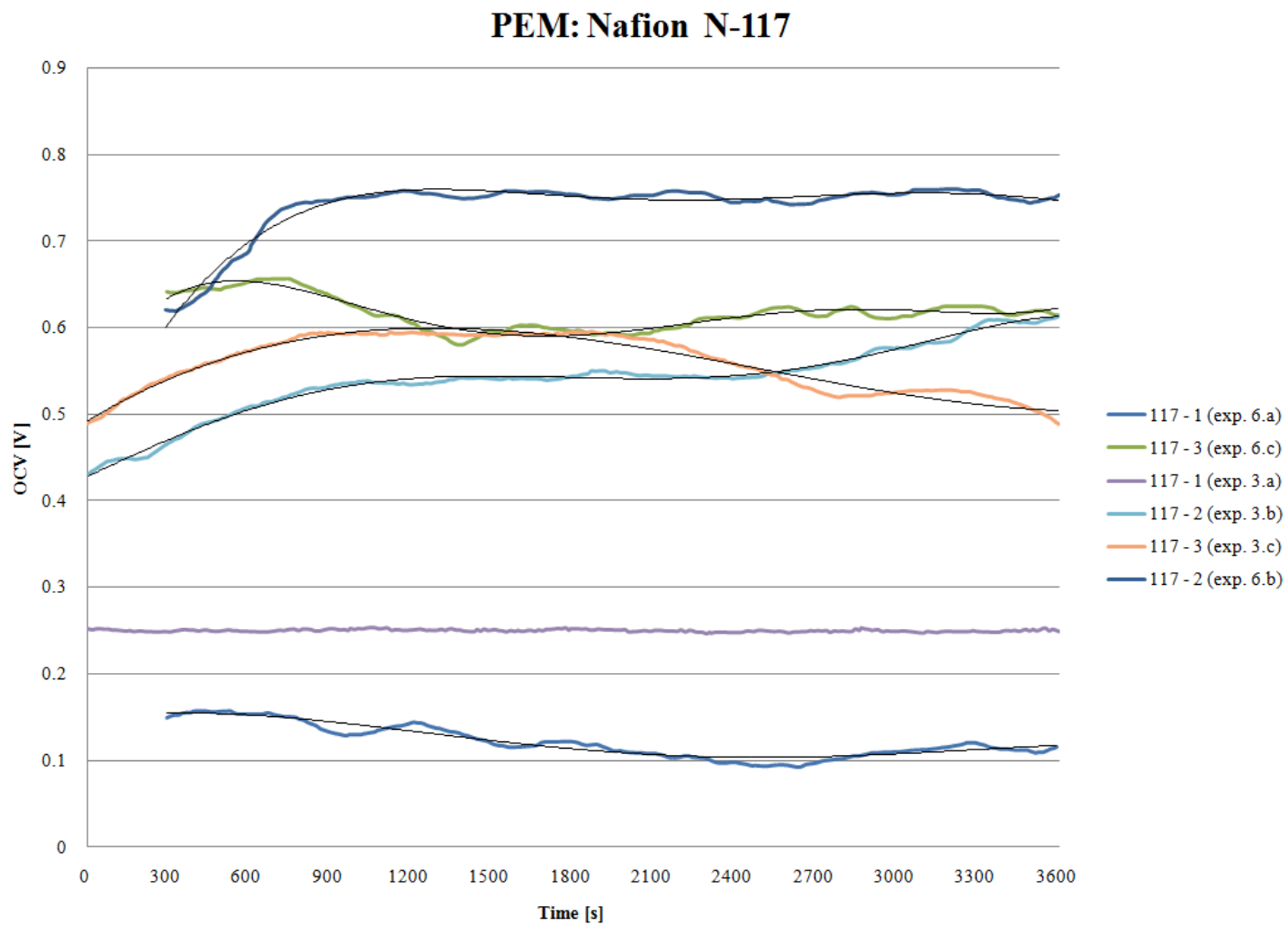
### A3: No-load performance of $\mu$ PSCs with Nafion 115 and various electrode configurations

(Discussed in Chapter 5 - Refer to Appendix A1 for details and parameters of the experiments)



## A4: No-load performance of $\mu$ PSCs with Nafion 117 and various electrode configurations

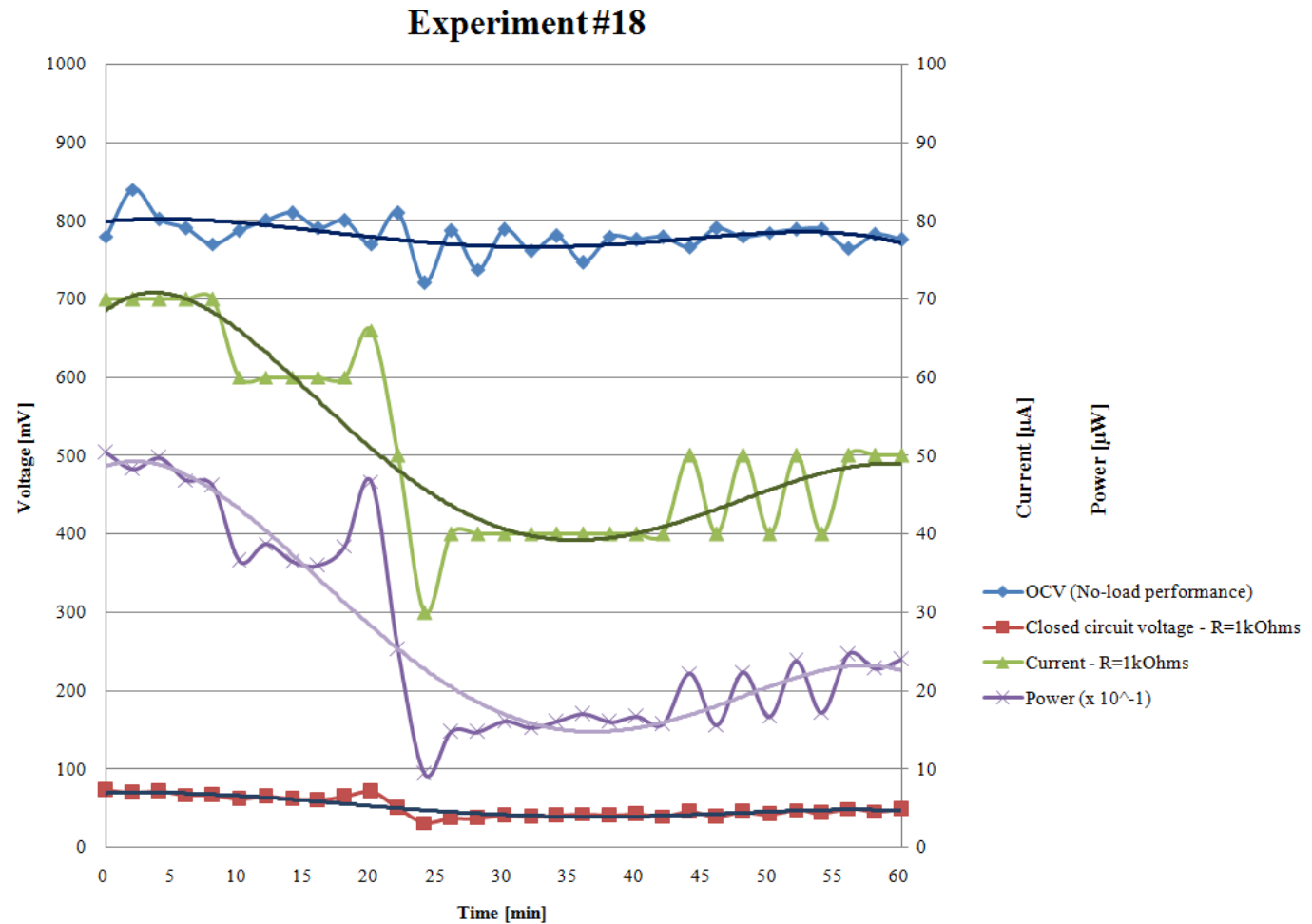
(Discussed in Chapter 5 - Refer to Appendix A1 for details and parameters of the experiments)



## A5: First trial experiment with external load of 1kOhms

Objectives: Confirmation of the functionality of the  $\mu$ PSC with external loading

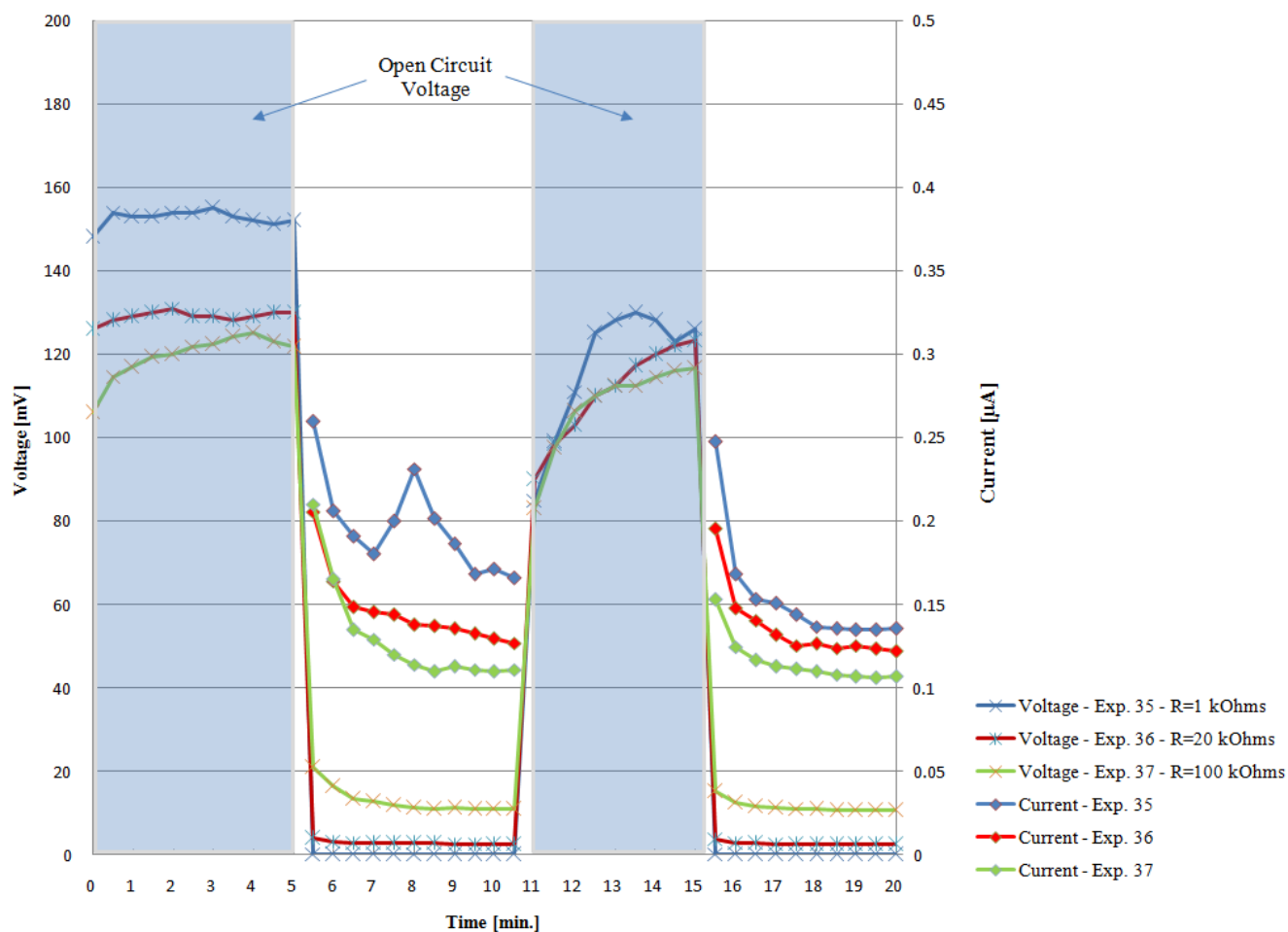
Device:  $\mu$ PCS with Nafion 117 and electrode configuration D2 - Refer to Appendix A1 for details and parameters of the experiment



## A6: Variations of voltage and current with three different external loads (PEM212/D3)

Objectives: Confirmation of the functionality of the  $\mu$ PSC with different loading scenarios (Trial experiment)

Device:  $\mu$ PCS with Nafion 212 and electrode configuration D3 - Refer to Appendix A1 for details and parameters of the experiment

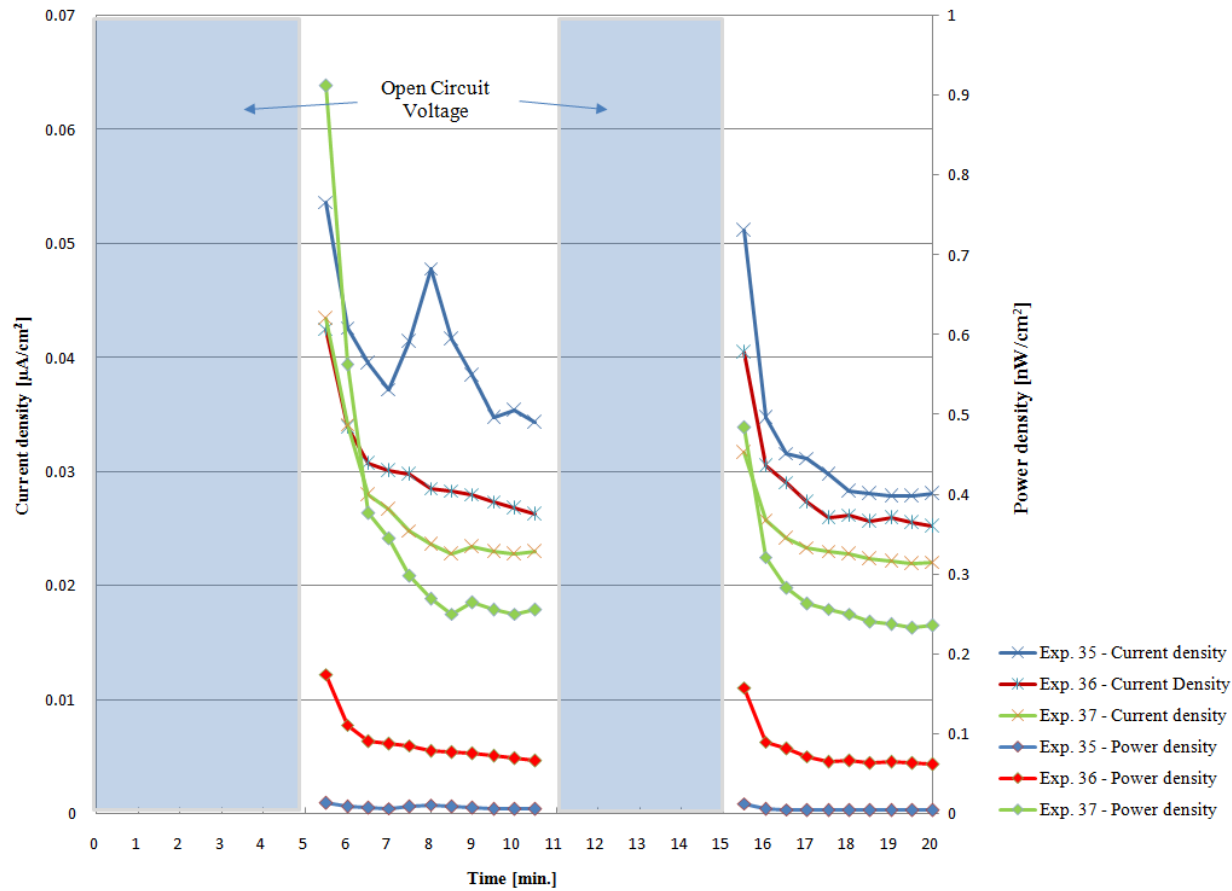


## A7: Variations of power and current densities with three different external loads (PEM212/D3)

Objectives: Observation of power and current densities variations with different loading scenarios (Trial experiment)

Device:  $\mu$ PCS with Nafion 212 and electrode configuration D3 - Refer to Appendix A1 for details and parameters of the experiment

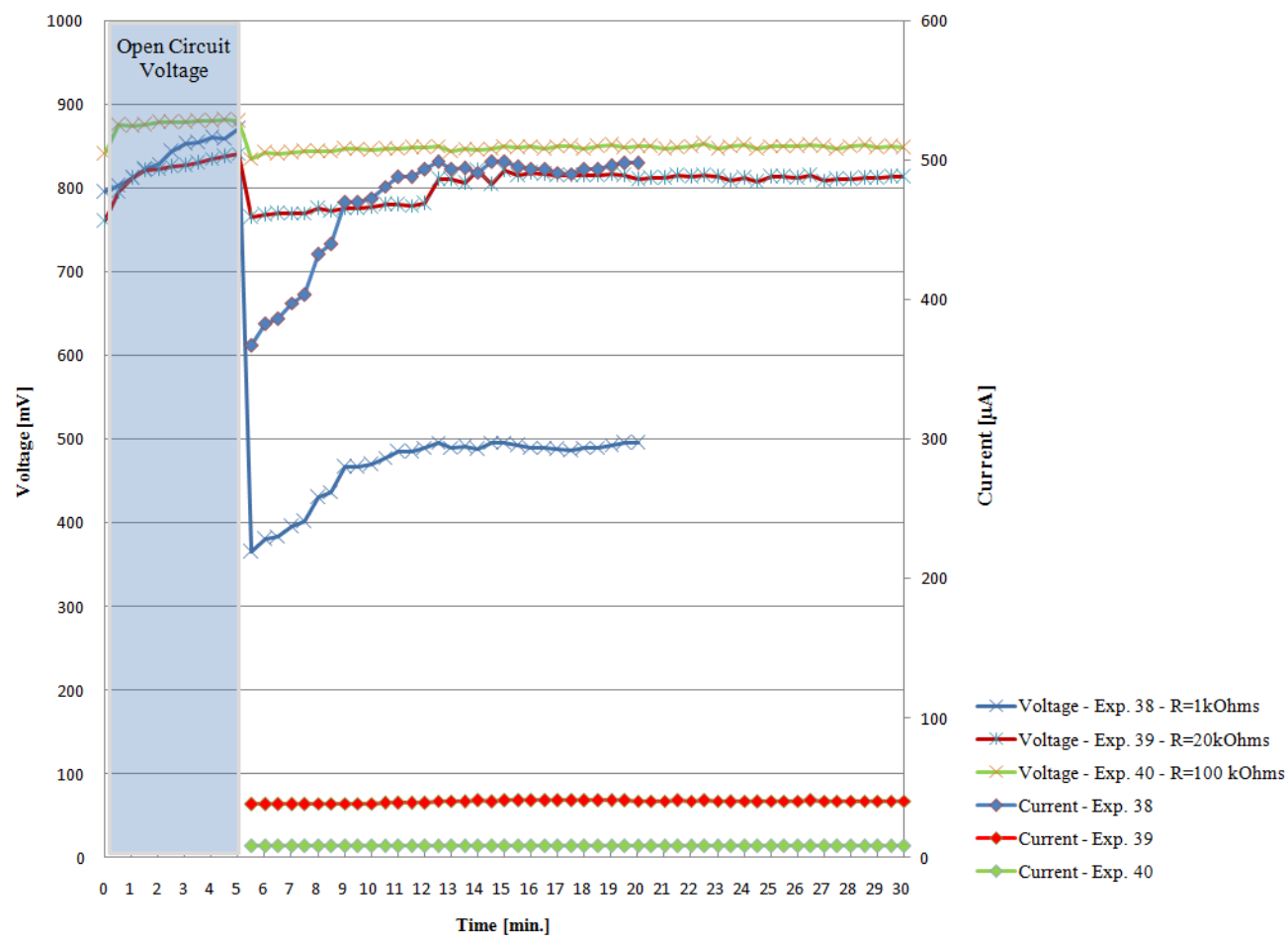
\* In the duration of OCV (no-load performance), no current is obtained. Consequently no current and power densities are available



## A8: Variations of voltage and current with three different external loads (PEM115/D3)

Objectives: Confirmation of the functionality of the  $\mu$ PSC with different loading scenarios (Trial experiment)

Device:  $\mu$ PCS with Nafion 115 and electrode configuration D3 - Refer to Appendix A1 for details and parameters of the experiment

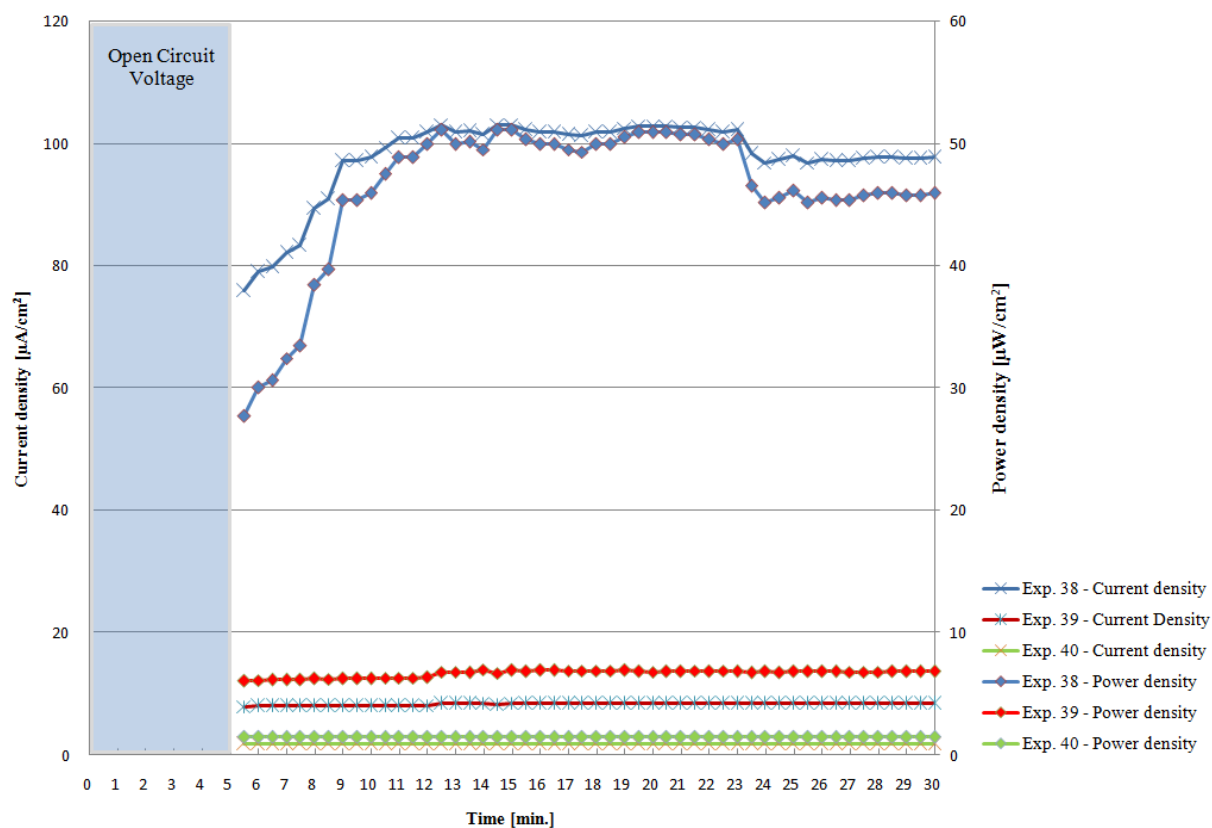


## A9: Variations of power and current densities with three different external loads (PEM115/D3)

Objectives: Observation of power and current densities variations with different loading scenarios (Trial experiment)

Device:  $\mu$ PCS with Nafion 115 and electrode configuration D3 - Refer to Appendix A1 for details and parameters of the experiment

\* In the duration of OCV (no-load performance), no current is obtained. Consequently no current and power densities are available

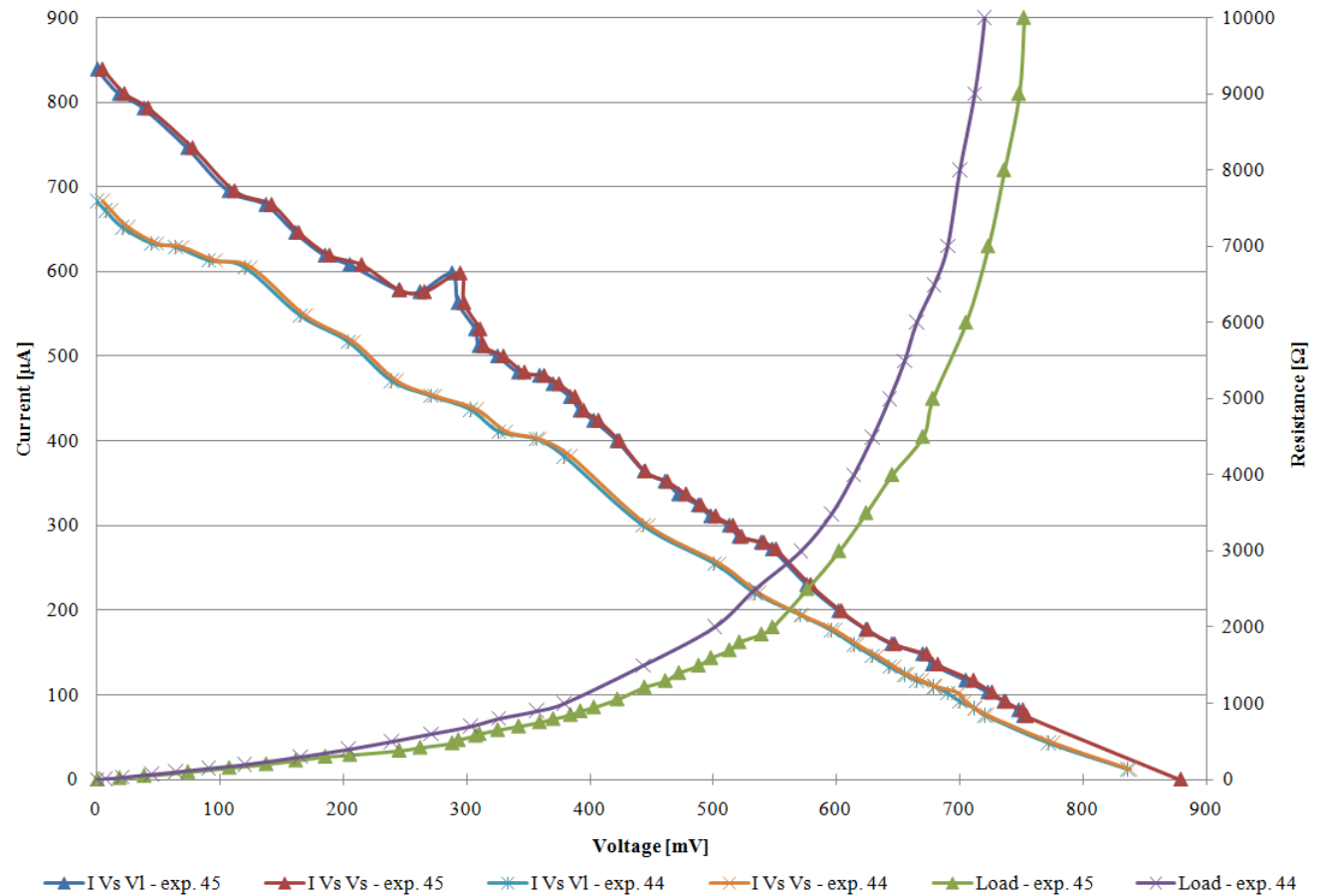


## A10: Voltage-Current ( $V$ - $I$ ) characteristics of two $\mu$ PSCs

Devices: Experiment 44:  $\mu$ PSC with Nafion 115 and electrode configuration D3

Experiment 45:  $\mu$ PSC with Nafion 117 and electrode configuration D2

(Refer to Appendix A1 for details and parameters of the experiment)



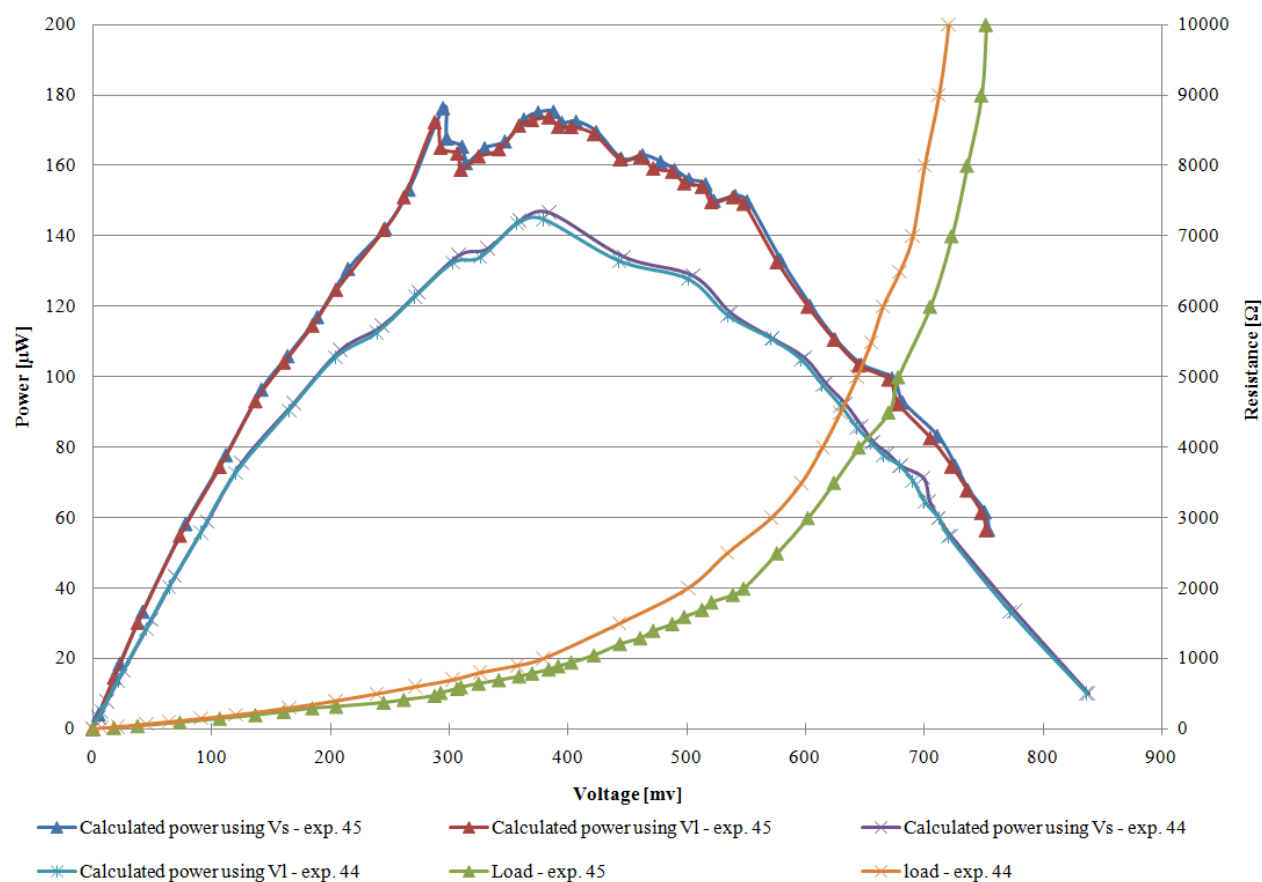
I: current  
 $V_l$ : voltage across the load  
 $V_s$ : voltage across the  $\mu$ PSC

## A11: Power generation curves of two $\mu$ PSCs

Devices: Experiment 44:  $\mu$ PSC with Nafion 115 and electrode configuration D3

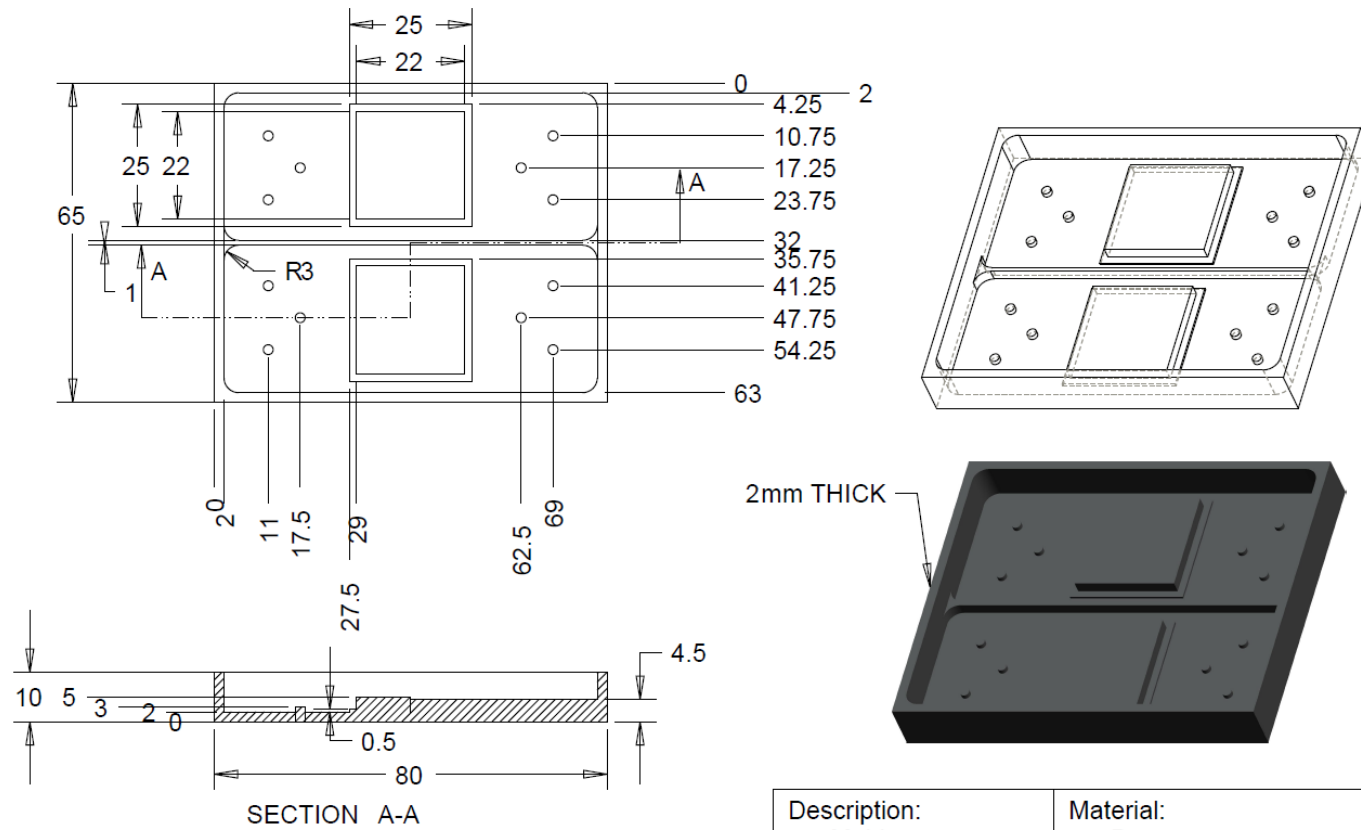
Experiment 45:  $\mu$ PSC with Nafion 117 and electrode configuration D2

(Refer to Appendix A1 for details and parameters of the experiment)



## A12: Mold design for PDMS fabrication

Material: Brass – Inner surface coated with gold using electroplating



Designer: Mahdi Shahparnia		Date: Sep. 08, 2008		Description: Mold		Material: Brass	
Dawing Number: MSH - 08 - 1		Ev. 13. 235 8482424 ext. 7098		Projection:		Scale: 1:1	
				Dimensions in: [mm]		Concordia University ENCS - Mechanical Eng.	